Analysis of transformer insulation systems with dielectric nanofluids

by

Daniel Pérez-Rosa

A dissertation submitted by in partial fulfillment of the requirements for the degree of Doctor of Philosophy in

Electrical Engineering Electronics and Automation

Universidad Carlos III de Madrid

Advisors:

Belén García, Juan Carlos Burgos

Tutor:

Belén García

July 2022

Acknowledgments

En primer lugar quiero agradecer a mis directores Juan Carlos y Belén por haber confiado en mí para participar en esta investigación, y desarrollarme como científico. Sus conocimientos guía y trabajo han sido fundamentales para la obtención de esta Tesis.

Gracias también a la Universidad Carlos III por darme la posibilidad de realizar la Tesis con los contratos predoctorales que ofrece, al tiempo que nos formamos como profesores. Agradezco también al departamento de Ingeniería Eléctrica por el apoyo y trabajo de sus integrantes. En especial tanto a Adrián Febrero como a Ángel Solanilla por su trabajo en los laboratorios del departamento.

Quiero también agradecer de forma muy especial al profesor Diego Garcia a su esposa Betty y su hija Ada Salomé, tanto por el trabajo que pude realizar en la Universidad del Valle, como por el enorme amor con el que nos trataron y por su enorme ayuda en los momentos complicados que nos tocó vivir allí.

No puedo pasar por alto tampoco a todos los profesores tanto de la UCM como de UC3M que me animaron a continuar aprendiendo e investigando. Son demasiados para citarlos a todos pero reitero mi más sincero agradecimiento a todos ellos.

A mis padres por la educación que nos dieron a mi y a mi hermano, y por la libertad que esa educación nos ha dado para buscar lo que queremos en la vida. Evidentemente a mi hermano porque siempre que podemos encontrarnos me hace aprender, reflexionar y crecer como persona. Como parte de mi familia también quiero agradecer a mis suegros Mari y Manolo que siempre han hecho lo posible por ayudarme en todo y sentirme querido.

Por supuesto tengo que agradecer a mis amigos Carmen, Eric, Jorge, Raúl, Alberto, Irene, Javi, sin ellos la vida sería, pero sería peor. Necesito guardar un agradecimiento especial para el Victor, gracias a él pude comenzar este proyecto, con él he compartido carrera, máster y tesis, es un sueño cumplido haber trabajado contigo.

A Sandra, por todo, por ella. Porque ella y yo sabemos todo el trabajo que ha llevado, todo el sacrificio que a veces ha supuesto. Gracias a ella lo malo ha sido menos malo y lo bueno siempre ha sido mejor.

Published and submitted content

- Title: Morphological analysis of transformer Kraft paper impregnated with dielectric nanofluids.
  Authors: D Pérez-Rosa, B García, JC Burgos, A Febrero
  Publication date: 20 August 2020.
  Journal: Cellulose.
  Publisher: Springer
  DOI: https://doi.org/10.1007/s10570-020-03386-1
  This material is wholly included in the thesis in chapter 4
  The material from this source included in this thesis is not singled out with typographic means and references
- Title: Dielectric Response of the Oil-Paper Insulation System in Nanofluid-Based Transformers.
  Authors: D Pérez-Rosa, B García, JC Burgos
  Publication date: 24 May 2021.
  Journal: IEEE Access.
  Publisher: IEEE.
  DOI: 10.1109/ACCESS.2021.3083368.
  This material is wholly included in the thesis in chapter 5
  The material from this source included in this thesis is not singled out with typographic means and references
- Title: Influence of Nanoparticles on the Degradation Processes of Ester-Based Transformer Insulation Systems.
  Authors: D Pérez-Rosa, B García, JC Burgos
  Publication date: 18 February 2022.
  Journal: Energies.
  Publisher: MDPI.
  DOI: https://doi.org/10.3390/en15041520
  This material is wholly included in the thesis in chapter 7
  The material from this source included in this thesis is not singled out with typographic means and references

- Title: Dielectric strength of nanofluid-impregnated transformer solid insulation.
  Authors: D Pérez-Rosa, A. Montero, B García, JC Burgos
  Submission date: 15th May 2022.
  Journal: High Voltage.
  Publisher: IET
  The material from this source included in this thesis is not singled out with typographic means and references
- Title: Temperature Dependency of the Dielectric Response of Nanofluid-based Transformer Insulation Systems.
  Authors: D Pérez-Rosa, B García, JC Burgos
  Publication date: 2nd June 2022.
  Conference: International Conference of Dielectric Liquids ICDL.
  Publisher: IEEE
  This material is wholly included in the thesis in chapter 5
  The material from this source included in this thesis is not singled out with typographic means and references

Other Research Merits

Journal papers and conferences

- Title: Evaluation of the Stability of Dielectric Nanofluids for Use in Transformers under Real Operating Conditions
  Authors: Victor A. Primo, Daniel Pérez-Rosa, Belén García, and Juan Carlos Cabanelas
  Publication date: 23 January 2019.
  Journal: Nanomaterials Publisher: MDPI
  DOI: https://doi.org/10.3390/nano9020143
- Title: AC Breakdown Voltage of Fe3O4 based Nanodielectric Fluids. Part 1: Analysis of Dry Fluids
  Authors: Victor A. Primo, Belén García, Juan Carlos Burgos, and Daniel Pérez-Rosa
  Publication date: July 2020
  Journal: IEEE Transactions on Dielectrics and Electrical Insulation. Publisher: IEEE
  DOI: 10.1109/TDEI.2019.008277
- Title: AC Breakdown Voltage of Fe3O4 based Nanodielectric Fluids. Part 2: Analysis of Fluids with High Moisture Content
  Authors: Victor A. Primo, Belén García, Juan Carlos Burgos, and Daniel Pérez-Rosa
  Publication date: April 2020
  Journal: IEEE Transactions on Dielectrics and Electrical Insulation.
  Publisher: IEEE
  DOI: 10.1109/TDEI.2019.008278
- Title: Investigation of the lightning impulse breakdown voltage of mineral oil based Fe3O4 nanofluids.
  Authors: Victor A. Primo, Belén García, Juan Carlos Burgos, and Daniel Pérez-Rosa
  Publication date: 28 November 2019.

Journal: Coatings.
Publisher: MDPI
DOI: https://doi.org/10.3390/coatings9120799

- Title: Analysing the Impact of Moisture on the AC Breakdown Voltage of Fe3O4 Based Nanodielectric Fluids.
  Authors: V. Primo, D Pérez-Rosa, B García, JC Burgos
  Publication date: July 2018.
  Conference: International Conference on Dielectrics
  ICD 2018.
  Publisher: IEEE
  DOI: 10.1109/ICD.2018.8514740
- Title: Analysis of water solubility in natural-ester based nanodielectric fluids
  Authors: D Pérez-Rosa, V. Primo, B García, JC Burgos Publication date: July 2018.
  Conference: International Conference on Dielectric Liquids ICDL 2019.
  Publisher: IEEE
  DOI: 10.1109/ICDL.2019.8796556
- Title: Analysing the impact of Moisture on the AC Breakdown Voltage on Natural Ester Based Nanodielectric Fluids.
  Authors: V. Primo, B García, D Pérez-Rosa, JC Burgos
  Publication date: July 2019.
  Conference: International
  Conference on Dielectric Liquids ICDL 2019.
  Publisher: IEEE
  DOI: 10.1109/ICDL.2019.8796675
- Title: Application of biodegradable fluids as liquid insulation for distribution and power transformers.
  Authors: B. García, A. Ortiz, C. Renedo, JC Burgos, D. García, D. Pérez-Rosa.
  Publication date: July 2020.
  Conference: International Journal of Environment and Electrical Engineering EEEIC 2020.
  Publisher: IEEE
  DOI: 10.1109/EEEIC/ICPSEurope49358.2020.9160569

Mobility

- Institution: Universidad del Valle

Location: Cali (Colombia)
Responsible researcher: Prof. Dr. Diego García
Period: 12/29/2019 to 06/18/2020

Grants

- PhD. Scholarship: "Personal Investigador Pre-Doctoral en Formación"
  Period: 09/12/2018 to 09/12/2022
  Funded by: Universidad Carlos III de Madrid
- Proyecto de Plan Nacional: Mejora de los sistemas de aislamiento de los transformadores mediante nanofluidos dieléctricos (DPI2015-71219-C2-2-R.)
  Period: 2015-2019
  Funded by: Ministererio de Economía y Competitividad.
- Proyecto de Plan Nacional: Gestión del ciclo de vida de transformadores aislados con fluidos biodegradables. (PID2019-107126RB-C21.)
  Period: 2021-2023
  Funded by: Agencia Estatal de Investigación (España)
- Marie Skłodowska-Curie Actions (MSCA): Raising knowledge and developing technology for the design and deployment of high-performance power transformers immersed in biodegradable fluids (BIOTRAFO) (H2020-MSCA-RISE-2018 Grant Agreement no 823969)
  Period: 2019-2023
  Funded by: European Comission (H2020)

Abstract

A number of authors have reported that the dispersion of small concentrations of nanoparticles may improve the dielectric and thermal properties of insulating oils. Extensive experimental work has been published reporting large improvements in the dielectric strength of these fluids compared with the properties of the base liquids.

However, even if those materials enhance the dielectric properties of conventional liquids, there are serious concerns about their applicability to real transformers in the future. The main difficulty is related with the long-term stability of the liquids at transformer service temperatures. This factor would only be improved if multidisciplinary research teams cooperate in the development of nanofluids which remains stable in the long term.

Another critical aspect is related with the interaction of nanofluids with other elements of the transformer, and the impact that they might have on the properties of these materials. In this field, the study of the interaction between nanofluids and transformer solid insulation is specially relevant. However only a small number of works have studied the topic up to date.

This PhD. Thesis carries out a research to get insight on the interaction between dielectric nanofluids and transformer's solid -insulation. An analysis on the morphological characteristics of nanofluid-impregnated paper was conducted that confirms the penetration of nanoparticles in the cellulose structure. Then several dielectric properties were investigated, including the dielectric strength and the polarization processes in nanofluid-impregnated solid insulation. Finally, the impact of the nanoparticles on the transformer ageing process was studied, to understand how the chemical reactions that lead to the degradation of solid materials on the transformer changes when the impregnation liquid is a nanofluid.

Research on nanodielectric fluids for transformer insulation is still a new field of study and these materials are still far from being of application to real transformers. The development of comprehensive studies, as the one presented in this Thesis, may contribute to the advance of this technology and to the promotion of new applications for these materials in the future.

Resumen

A lo largo de la última década, varios autores han publicado estudios que muestran que la dispersión de pequeñas concentraciones de nanopartículas puede mejorar las propiedades dieléctricas y térmicas de los aceites aislantes. Hasta la fecha se han publicado un número significativo de trabajos experimentales que constatan grandes mejoras en la rigidez dieléctrica y en otras propiedades de estos fluidos en comparación con las propiedades de los fluidos base.

Sin embargo, a pesar de que estos materiales parecen mejorar las propiedades dieléctricas de los líquidos convencionales, existen serias dudas sobre la posibilidad de que puedan ser empleados en transformadores reales en un futuro próximo. La principal dificultad está relacionada con la pérdida de estabilidad de estos líquidos a las temperaturas de servicio del transformador. Este aspecto solo podrá mejorarse mediante el desarrollo de investigaciones en las que colaboren investigadores de distintas áreas que logren desarrollar nanofluidos que con suficiente estabilidad a largo plazo. Otro aspecto crítico está relacionado con la interacción de los nanofluidos con otros elementos del transformador y su impacto en las propiedades de estos materiales. En este contexto, el estudio de la interacción entre los nanofluidos y el aislamiento sólido del transformador es de especial relevancia. A pesar de ello los estudios desarrollados sobre esta temática hasta la fecha han sido escasos.

En esta tesis doctoral se lleva a cabo un estudio integral sobre la interacción entre los nanofluidos dieléctricos y el aislamiento sólido del transformador. Dentro de la tesis se ha realizado un análisis de las características morfológicas del papel impregnado con nanofluido, que confirmó la penetración de las nanopartículas en la estructura de la celulosa y la formación de enlaces entrea ambos elementos. A continuación, se investigaron varias propiedades dieléctricas, incluida la rigidez dieléctrica y los procesos de polarización en aislamientos sólidos impregnados con nanofluidos; estos son aspectos de especial relevancia para el diseño de los transformadores. Finalmente, se estudió el impacto de las nanopartículas en el proceso de envejecimiento del transformador, para entender cómo influye la presencia de estos elementos en las reacciones químicas que dan lugar a la degradación de los materiales sólidos del transformador.

La investigación sobre fluidos nanodieléctricos para el aislamiento de transfor-

madores es un campo de estudio novedoso, y estos materiales aún están lejos de ser de aplicación en transformadores reales. El desarrollo de estudios integrales, como el presentado en esta Tesis, puede contribuir al avance de esta tecnología y al desarrollo de nuevas aplicaciones para estos materiales en el futuro.

Contents

List of Tables

List of Figures

Chapter 1

Introduction

1.1 Motivation

Transformers are one of the most important components of an electrical system. They are responsible for raising the voltage level of the energy to transport it with low power losses and reduce the voltage level near the consumption points. The reliability of these elements is essential for the proper operation of electrical networks and, in some cases, transformer failures have led to power outages and serious accidents that result into high economic losses [1–3].

One of the main elements that makes possible the safe operation of transformers is the insulation system, which is divided into liquid and solid insulation. Transformer solid insulation is composed of different types of cellulose based materials such as Kraft paper and pressboard [4]. The liquid insulation of transformers is commonly mineral oil (MO), a petroleum derivative, that fills the transformer tank accomplishing a double mission as electrical insulator and coolant agent. The insulating fluid impregnates the cellulose insulation enhancing its dielectric strength and protecting it from excessive aging. With the aim of improving safety and environmental protection, other liquids such as natural and synthetic esters have begun to be used as an alternative to MO.

In the last 20 years the application of nanotechnology has generated multiple research lines and innovation in almost every field of the science and engineering [5–7]. The development of new nanotechnology-based materials has also become a field of interest in high voltage engineering. In particular, the addition of NPs to transformer liquid insulation has been proposed as an attempt to improve the electrical and thermal properties of conventional insulating liquids [8–10]. Some authors claim that the development of new dielectric NFs with superior dielectric and thermal properties could lead to the manufacturing of transformers of smaller sizes and higher reliability in the future [11].

A number of authors have demonstrated that the presence of small concentrations of NPs can significantly improve the dielectric [12, 13] and thermal [14] properties of the oils. Published experimental works report large improvements in Alternating Current (AC) and Direct Current (DC) breakdown voltage (BDV), partial discharge inception voltage (PDIV) and impulse breakdown voltage of these liquids compared to those of the base fluids [15–18].

Several NFs have also shown better performance in some properties that are key to transformer design. Some authors have found important improvements in breakdown voltage [19–21] using ZrO_2, TiO_2 and Al_2O_3 NPs. Some other authors studied positive and negative impulse breakdown [22, 23] observing great improvements for positive impulse and less important improvements for the negative waves with Fe_3O_4 and aluminium nitride.

Another aspect studied is the influence of moisture in the performance of NFs. The presence of water particles in oil is one of the main factor that conducts to failures and degradation inside a transformer. NFs tend to accumulate more water molecules than MO or esters [24] due to the polarity of the NPs. So, several authors have shown that the NFs with higher values of moisture presents better performance when compared with their base fluids [25–27]. The reported studies conclude that NP's attract water molecules avoiding this molecules to form water bubbles or paths inside the dielectric oils that are responsible to generate electrical discharges.

Another main function of the dielectric oil is to allow cooling of the transformer due to its thermal conductivity. Studies conducted with NFs on this topic concluded that NPs do not have much influence on thermal conductivity. Only a few authors studied this topic observing small improvements for TiO_2, Fe_3O_4 and SiO_2 NPs [28–30].

Nevertheless, even if the properties of insulating liquids are improved by the addition of NPs there are still serious concerns that hinder their application in practice. One of the main issues is related with the long term stability of these colloids. A lot of progresses have been made on this subject in the last years, form studies that observed a stability of days [31–34], to obtain a stability of several months [35].

Also related to the long-term performance of the NFs some authors studied the aging process of the NFs [36–38]. The authors studied the properties of the NF after an accelerated thermal aging process, the conclusions obtained from the studies are that the NF maintain better dielectric properties even after the aging process.

Due to the advances in the development of NFs for transformer insulation system, some other questions have gain relevance. One of this questions is how the NF will interact with other components of the transformer.

The cellulose materials are an important part of the transformer insulation system, and interact very closely with the dielectric oil. Transformers are insulated using two main cellulose components: Kraft paper and pressboard. This interaction in the case of NF impregnated cellulose, Kraft paper or pressboard, is currently a main research topic to advance towards a commercial use of NF as dielectric liquids in power transformers.

When the cellulose insulation is impregnated with a NF, it is very likely that a part of the NPs suspended in the NF will penetrate into it. The presence of NPs could affect several properties of the solid insulation, which would have an impact on the overall performance of the transformer. The dielectric strength of the solid insulation could change; this would modify the allowable electrical stress in the oil-paper insulation. Also the permittivity values of the solid and liquid could change what would have an impact on the electric field distribution within the transformer. Additionally, the physic-chemical interaction between the NPs and the cellulose could cause changes in their properties what may affect some processes as the moisture dynamics or the aging

rate of the cellulose.

Despite of the relevance of the topic, very few authors have studied the influence of the NPs dispersed in the oil on the cellulose performance and the vast majority of the publications on dielectric NFs are focused on the the characterization of the liquids as insulators. This PhD. thesis studies some aspects related to the interaction between dielectric NFs and cellulose insulation with the aim of contributing to the advancement of this technology and to promote the future application of these materials in real units.

1.2 Objectives of the Thesis

The main objective of the PhD Thesis is to investigate how the use of NFs impacts the global behaviour of the solid insulation of a transformer.

The Thesis considers several NFs based in Fe_3O_4 NPs which had been fully characterized in a previous work [39]. The interaction between these fluids and the cellulose insulation is studied in this Thesis from several perspectives to get insight into how the oil-paper insulation of transformers would behave if the transformer tank were filled with NF instead of MO.

Although the experiments were carried out using only Fe_3O_4 based NFs it is likely that the results can be extended to insulation systems based on other types of conductive NPs (as Fe_3O_4 is a NP with conductive properties).

Some specific objectives have been proposed in the Thesis:

1. Proposing an experimental methodology to emulate the impregnation process of cellulose insulation in transformer factories, and apply it to the impregnation of paper insulation with NFs.
2. Studying if there is any chemical interaction between the cellulose and the NF that impregnates it. Characterize the morphology of the NF-impregnated cellulose.
3. Compare the dielectric response of the NF-impregnated paper with that of the MO-impregnated materials. Characterize the dependence of the dielectric response on NPs concentration and temperature.
4. Investigating the dielectric strength of NF-impregnated cellulose insulation compared with the performance of conventional materials. To this aim AC BDV and lighting impulse tests will be carried out on NF-impregnated paper samples and on MO-impregnated ones.
5. Performing accelerated thermal aging tests on NF-cellulose systems and compare the ageing processes in these systems with those that take place in conventional oil-paper insulation.

1.3 Outline of the document

The PhD. thesis is structured in eight chapters:

In Chapter 1 a general introduction is presented. The objectives of the thesis are set and a outline of the document is exposed.

Chapter 2 reviews the state of art of the topic. The studies carried out by other authors and their results are presented and discussed.

Chapter 3 describes the materials and the experimental methods and instruments used in the preparation of the samples.

Chapter 4 presents the study about the morphology of NF-impregnated samples and the comparison with conventional oil-paper systems, proposing interaction mechanisms between NPs and cellulose.

Chapter 5 shows the study on the dielectric response of the NF-based insulation systems.

Chapter 6 presents the investigation about the dielectric strength of NF-impregnated Kraft paper including the AC and the lighting impulse BDV and compares the results with those obtained on MO-impregnated samples.

Chapter 7 shows the results and observations of the accelerated aging experiments on NF and NE-immersed paper samples carried out in the Thesis.

Finally, Chapter 8 summarizes the main conclusions and contributions obtained from the thesis and outlines some possible future works.

Chapter 2

State of the art

In the present chapter a review of the state of the art related with the interaction of the NFs and solid insulation of transformers is presented. The results obtained by several authors are described and compared. The chapter reviews materials published on the topic focusing in four aspects: morphology, dielectric properties, breakdown voltage and aging.

2.1 Morphology studies

When studying the properties of the solid insulation impregnated with NFs, it is necessary to understand how the NPs interact with cellulose, which is by far the main component of the solid insulation of the transformer.

This section revise two types of studies that describe the interaction of NPs with cellulose. Most of authors use NFs to impregnate cellulose materials and study the interaction of both materials. Other authors modify the cellulose pulp or its surface with NPs to create a NP-doped Kraft paper[40, 41]. The objective in both cases is to improve the dielectric properties of the cellulose-dielectric fluid system to obtain superior material for the use in power transformers.

2.1.1 Characterization techniques

Several techniques can be used to get insight into the morphological structure of NF-impregnated cellulose. Scanning electron microscopy (SEM) , Fourier transformed infrared spectroscopy (FTIR), X-ray photoelectron microscopy (XPS) were used by several authors in their works for that purpose.

SEM is a widely used technique for the analysis of materials' surfaces. In this technique the analyzed material is illuminated with an electrons' beam. That beam can be focused with several lenses to observe the material at nanometre scale. The images obtained are useful to identify differences in the composition [42, 43] or defects in materials [44]. The presence of a multitude of radiations resulting from the interaction of the electron beam and the studied materials allows the combination of SEM with other qualitative and quantitative analysis that can complete the information provided by the SEM images.

FTIR analysis a is routine technique that is widely used to identify the covalent bonds in several solid [45] and liquid [46] materials. The samples are subjected to an infrared radiation which is absorbed by the material at a range of frequencies which is related with the presence of different covalent bonds of the material. As a result of the analysis a spectrum is obtained in which it is possible to identify multiple covalent bonds. FTIR is one of the most powerful techniques to identify multiple compounds

formed by covalent bonds. On the one hand is a useful technique for qualitative analysis, on the other hand is quite difficult to obtain quantitative results due to the low repeatability of the measures on the samples.

XPS analysis is a widespread technique which is used to identify the composition and oxidation state of multiple elements using an X-ray beam under high vacuum conditions. XPS is a powerful technique to observe chemical changes in comparable samples[47]; it is also widely used to quantify elementary composition changes [48].

2.1.2 Previous works on morphology of NF-based materials

One of the main questions about the interaction of NFs with solid insulation is whether the NPs migrate from the dielectric liquid to the paper. In case it happens, it is necessary to know if there is a chemical interaction between the two materials. In this sense, the main objective of the morphology studies is to know if chemical bonds in NF-impregnated cellulose differ from those present in the cellulose impregnated with conventional insulating liquids or non-modified cellulose.

Authors usually apply one or two of the techniques mentioned above to identify the presence of NPs in the NF-impregnated cellulose before performing dielectric tests, thermal tests or other tests to investigate material's properties. It may be noted that the main focus of those works is the analysis of other properties of the materials and thus the morphology analysis is generally not exhaustive.

In [49], the authors used SEM to investigate the structure of TiO_2 based NF-impregnated pressboard. They observed that there were NPs between the pressboard fibers and concluded that NP can pass through the pressboard, and this fact can modify the dielectric performance of the NF-impregnated samples compared to those impregnated with MO.

Keeping the same working structure Du et al. [12] used FTIR (Fig. 2.2) to trace the changes produced in the pressboard samples that they used in further investigations when those were impregnated with a TiO_2 based NF. They observed major differences at 1500-1700 cm^{-1}, concluding that NPs affect to the internal structure of the oil-cellulose composite structure. After observing the changes that the presence of NPs produced in the FTIR spectrum they performed space charge tests and electrical field distribution tests.

Kai-Bo et al. [50] studied the morphology of TiO_2 NF impregnated Kraft paper samples using SEM and EDX analysis. They prepared the NFs and impregnated Kraft paper samples. After that they studied the fresh samples and compared those with temperature accelerated aged samples. The main focus of the study was related with the comparison of the properties of the NF-impregnated new and aged samples. In

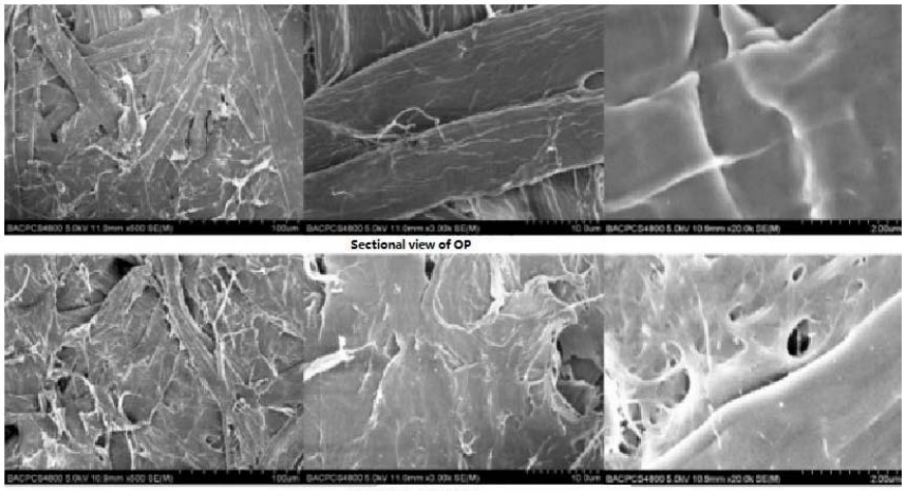

Figure 2.1. SEM images of sectional view of MO-impregnated pressboard (top) and NF-impregnated pressboard (bottom). Taken from [49]

.

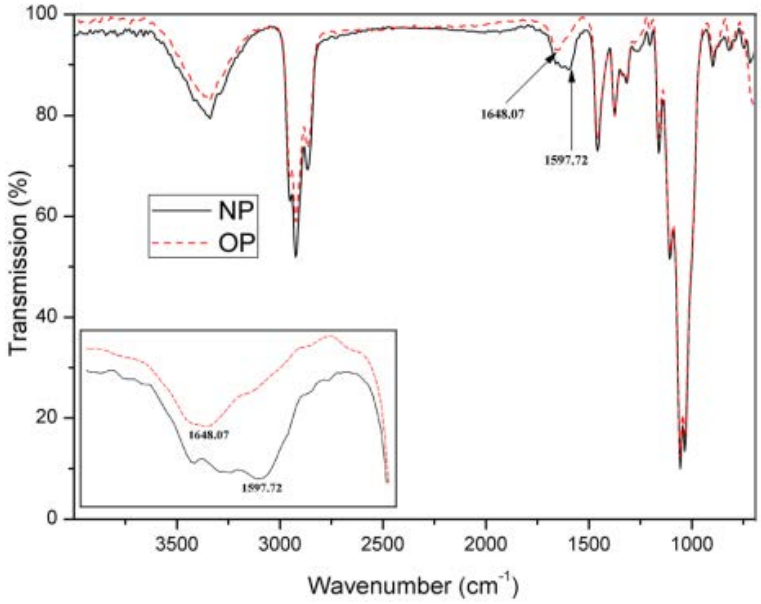

Figure 2.2. FTIR spectrum of TiO_2 NF-impregnated pressboard (NP) and MO-impregnated pressboard (OP). Taken from [12]

.

relation to the morphology, the authors observed and analyzed some impurities on the paper surface, concluding that despite the presence of these particles, the dielectric strength of the NF impregnated samples is enhanced for both fresh and aged samples.

Also Mo et al. [51] studied the structure of AlO_x NP modified insulating paper samples. Unlike the two cases before the authors prepared Kraft paper samples coating the surface of the cellulose with Al_2O_x NPs, instead of impregnating the cellulose with a NF. They used XPS analysis to identify the evolution of the modified paper samples

(Fig. 2.4), and completed the morphological study using SEM images. The SEM images obtained reveal the micro-morphology differences between the blank paper and the alumina coated paper, the authors also observed the different sizes of the alumina particles when coating time is increased. The average size of the particles after 30 minutes of coating was less than 45 nm, when after 60 minutes the sizes of the particles were between 50 and 100 nm as shown in Fig. 2.3. Finally the authors evaluated the electrical space charge changes when adding AlO_x NPS, observing a important reduction of the space charge, specially on the surface of the cellulose. The total charge accumulation of the 60 min coated paper was 34.8% lower than that of the blank paper. The authors concluded that coating the Kraft paper with alumina NPs is a effective method to improve the space charge behaviour of the paper.

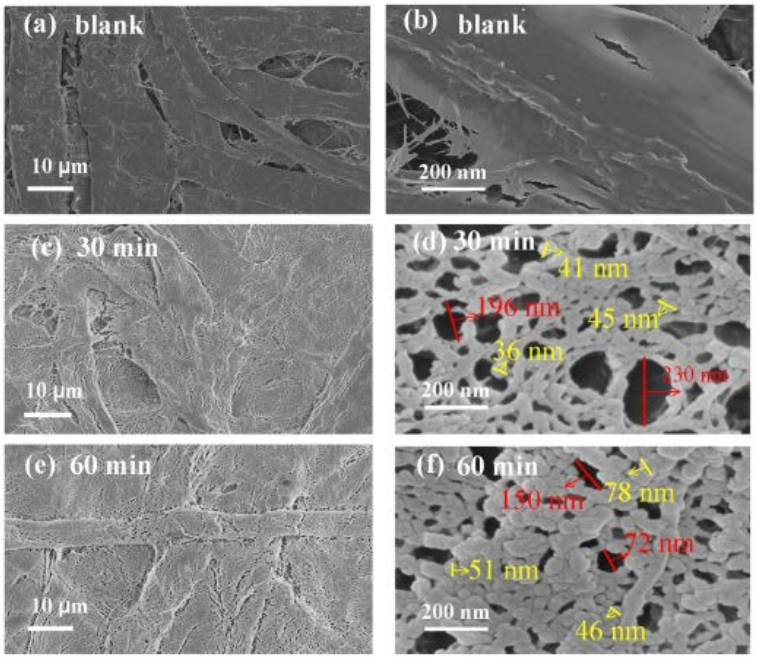

Figure 2.3. SEM images of blank paper(a, b); paper coated for 30 minutes(c, d); and paper coated for 60 minutes (e, f). Taken from [51]

Hollertz et al. [40] studied the morphology of silica-modified Kraft paper .They produced the paper from a cellulose pulp modified to permit the adsorption of the NPs. They observed the structures formed when adding the NPs in several quantities using SEM concluding that it was possible to create a silica NPs multi-layer supported on the cellulose structure, they observed NP sizes from 5 to 12 nm. After the morphological analysis the authors analysed the dielectric properties of the insulating Kraft paper.

A summary of the materials, characterization techniques and conclusions of the morphological studies performed by other authors in previous works is presented in Table 2.1. Observing the morphological studies and its conclusions, it is possible to observe that NPs could been identified in the cellulose and form stable layers when

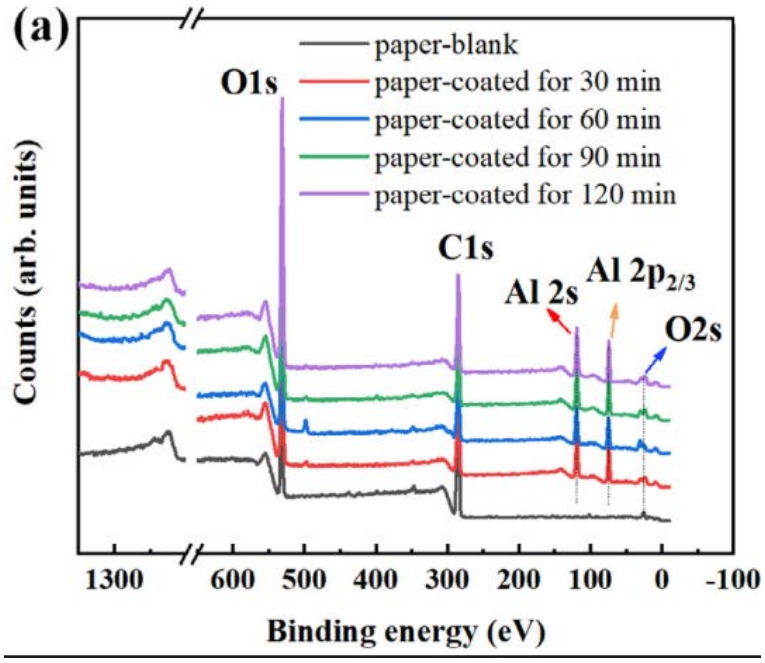

Figure 2.4. XPS analysis of AlO_x modified paper. Taken from [51]

the cellulose is modified with NPs and then impregnated with the dielectric oil. This fact is due to the higher concentration of NPs that are used when modifying cellulose. On the other hand the characterization of the properties of modified-cellulose tend to focus on the surface of the samples. For NF-impregnated cellulose studies it is harder to identify the NPs, as much lower concentrations are used to ensure the NF's stability. Despite of that the properties of the NF-impregnated cellulose change significantly and the improvements are quite relevant.

Table 2.1. Summary of the previous studies related with the morphological analysis of NF-based cellulose insulation

Ref	Materials	Manufacturing method	Characterization techniques	Conclusions
[49]	TiO_2 Pressboard	Impregnation with NF	SEM	NP flow trough the pressboard
[12]	TiO_2 Pressboard	Impregnation with NF	FTIR	NPs affect to internal structure of cellulose
[51]	Al_2O_x Kraft paper	NP modified cellulose	XPS,SEM	34.8% reduction of total space charge
[50]	TiO_2 Kraft paper	Impregnated with NF	SEM, EDX	BDV enhanced
[40]	Silica Kraft paper	NP modified cellulose	SEM	Stable multilayer silica NP created

2.2 Dielectric properties

The dielectric properties of NF-impregnated paper are among the key factors that define the possibility for the NFs to be used in real operation transformers. The NFs must prove that their dielectric behaviour is better than that of traditional oils; the same is of application for the solid insulation impregnated with those liquids.

One of the main consensus about the NF research is that the presence of NPs distort the properties of the dielectric oil due to the formation of an electrical double layer [52] around the NPs. This effect is caused by the fact that NPs present a negative charge on their surface. The negative charge creates an electric field that attracts a second layer of charges around every NP, as can be observed in Fig. 2.5. The electrical double layer modifies the behaviour of the dielectric oils when they are exposed to an electrical field [53].

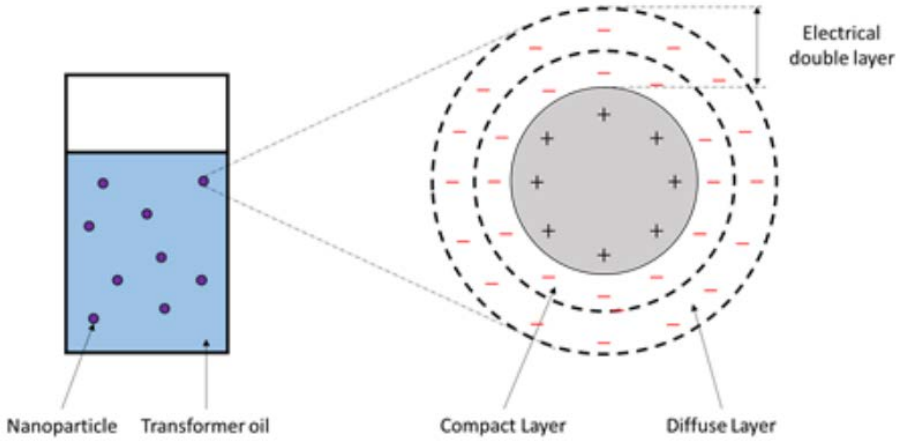

Figure 2.5. Electrical double layer formation. Taken from [39]

The characterization of the dielectric properties of NF-impregnated cellulose encompass the performance of a significant number of different tests aiming to understanding how NF-impregnated cellulose would perform in real operation conditions. In this sense creeping of the pressboard, volumetric breakdown (under both lightning and AC BDV) and dielectric permittivity are factors that play an important role in transformer's design. It is also important to investigate the partial discharge inception voltage (PDIV), as International Standards limit the maximum admissible level of PD activity in a transformer.

In this context some authors focused their work on understanding the dielectric properties of the interface NF-cellulose while others carried out volumetric studies in the materials.

2.2.1 Creeping properties of NF-impregnated cellulose

Creeping phenomena occurs when an electrical discharge spreads across the surface of a cellulose material. This kind of discharges takes place on the interface cellulose-NF, and as stated before, the characteristics of the dielectric double layer are strongly related with these discharges. Creeping studies are performed using a plate electrode and a needle electrode on the surface of the used cellulose material.

Rafiq et al. [54] studied the creeping performance of the oil-pressboard interface when a NF based on Al_2O_3 nanorods was used as insulating liquid; the authors observed an enhancement in the creep voltage with respect to that obtained when using MO. They reported an improvement of the creeping flashover voltages within 11 and 15%, depending on the electrode distance and the polarity of the of the overvoltage (Fig. 2.6).

Positive creeping flashover voltages of OIP and NIP

Gap distance (mm)	OIPs		NIPs		Improvement (%)
	Mean value (kV)	SD (kV)	Mean value (kV)	SD (kV)	
20	51.22	2.3	56.9	3.1	11
30	62.14	1.7	71.5	2.1	15

Negative creeping flashover voltages of OIP and NIP

Gap distance (mm)	OIPs		NIPs		Improvement (%)
	Mean value (kV)	SD (kV)	Mean value (kV)	SD (kV)	
20	64.1	1.9	72.4	2.4	12
30	78.06	1.7	88.98	3.9	14

Figure 2.6. Negative and positive creeping flashover voltages for presboard with Al_2O_3 nanorods. Taken from [54].

Shan et al. [55] studied the creeping phenomena under lighting impulse, using a NF prepared with Fe_3O_4 NPs. They observed a reduction in the creeping flashover probability for the same voltage for NF-impregnated pressboard.

Huang et al. [56] tested the oil-pressboard interface under impulse using a TiO_2 NPs based NF. They tested the influence of using several NP sizes from 5 to 30 nm on the creeping flashover voltage under AC stress. The study showed important improvements of the flashover voltage (Fig. 2.7), which reached a 30% when NPs of diameter 5 nm were used. For other NP-sizes there were improvements but less important than in the case of the smallest NPs.

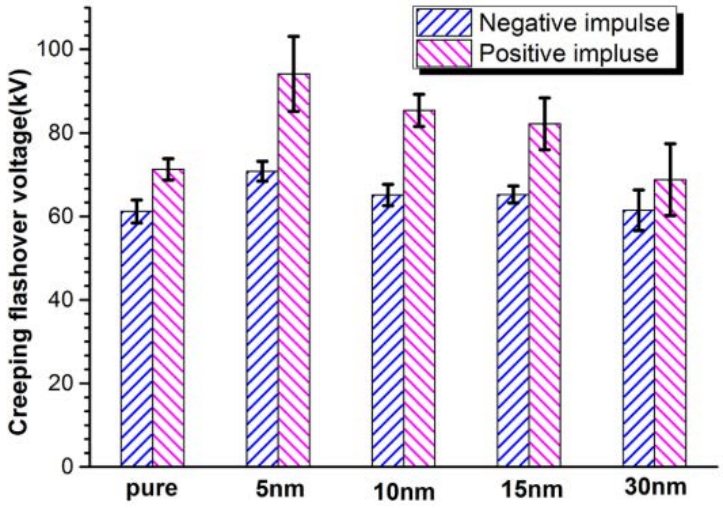

Figure 2.7. Negative and positive creeping flashover voltage of TiO_2 based NF-impregnated and MO-impregnated pressboard for several NP sizes. Taken from [56]

2.2.2 Breakdown voltage of NF-impregnated cellulose materials

BDV is one of the most important properties of dielectric materials. BDV of the materials that constitute the insulation system of an electric equipment has a significant impact on its size and cost. For this reason obtaining materials with as high as possible BDV is needed. Several authors focused their studies in obtaining information on the BDV of NF-impregnated cellulose materials.

In the study performed by Shan et al. [57], the effect of the NPs diameter on the DC BDV of NF-impregnated Kraft paper was observed. As in the previous case, the study compared the properties of materials obtained using NPs of several sizes. The authors observed, as did Huang et al., that the smaller the NP size the larger the BDV of the resulting cellulose samples is. The authors observed a better performance of all NF-impregnated samples versus MO-impregnated samples, where the maximum improvement correspond to the 5 nm NPs that was a 12.9%. They also reported a strong decrease in the breakdown strength as the NP size increases (Fig.2.8).

Liao et al. [58] studied the influence of the concentration of NPs in TiO_2 NP-modified pressboard on the dielectric strength, observing an increase in the dielectric strength of the modified pressboard. For samples with high NP's concentration (i.e. above 3 wt%) the samples started to show a decrease of the dielectric strength.

Maharana et al. [59] studied the AC breakdown voltage (BDV) of pressboard impregnated with NFs. They compared the dielectric strength of NF-impregnated pressboard under several aging conditions with the performance of MO-impregnated pressboard with the same ageing degree, concluding that for fresh samples the improve-

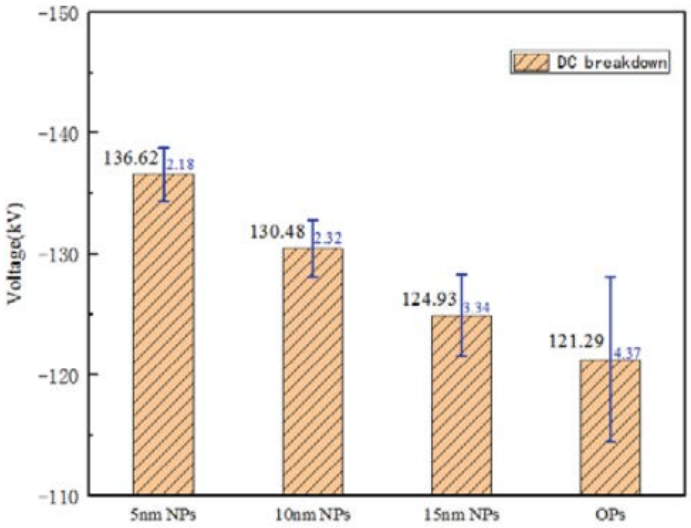

Figure 2.8. Negative DC breakdown voltage of oil-impregnated pressboard taken from [57]

ment in BDV is about 2 %.

All the results obtained by the authors on creeping flashover voltage and BDV are summarized in Table 2.2

Table 2.2. Summary of the studies published by different authors on the characterization of the creeping flashover voltage and BDV of cellulose materials with NPs

Ref	NPs	Cellulose material	Tests performed	Improvement in BDV	Comments
[54]	Al_2O_3	Pressboard	Creeping flashover AC	7%	-
[54]	Al_2O_3	Pressboard	Creeping flashover impulse	14% Negative 15% Positive	-
[56]	TiO_2	Pressboard	Creeping flashover AC	18.8%	NP sizes 5 to 30 nm
[55]	Fe_3O_4	Pressboard	Lightning impulse creeping flashover	15-17%	Two distance for electrodes used
[59]	h-BN	Kraft paper	AC BDV	2%	Compared fresh and aged samples
[57]	TiO_2	Pressboard	DC BDV	12.9%	Several NP sizes 5 to 15 nm
[58]	TiO_2	NP doped Kraft paper	AC BDV	20.83%	Several wt% of NP

2.2.3 Dielectric response

The dielectric response is a widely used technique for the diagnosis of insulation systems. The frequency response tests consist of applying a voltage with a variable fre-

quency between a few kHz and a few mHz and obtaining the real and imaginary parts of the complex capacity. The real part is related to the permittivity of the material, while the imaginary part is related to the dielectric losses. The traditional MO-impregnated cellulose is a well known system in which any unexpected change could be correlated with its dielectric response. For the case of the NF-impregnated samples it is necessary to identify how NP interacts with oil and cellulose and how it modifies the dielectric response.

In [60] the authors studied the dielectric response of TiO_2 NF-impregnated Kraft paper. The study was performed with two NP concentrations in the NF: 0.01 g/L and 0.02 g/L. The authors observed a decrease in the dielectric constant of the NF-impregnated samples due to the presence of NPs on the interface, also they observed lower values of dielectric losses that are result of the affinity of the NP to water molecules. They performed BDV test of the same samples obtaining similar values to those of the MO. This last result is compatible with the results observed in the previous section 2.2.3 were the authors observed enhancements in the BDV but using higher concentrations of NPs.

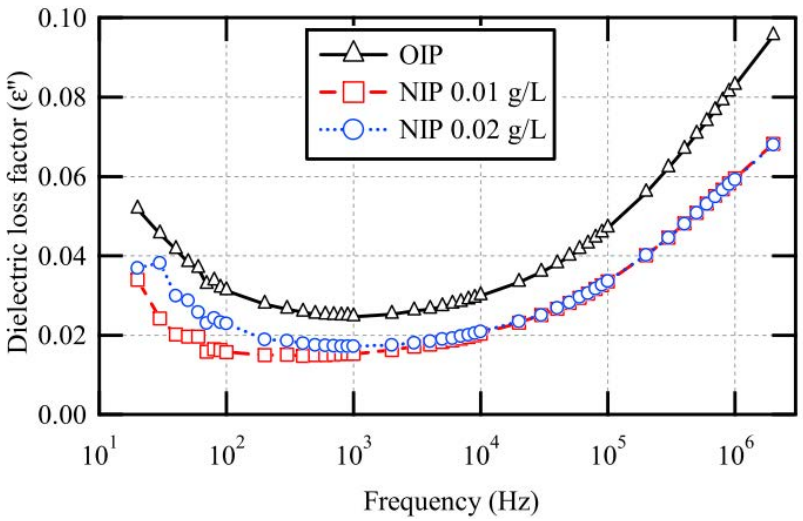

Figure 2.9. Dielectric loss factor of NF- impregnated paper and MO-impregnated paper. Taken from [60]

Yan et al. studied in [61] the dielectric response of Al_2O_3 NPs doped Kraft paper. They prepared samples with and without NP, impregnated with oil After that they prepared an aging observe how the dielectric response, AC BDV vary trough the time. Finally the authors studied also the tensile strength of the doped Kraft paper. The conclusions obtained reveal a general improvement in the properties, as the authors explain the NP contribute to maintain the paper properties trough the aging experiment.

2.3 Aging

An important aspect that needs to be studied before NFs could be used as dielectric liquids in real power transformers, is its long-term performance and how the presence of NPs influences the aging process of the Kraft paper and pressboard insulation. Power transformers can be in service for years, so the dielectric NF must contribute to the optimal conservation of the cellulosic materials inside the transformer.

Aging studies of cellulose materials are commonly carried out by means of accelerated aging experiments that consider temperatures high enough to emulate the long term aging processes that take place in service transformers. After the accelerated aging several studies are performed on the samples to assess the aging condition of the cellulose material. The main parameters that are used to quantify the degradation are the polymerization degree, which represents the average number of glucose monomers in the chains that compose the cellulose, and the tensile strength, which is related with the force that must be applied to break a strip of paper of certain dimensions, so it is a measurement of the mechanical properties.

Several authors have carried out ageing tests in NF-impregnated cellulose materials. Some of these studies are focused towards the evaluation of the evolution of the dielectric properties of the materials as they age.

Swati et al. [62] carried out accelerated aging experiments at 120^o C and 145^o C for 6 days, using Kraft paper-impregnated with a TiO_2 NPs and MO-based NF. They evaluated the aging from two points of view, the electrical behaviour and the physic-chemical analysis. From the electrical point of view the most relevant result confirms a lower accumulation of charge for the NF-impregnated samples. The results of the physical-chemical analysis are less clear since the authors could not observe clear differences when NF was used as dielectric oil.

In [63] Ibrahim et al. evaluated the aging of ZnO NF impregnated cellulose insulation, using Kraft paper and pressboard samples. For that purpose they aged impregnated cellulose insulation samples for 20 days at 120^o C. After the aging process they evaluated the tensile strength (TS), AC BDV, and moisture content. They observed no improvement in the TS for the NF-impregnated samples and obtained almost the same results in the moisture test. The most relevant result obtained in the study is the improvement observed on the AC BDV that reached a 10%.

Cimbala et al. in [64] studied a Fe_2O_3 based NF that impregnated pressboard samples. They carried out an accelerated aging experiment maintaining the NF and MO impregnated samples at 90^o C for 1000 hours. During the aging process they removed samples from the oven at different aging times (100, 250, 400, 600, 800 and 1000 hours), comparing the results to observe how the aging process take place. To

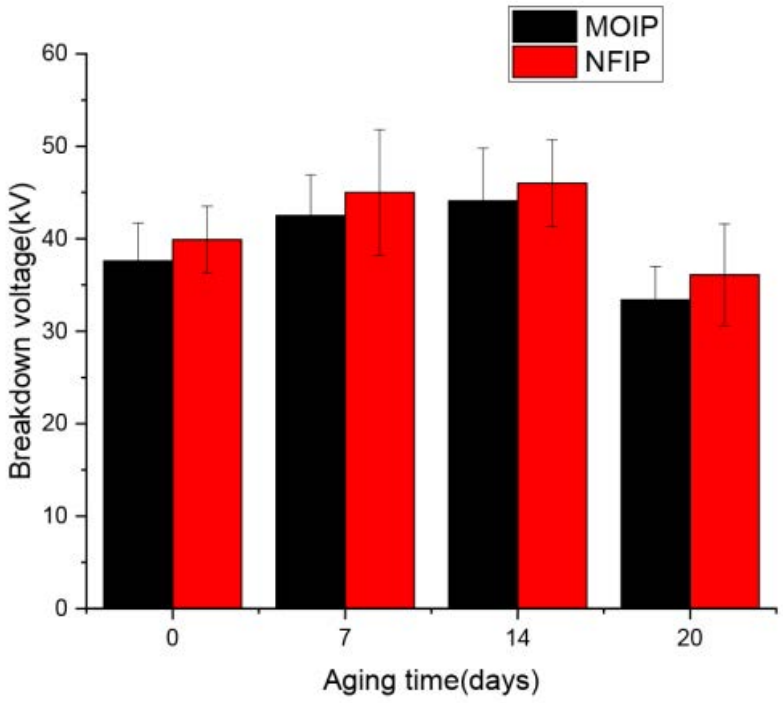

Figure 2.10. AC BDV of pressboard samples impregnated with NF and with MO at different aging times. Taken from [63]

evaluate the aging state of the samples analyzed they studied the dielectric response using FDS method. The results obtained by Cimbala et al. reveal that all the NF impregnated samples present less change in its dielectric behaviour as ageing progresses, compared with the MO-impregnated samples which suffer significant changes in the dielectric response with ageing.

In [59] Maharana et al. studied the aging process of Kraft paper impregnated with a NF based on MO and BN NPs. They used pre-aged Kraft paper and impregnated it NFs with two different NP contents, 0.1 and 0.01 wt%. to evaluate the influence of the NPs on the dielectric and mechanical properties of these samples. They measured the AC BDV and the TS of the NF-impregnated paper and the MO-impregnated samples. On the one hand they observed a similar performance on the NF-impregnated samples compared with the MO-impregnated ones for the AC BDV. On the other hand they observed an improvement in the TS of the NF impregnated samples, reporting an improvement for this parameter from the 3 to the 25%.

A summary of the studies performed in relation to the ageing process of NF-based cellulose insulation is provided in Table 2.3.

Table 2.3. Summary of the studies published by different authors on the ageing process of cellulose materials with NPs

Ref	Materials	Cellulose sample	Aging conditions	Evaluation method	Test performed
[62]	TiO_2-MO	Impregnation with NF	120^o,145^o C for 6 days	FTIR UV-Visible	Surface discharges
[63]	ZnO- MO	Impregnation with NF	120^o C for 20 days	TS moisture test	AC BDV
[64]	Fe_2O_3	Impregnation with NF	90^o C for 1000 h	Dielectric response	
[59]	BN-MO	Impregnation with NF	Pre-aged Kraft paper	TS	AC BDV

2.4 Conclusions

Some authors have studied the properties of different NF-impregnated cellulose materials, although the number of publications is significantly lower than the studies on the properties of NFs.

The morphology studies suggest that the NPs that are suspended in the NF clearly penetrate in the cellulose structure during the impregnation process and interact with it. However, the interaction modes between cellulose the cellulose molecular structure and the NPs are not well described yet.

The main topic of interest has been the characterization of the dielectric properties of NF-impregnated cellulose materials. Evidences have been found of a significant improvement on the dielectric strength of these materials compared with those of MO-impregnated samples. The degree of improvement depends on the experimental conditions and on the sample-preparation process though. A few works have proved that the dielectric response is also affected by the presence of NPs. Given the relatively small number of published works, it is difficult to extract conclusions on the impact of the NPs nature (i.e. conductive, semiconductive and insulating) in the results.

Finally, some accelerated ageing experiments have been reported which suggest that the NPs do not have a negative impact on the ageing processes of cellulose. Some works even show some improvements on the long term performance of NF-impregnated cellulose. As with other factors, the number of references and the depth of the studies published up to date is not enough to extract general conclusions on the subject.

Chapter 3

Materials and sample preparation

This chapter describes the materials used during the experimental stage of the Thesis. The experiments that are reported in Chapters 4 to 7 were carried out using similar materials and preparation procedures, although some variations were introduced in every case to adapt the setup to the particularities of each experiment. A general overview of the materials and preparation methods of the Thesis is presented below. Additionally, each chapter of the document describes the experimental procedure considered for the reported test.

3.1 Materials

3.1.1 Cellulose insulation

The main objective of the Thesis is to study the behaviour of the transformer solid insulation when it is impregnated with a NF and to compare it with the behaviour of the solid insulation impregnated with conventional insulating liquids.

The solid insulation considered for all the tests of the Thesis was Kraft paper. This type of paper is typically composed of 75-85 % alpha cellulose, 10-20 % hemicellulose and 2-6 % lignin [65]

The Kraft paper used for the experiments of Chapters 4 to 6, was provided by a transformer's manufacturer and is standard Kraft paper for electrotechnic purpose. The paper is supplied in layers of thickness 62.5 μm and grammage 0.75 g/cm^3. The thermal class of the paper is 105^o C. As will be explained in further chapters, for some experiments of the thesis simple layers of paper were used, while for others the paper was wired around a metallic core forming coils with several layers of paper (Fig. 3.1).

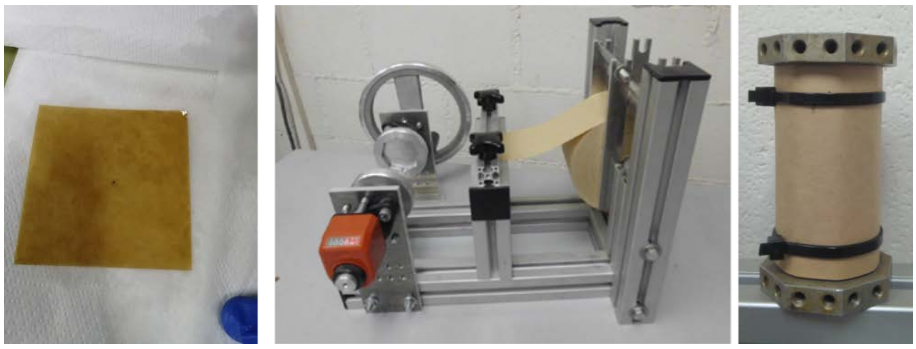

Figure 3.1. Paper sample used in chapters 4,5 and 7 .

For the aging experiments of Chapter 7, a different type Kraft paper was used, taken from a Kraft-paper-insulated copper conductor wire. The insulated wire was supplied by the manufacturer Vicente Torns (Spain). The copper conductor was unwrapped

(Fig. 3.2), and the paper was placed in glass vials for accelerated aging. The paper grammage is 0.75 g/cm^3, the thickness 50 m and the temperature index 105^o C.

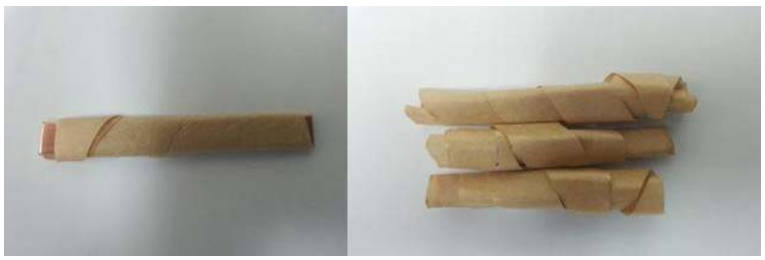

Figure 3.2. Kraft paper used for the aging experiment.

3.1.2 Insulating fluids

As was explained before, all the experiments of the Thesis were carried out in duplicate: first considering a conventional fluid (MO or NE) as cellulose-impregnation liquid, and then repeating them using a NF as cellulose-impregnation liquid. The NF was prepared by dispersing Fe_3O_4 NPs in the conventional fluid that was used for the reference tests.

The conventional insulating fluids used in the Thesis were the MO Nytro 4000X (Nynas, Sweden) and the NE Bioelectra (Repsol, Spain). The main characteristics of those liquids are summarized in Table 3.1.

Table 3.1. Main properties of the dielectric oils used in the Thesis

Property	Nynas Nytro 4000x	Repsol Bioelectra
Kinematic Viscosity (40^o C)	9.1 cSt	39.2 cSt
Flash point	146^o C	330^o C
Pour point	-54^o C	-21^o C
Density (20^o C)	0.866 g/cm^3	0.91 g/cm^3
Water content	20 mg/Kg	100 mg/Kg

The MO and MO-based NFs were used for the experiments of Chapters 4, 5 and 6 while the NE was used for the ageing experiments reported in Chapter 7. The reason of using a different base liquid for the ageing tests is that the NE-based NFs prepared in our laboratory remained stable for several moths at temperatures up to 105^o C, while the stability of the MO-based NFs at temperatures above 80^o C was not good [35].

3.1.3 Preparation of the nanofluids

The NFs were manufactured by dispersing Fe_3O_4 NPs in the MO Nytro 4000 X and in the NE Bioelectra.

The Fe_3O_4 NPs were supplied in form of NP suspensions by the company Magnacol (United Kingdom). The NPs were produced in the laboratory of the company by means of a one-step manufacturing process, i.e. they were produced directly in a solvent. A surfactant was added by the manufacturer to avoid NP aggregation. The diameter of the Fe_3O_4 NPs in the NP suspension was about 10 nm, and its concentration 60% in weight.

Since two different dielectric liquids were used to prepare the NFs of this work (a MO and a NE), it was necessary to use two NP suspensions to ensure the correct dispersion of the NPs in both liquids:

1. For the MO Nytro 4000X the NP suspension that was added was custom-made and used the MO Nytro 4000X as solvent.
2. For the NE Bioelectra the NP suspension was prepared in a hydrocarbon base.

All the NFs were prepared by mixing one the dielectric oils with a Fe_3O_4 dispersion. No additional surfactant was added to the mixture, so the one present in the commercial NP dispersions was the only used.

The prepared NFs considered NPs concentrations between 0.1 and 0.4 g/L. Those concentrations were chosen because, in previous studies, the NFs with these concentrations of NPs showed fair AC BDV and impulse BDV, while for higher concentrations the AC BDV of the liquid decreased [66].

The preparation process was as follows: The selected quantity of commercial suspension was added to 500 mL of the dielectric base liquid. The mixture was performed using a sonicator Sonics& Materials, Inc model VC 750 Watt (Fig. 3.3). The sonicator is an ultrasonic liquid processor, which generates ultrasounds that are capable to disperse NPs within the base fluid to obtain a uniform colloid. The mixture was homogenized with the sonicator at 40% of the rated power (i.e., power 300 W and ultrasound wave intensity 268 W/cm^2) for two hours in intervals of 30 seconds of agitation and 30 s of pause to avoid overheating of the mixture.

A picture of the obtained NFs are shown in Figs. 3.4 and 3.5.

The stability of the colloids was evaluated in a previous work [35] using two different methods: visual inspection and particle-size evaluation by dynamic light scattering. It was observed that the MO-based NFs remained stable at ambient temperature for more than one year and had a typical distribution of NP diameter between 10 and 16 nm. The NE-based NFs also remained stable for more than two months at temperatures up to 110^o C.

Figure 3.3. Ultrasounds stirrer used to produce the NFs through the Thesis.

Figure 3.4. NFs prepared from the NE Bioelectra with several NP concentrations.

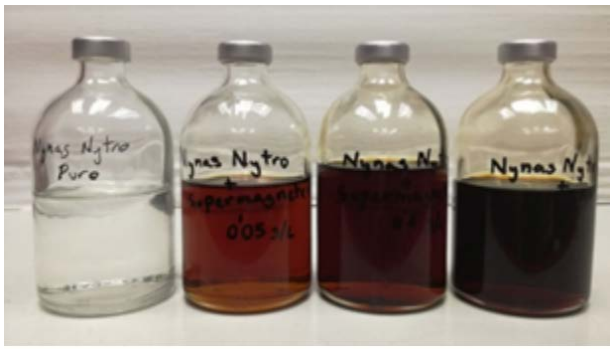

Figure 3.5. NFs prepared from the MO Nytro 4000x with several NP concentrations.

3.2 Impregnation process

All the cellulose samples included in the Thesis were subjected to drying under vacuum and then impregnated with conventional liquid or NF. Before every impregnation the insulating liquids were dried under vacuum at 60^o C for 24 hours. The cellulose was also dried under vacuum at temperature of 60^o C for 24 hours.

The main objective of the impregnation process is to emulate the impregnation that takes place in transformer factories. The impregnation of a transformer in an industrial plant takes place at temperature and under vacuum. The temperature makes the oil less viscous and, when subjected to vacuum conditions, creates an spray that favors a good impregnation of the cellulose.

An impregnation plant was used for the sample preparation (Fig. 3.6) which is composed of two chambers connected by a hosepipe. Chamber 1 has a heating resistor inside it and a thermometer to control the temperature. Chamber 2 is provided with a vacuum pump and a manometer.

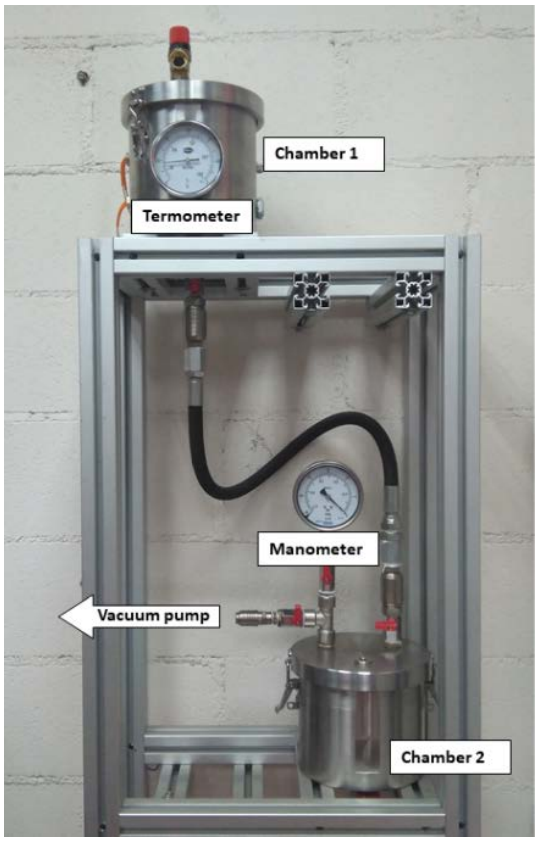

Figure 3.6. Impregnation plant

In the first step the fluid is placed in Chamber 1, where it is preheated at 40^o C until the temperature is homogeneous. The cellulose samples are placed in Chamber 2 and vacuum is applied in order to keep the Kraft paper as dry as possible. The

fluid in Chamber 1 is preheated to temperature 40^o C. When temperature is stable, the hosepipe is filled with the fluid. Finally, in the last step, the fluid passes from the hosepipe to Chamber 2, while applying vacuum in order to obtain a spray effect.

After the impregnation, the oil and the solid insulation specimens remain under vacuum for 30 minutes. Finally the oil in Chamber 2 is drained by means of a valve located at the bottom of the chamber.

The process described above was used for the impregnation of all the cellulose samples analysed throughout the Thesis. The plant was used either to impregnate samples of paper with NF and with MO or NE. Between two imprecations with different liquids the plant was subjected to a cleaning process that removed all the remains of the last used fluid.

3.3 Conclusions

This chapter presents the materials and preparation methods used in the Thesis. Some particular aspects that concern each particular tests are included in further chapters though.

Chapter 4

Morphology study

Liquid and solid insulation are in continuous interaction in transformers. After being manufactured, the transformer active part is subjected to an impregnation process through which oil passes to fill the voids of the cellulose insulation, improving its dielectric properties and its protection against oxidation. Additionally oil fills the tank and acts as a cooling agent that circulates throughout the transformer during its operation.

In the event that a NF was used as transformer insulation, the cellulose would be impregnated with it and it is likely that the NPs would penetrate in the cellulose structure and interact with it. However this is a hypothesis that needs to be proven. This chapters it es dedicated to it.

The first step to analyse the impact of the NF on the behaviour of the oil-paper insulation, is to understand how NPs interact with cellulose insulation from a morphology point of view. This chapter carries out a morphology analysis of samples of Kraft paper impregnated with a NF and with a MO. Characterization with several analytical techniques was carried out to investigate the interaction between the NPs and the Kraft paper structure when paper is impregnated with a NF.

4.1 Preparation of the Kraft paper samples

The analysis was carried out on coils of Kraft paper, emulating the insulation of the winding's conductors, which are composed of several layers of paper.

The paper coils were prepared according to the procedure described in Chapter 3. 14 layers of Kraft paper were rolled on an aluminium core using to this aim a winding machine to wrap the paper layers around the core to a thickness of 1 mm (Fig. 4.1). The arrangement emulates the solid insulation system of a transformer winding.

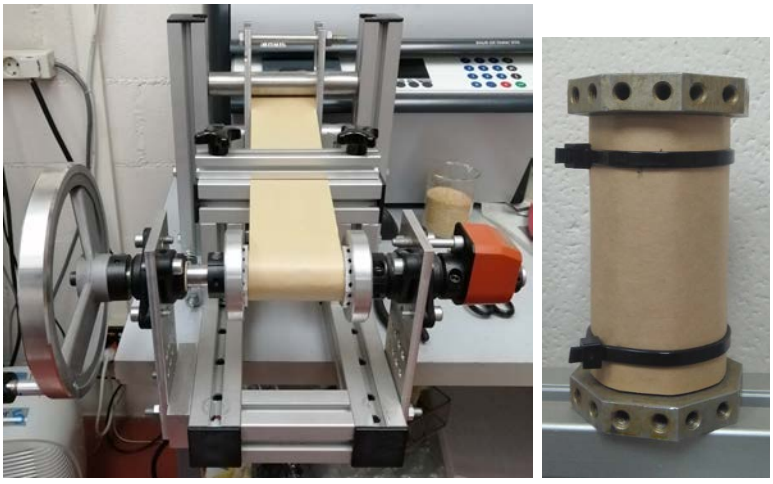

Figure 4.1. Solid insulation test specimens

The solid insulation test specimens and the NFs were subjected to drying process at temperature 60^o C and vacuum 1 mbar for 24 hours in a Binder VD 53 vacuum oven before starting the impregnation process. The moisture content of the solid insulation specimens at the end of the drying process was evaluated using Karl Fischer titration, obtaining moisture contents ranging between 0.5 and 0.9 % in weight in all cases.

As explained before, the main objective of the study is to analyze the interaction between the Fe_3O_4 NPs, that are suspended in the prepared NFs, and the cellulose insulation during the manufacturing process of the equipment when a dielectric NF is used as an insulating liquid for the transformer. Aiming at analysing that interaction, three different types of solid insulation samples were investigated: solid insulation samples impregnated with MO, solid insulation samples impregnated with Fe_3O_4 based NF, and samples that had been initially impregnated with NF and subsequently treated with chloroform to remove the impregnating NF.

The solid insulation test specimens were subjected to an impregnation process that emulates what is typically done to impregnate the solid insulation of the transformer active part in factory. The impregnation process was described in Section 3.2.

The impregnation process was evaluated by weighing samples taken from the 14 layers of paper of several solid insulation test specimens. No significant differences in weight were observed between the evaluated samples which suggests that the impregnation degree of the paper at the different layers was similar and that the impregnation process was repetitive.

To analyse the different scenarios described before, identical solid insulation test specimens were impregnated with MO and with Fe_3O_4 based NFs with NP concentrations 0.2 g/L, 0.3 g/L and 0.4 g/L.

Finally, smaller samples of paper were taken from the solid insulation test specimens to be tested with the analytical techniques that are described next. For that purpose, a hollow drill bit of 7 mm of diameter was used (Fig. 4.2). The samples used for testing were taken in all cases from the central layers of the solid insulation test specimens (i.e. layers 7 and 8).

4.2 Characterization of the samples

The samples were evaluated using three different techniques: Inductively Coupled Plasma mass spectrometry (ICP), Scanning Electron Cryomicroscopy (Cryo-SEM) and Energy Dispersive X-ray Spectrometry (EDX). Additionally the FTIR spectra of the samples was obtained to get insight on the types of bonds that are formed between the cellulose and the NPs.

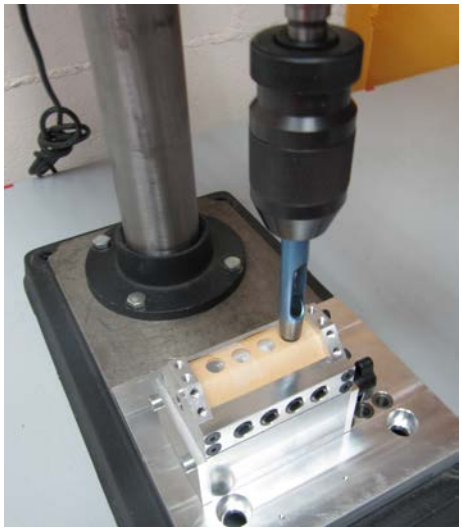

Figure 4.2. Extraction of samples from the paper coil

ICP is an element identification technique that is suitable to identify the presence of Fe or other elements in solid samples. It was used in this study to identify the presence of Fe_3O_4 NPs in Kraft paper that had been impregnated with NF of different NP concentrations after the oil had been chemically removed from the Kraft paper. The ICP measuring process starts by cleaning the NF from the impregnated paper using chloroform as solvent; after that the samples are crushed and dried. In order to obtain a solution for the ICP determination a 24 hours digestion is carried out in acid medium (HCl 50%).

An important objective of the characterization process is being able to observe the presence of NPs within the paper while it is impregnated with a NF. This aspect is one of the main difficulties of the study, since even a small quantity of MO could be quite corrosive to the components of the Scanning Electron Microscopy (SEM) classic equipment because of to the high vacuum conditions required to observe the samples.

Transmission electron microscopy (TEM) has been widely used by some authors [67–69] for morphological characterization of solid samples and observation of NPs within solid materials. However, the application of TEM was not possible in this case, since it would require the transference of the NPs to a hydrophilic solution, what would lead to a removal of the oil that supports the NP dispersion.

To observe the interaction between NPs and the cellulose fibres, Cryo-SEM was used. This technique enables the observation of cellulose samples in presence of oil or dielectric NF. For the Cryo-SEM characterization, the samples are set on carbon film in a Cryo-holder and transferred in a Cryo-SEM preparation system PPT2000 with Cryo-transfer (Quorum Technologies), to be analyzed in a cryogenic dual beam microscope, NOVA Nanolab 200 (FEI). The Kraft paper samples are treated at low temperature

using liquid nitrogen and vacuum. Samples are fast frozen in liquid nitrogen in order to preserve the natural state of the sample and then transferred, under vacuum, into a preconditioning chamber. Surface frost is removed by subliming the sample at -90^o C for 5 min. The samples are then platinum-coated using plasma sputtering and subsequently inserted in the microscope chamber and kept at temperature -130^o C and vacuum. As explained before, samples impregnated with nanodielectric oil and cleaned with chloroform were also observed with Cryo-SEM.

The microscope NOVA Nanolab 200 used in this work is also equipped with an Energy Dispersive X-ray Spectrometer (EDX) (Oxford INCA). EDX analysis of the samples was carried out to complete the study, for that purpose the surface and the cross section of the cellulose samples were analyzed at several regions. An accelerating voltage of 30 kV was applied to determine the Fe presence with the peak intensity of the Fe K-α X-ray line (6.398 keV).

4.3 Results and discussion

4.3.1 ICP Analysis

ICP analysis is can not be used on paper-impregnated samples, as the ICP apparatus is not compatible with oil. For this reason, ICP analysis was only performed on samples in which the oil had been removed.

The results of the ICP analysis performed on samples washed with chloroform are shown in Table 4.1 for different concentrations of NP in the NF used to impregnate the paper. As it can be seen, all the samples showed measurable quantities of Fe, even though those samples had been treated in an acid medium and digested, which is a chemical process capable of eliminating most of the Fe in the samples. The presence of Fe in the samples seems to indicate that the NPs dispersed in the NF tend to migrate towards the Kraft paper and bind to cellulose fibres.

It must be noted that there are important differences between the ppm of Fe obtained on twin samples prepared at identical conditions (i.e. impreganted with a NF with the same NP concentration). Additionally, the results do not show a clear relation between the presence of Fe and the concentration of NPs in the NF as the ppm of Fe determined from the different samples do not keep a monotonous relation with the NP concentration in the oil.

Although ICP measures provide a clear evidence of the presence of NPs in the washed cellulose samples, they are insufficient to clearly report a direct relationship between the NP concentration in the oil and the concentration of Fe in the Kraft paper. The lack of consistency observed in the Fe concentrations might be caused by

Table 4.1. ICP analysis results

Sample	Paper weight (g)	Fe (ppm)	Mean
0.2 g/L	0.5095	115	220
	0.5055	325	
0.3 g/L	0.5009	270	170
	0.4640	70	
0.4 g/L	0.5099	135	440
	0.5030	672	

the chemical digestion process and the use of HCl as acid medium, which can eliminate a non constant amount of Fe_3O_4 NPs.

4.3.2 Cryo-SEM and EDX

Circular paper samples 7 mm diameter extracted from the test specimens shown in Fig. 4.1, were characterized using Cryo-SEM.

Three different types of samples were evaluated to understand the interaction between NPs and Kraft paper:

1. NF-impregnated Kraft paper samples. Further referred to as NFS.
2. MO-impregnated Kraft paper samples. Further referred to as MOS.
3. NF impregnated Kraft paper samples that had been treated with chloroform to remove the oil. Further referred to as NFScl.

The main objective of the study is to compare the morphology of the three types of samples (NF, MOS and NFScl) and to identify the NPs attached to the cellulose fibres in those cases where NFs were used to impregnate the paper. The samples were analyzed from two different points of view. On one hand, a cross section of the Kraft paper was observed using Cryo-SEM microscopy; then the surface of the Kraft paper was observed with the same technique.

The NF-impregnated samples (NFS and NFScl) characterized with Cryo-SEM were extracted from the solid-insulation test specimen impregnated with the NF with highest NP concentration (i.e. 0.4 g/L). The reason to choose the samples with the highest content of NP is to facilitate the observation of the NPs.

Initially the samples were observed using the Back Scattered Electron (BSE) mode, to distinguish the Fe_3O_4 NPs from the cellulose fibres in brightness, due to the different atomic numbers of the elements. After some attempts it was concluded that it was not

possible to detect a significant difference in brightness and the Secondary Electrons (SE) mode was used instead, which provides deeper information about the morphology and allowed to obtain clearer images of the samples.

Fig. 4.3 shows the cross section image of the NF-impregnated Kraft paper sample (NFS). The image is quite clear and it is possible to identify the cellulose nanofibres on the right bottom part of the image and on the centre of the image. It is also possible to observe a large number of bright spherical forms that were identified in a first moment as Fe_3O_4 NPs (some of them are highlighted with yellow circles).

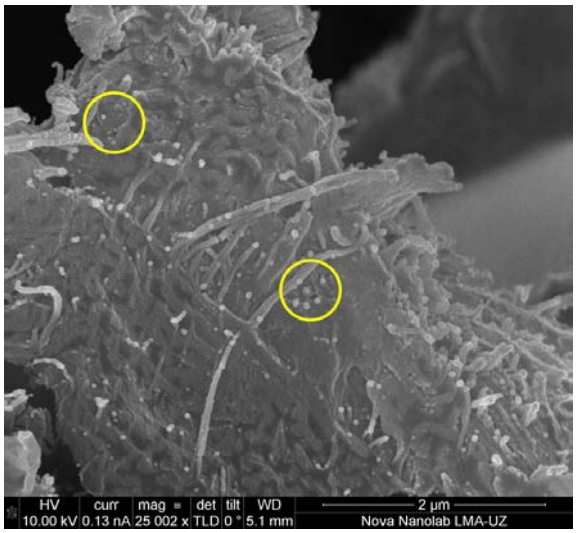

Figure 4.3. Cryo-SEM image of the cross section of a NF impregnated paper sample (NFS)

Fig. 4.4 compares two images of the cross section of a MO-impregnated paper sample (MOS) (b), and a NF-impregnated paper (NFS) (a). Both images clearly show the cellulose nanofibres, which are part of the cellulose macrofibres. It can be observed how, depending on the orientation of the nanofibres, they are visible as spheres or cylinders.

The comparison of the two images in Fig. 4.4, in which one of the samples was impregnated with MO (i.e. without presence of NPs) and the other one was impregnated with NF (i.e. with presence of NPs), suggests that, because of the shape and the size of the cellulose nanofibres, these can be confused with NPs. Thus, it must be concluded that although presumably some of the circular shining forms observed in Figs. 4.3 and 4.4 (b) are Fe_3O_4 NPs, it is not possible to assert it with total confidence.

To complete the study, a Cryo-SEM evaluation of the surface of three additional samples of types NFS, MOS and NFScl was carried out. These analysis were complemented by obtaining the EDX spectra of the three samples, in order to provide a precise evidence on the presence of Fe_3O_4 NPs in paper, and to make possible a quantification of the NP content in the different samples.

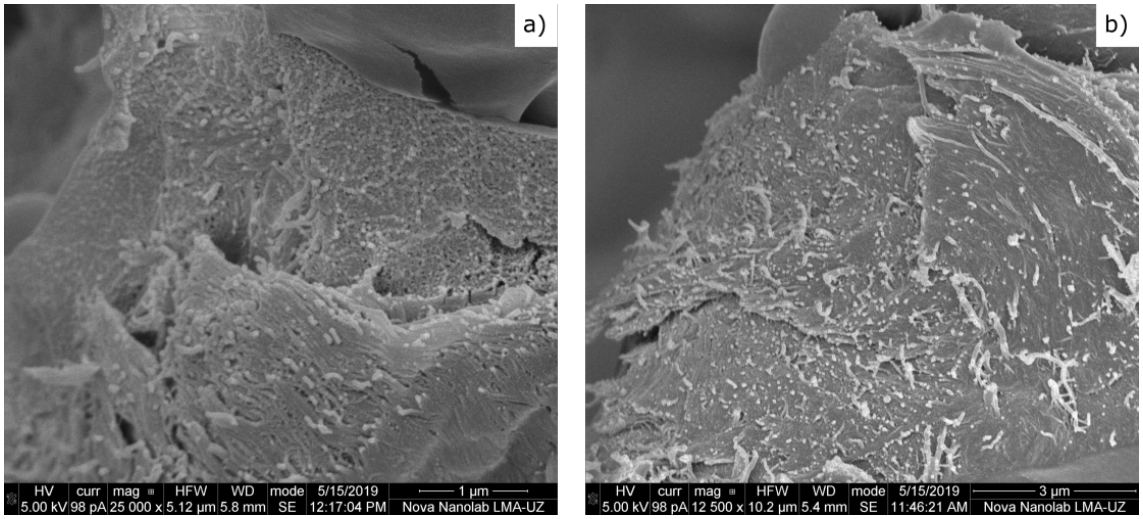

Figure 4.4. (a) Cryo-SEM image of a cross section of MO impregnated paper (MOS).(b) Cryo-SEM image of cross section of NF impregnated paper (NFS)

Figs. 4.5, 4.6 and 4.7 show the images of the three samples observed with Cryo-SEM and the spectra measured by EDX.

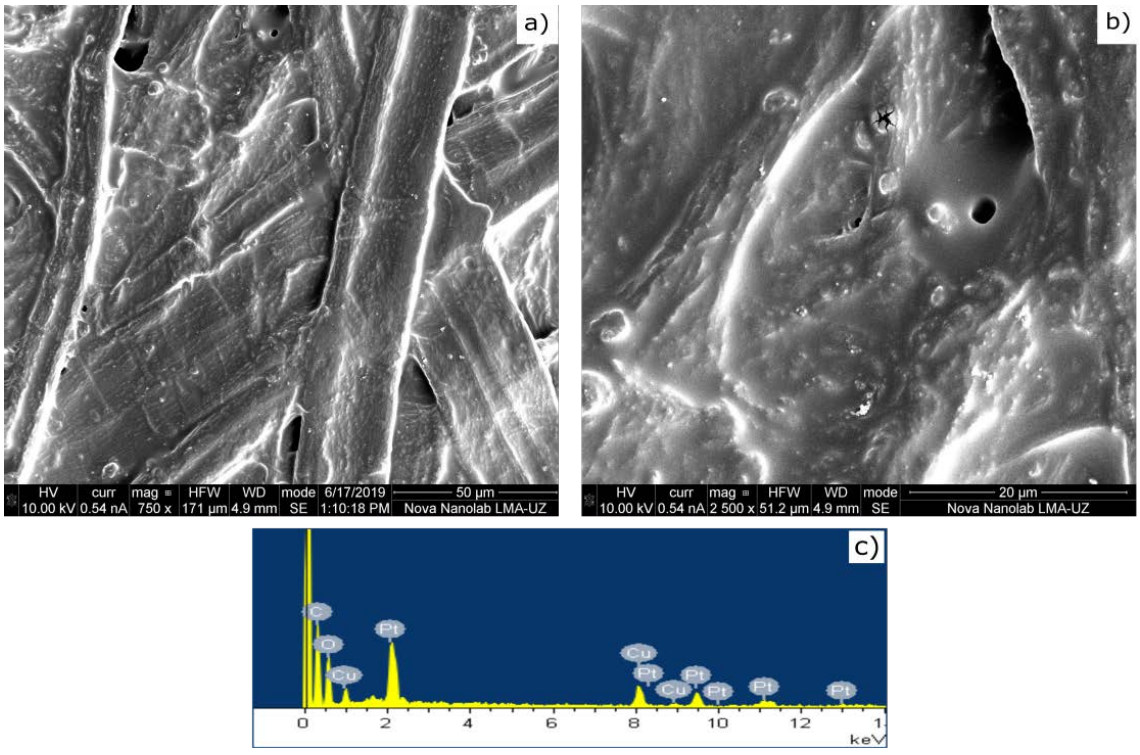

Figure 4.5. (a)(b) Cryo-SEM images of the MO impregnated paper (MOS). (c) EDX analysis of oil impregnated paper (MOS)

Fig. 4.5 shows the surface of a Kraft paper sample impregnated with MO (MOS); that sample is used as blank sample to be compared with those impregnated using NFs (both, NFS and NFScl). In Fig. 4.5 (a) the cellulose structure can be clearly seen as a

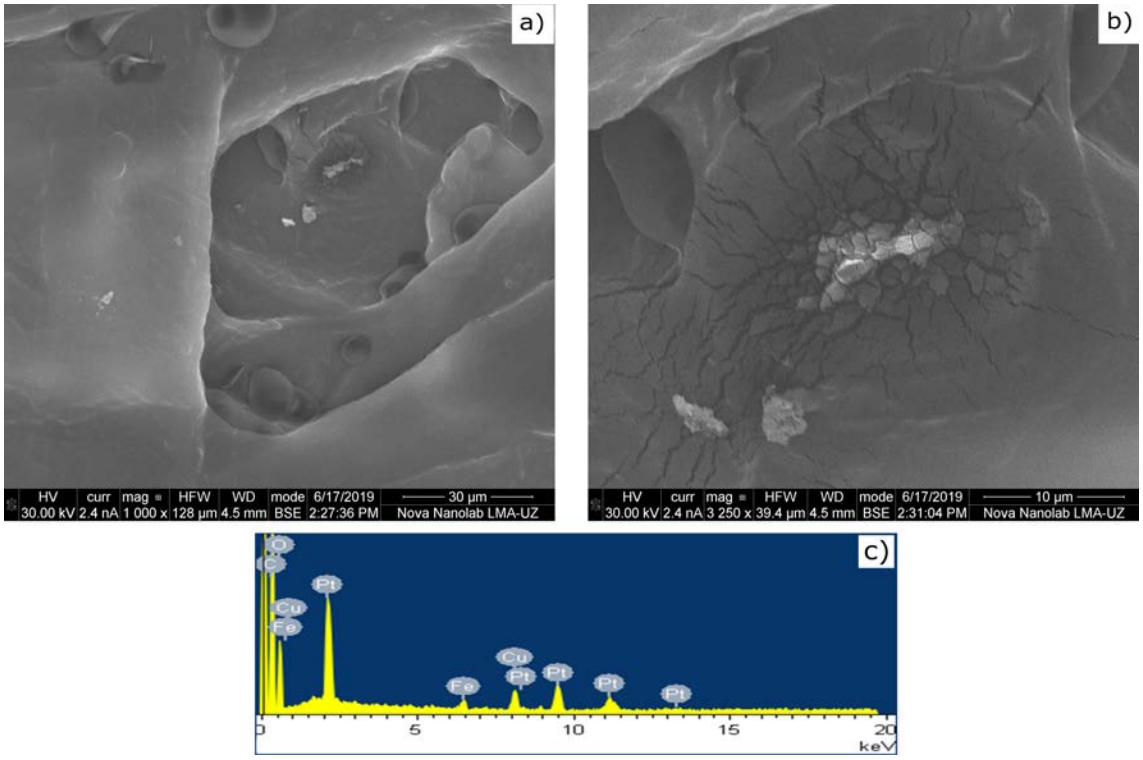

Figure 4.6. a)b) Cryo-SEM images of the NF impregnated paper (NFS). c) EDX analysis of NF impregnated (NFS)

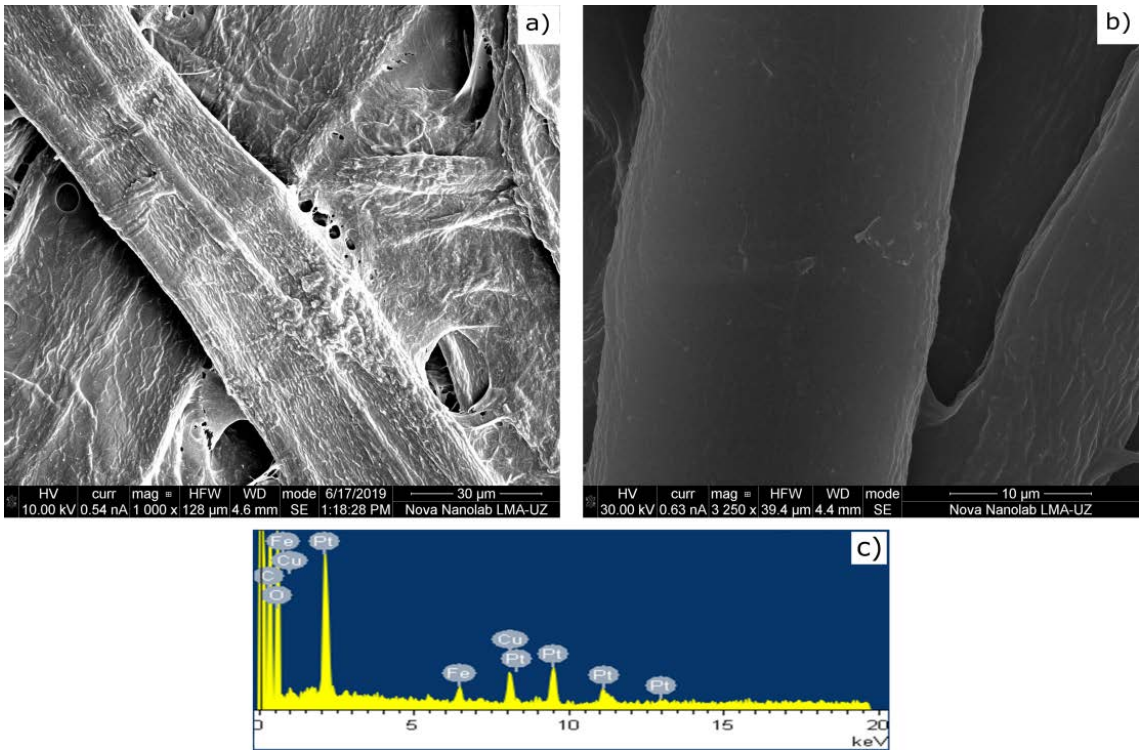

Figure 4.7. (a)(b) Cryo-SEM images of the NF impregnated Kraft paper (NFScl). (c) EDX analysis of NF impregnated Kraft (NFScl)

randomly crossing fibres structure. A detail of the same section of Kraft paper surface is shown in Fig. 4.5 (b). Finally, in Fig. 4.5 (c) an EDX spectra is shown, which was taken on the surface of the Kraft paper. As can be observed in the EDX spectra, the composition of the sample corresponds mainly to the cellulose element components (C and O); the platinum coating used to improve the resolution of the technique is also present in the EDX spectra.

Fig. 4.6 (a) and (b) shows the surface of a Kraft paper sample impregnated with NF (NFS). As can be seen the Fe_3O_4 NPs are not easily visible on the cellulose surface shown in (a). In Fig. 4.6 (b), which is a detail of the cellulose fibres, some regions could be identified as NP agglomerates, although, as in the case of the cross-sectional sample, it is not possible be absolutely certain of it. Fig. 4.6 (c) shows the results of the EDX spectra of the sample surface. The presence of Fe in it confirms the presence of the NPs on the surface of Kraft paper.

Fig. 4.7 shows the surface of a Kraft paper sample NFScl type, which was first impregnated with NF and then cleaned with chloroform to remove the NF. As in Fig. 4.6, the NPs on the surface of the sample can not be made certain, although it seems highly probable that some of the bright regions in the figure are NPs and NP-agglomerates. In this case the images are more clear than in the previous ones and the cellulose fibre structure can be very clearly appreciated. It must be noted that the presence of oil in the cellulose samples reduces the resolution of the Cryo-SEM method; in NFScl samples the oil that impregnated the cellulose has been removed what allows to distinguish the presence of NP agglomerates on the paper surface surface and even to measure their diameter.

Fig. 4.7 (c) shows the EDX spectra of the sample. One of the important things that can be noticed in it is that, although the NF has been removed from the cellulose in this case, a remarkable amount of the Fe stays bounded to the cellulose fibres.

Bonding between cellulose fibres and NPs was also reported by [70] who proposed an interaction mechanism between both elements, according to which bridges may be formed from an organic carbon molecule to the inorganic Fe_3O_4 NPs.

Fig. 4.8 shows the image of a NP-agglomerate that remained in the cellulose surface when the oil was removed and the EDX spectra of the agglomerate. The results of the spectra are quite clear: the visualized agglomerate is composed of Fe and the rest of elements appearing in the spectra are the same that in the previous one: carbon, oxygen, platinum and copper (these elements belong to the cellulose structure or the coating).

Fig. 4.9 shows an impurity macroparticle that was found on the surface of the Kraft paper sample treated with chloroform (NFScl). It can be observed how a number of NPs are attached to the paper. Those NPs were measured with the Cryo-SEM equipment

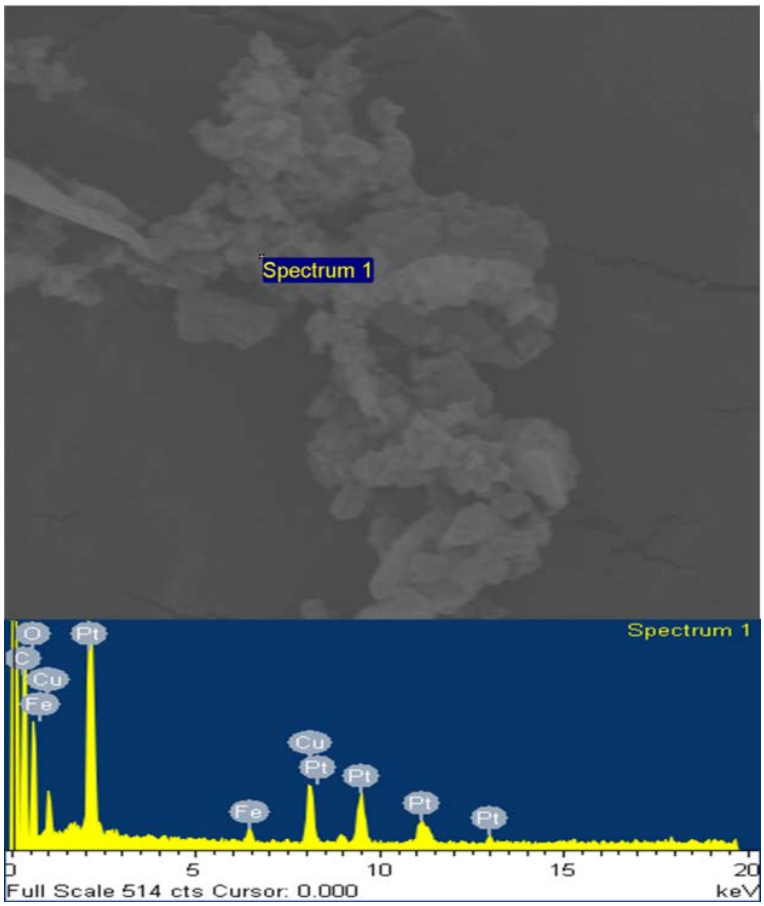

Figure 4.8. NP Agglomerate detail

to obtain a relation of sizes. The measured NP sizes are within 19 and 40 nm, what is in agreement with the sizes of NPs measured in the NF in a previous work carried out on the same materials [35].

According to the images and the EDX spectra shown in Figs. 4.7, 4.8 and 4.9, it can be concluded that when removing the oil the NPs can behave in three different ways: they can remain bounded to cellulose, they can form agglomerates that deposit on the cellulose surface or they can deposit on impurities. The presence of agglomerates or a non uniform distribution of NPs on the surface of the cellulose could affect to the insulation properties such as partial discharges.

Table 4.2 summarizes the results of the EDX spectra on all the analyzed samples and on the NP agglomerate.

It is possible to observe how Fe does not appear in the sample impregnated with MO. This sample is used as blank and compared with the others. The amount of the main elements of cellulose (C and O) present in all the samples is similar; the same happens with Pt, which is the metal that is used to coat all the samples. The presence of Cu in all samples, can be explained as the Cu is present in an important amount, in

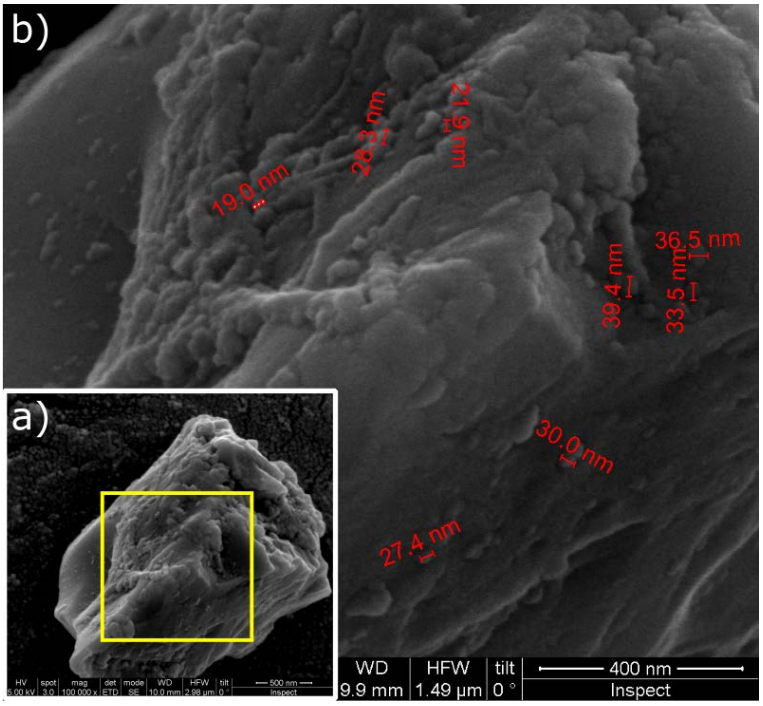

Figure 4.9. (a)Macroparticle with NPs attached, (b)NPs detail

Table 4.2. Comparison of the results of EDX spectra

Element	Samples			
% Weight	MOS	NFS	NFScl	NP agglomerate
C	47.53	52.98	50.44	51.34
O	35.09	30.03	37.08	36.12
Fe	-	0.78	0.26	0.23
Pt	12.72	13.53	11.30	10.52
Cu	4.66	2.68	0.92	1.79

the commercial aluminium alloys [71], used in this case as core to wound the insulating paper test specimens.

On the other hand, the presence of Fe in the samples that are impregnated with NF or in those that were impregnated with it and subsequently washed is clear. The sample containing NPs and oil presents the higher weight percentage of Fe, but it is remarkable how Fe is also detected in the sample washed with chloroform (NFScl). Additionally, it was possible to detect the Fe NPs aggregates formed when the NF was removed from the samples.

An extensive microscopy study was performed to obtain the maximum information of the studied materials. The more relevant images are those presented in the present chapter, however other images obtained during the study that might be of interest are presented in AppendixA.

4.3.3 FTIR analysis

In order to complete the analysis, samples of paper 7 mm diameter were extracted from the solid insulation test specimens to be characterized using FTIR. Fig. 4.10 shows the results of the analysis. Fig. 4.10 (a) corresponds to a sample taken from a test-specimen impregnated with MO, Fig. 4.10 (b) to a sample impregnated with NF and NP concentration 0.4 g/L and subsequently washed with chloroform, and Fig. 4.10 (c) shows the results on a sample impregnated with NF and NP concentration 0.4 g/L.

As it can be seen, comparing Fig. 4.10 (b) and (c) with reference Fig. 4.10 (a), small changes appear in the Fe-O stretching vibration at 569 cm^{-1}. It can be also seen how the multiple C-O vibrations signals at 1370, 1208 and 1025 cm^{-1} changes from 4.10 (a) to (c). The small changes on the FTIR spectra correspond to the vibration of C-O bonds (1370, 1208, 1025 cm^{-1}) and Fe-O stretching vibration (569 cm^{-1}) might be explained as changes on the chemical environment when ferrite-lignin bridges are formed.

Although the changes in the spectra are quite small, it can be noted that the chemical environment changes even when the NP concentrations are as small as 0.4 g/L. These variations are in agreement with the results of other analysis and also with the results presented in [70].

4.4 Conclusions

In the present chapter the morphological structure of NF-impregnated Kraft paper was evaluated. It was proved that the Cryo-SEM technique combined with EDX spectra is an suitable way to evaluate the structure of the cellulose, even when the samples are impregnated with oil, which can be corrosive to the components of the SEM classic instruments.

As it was shown in this paper, for a clear identification of the presence of NPs in the paper, the combination of both characterization techniques (EDX and Cryo-SEM) is required. Although the visual differentiation between NPs and cellulose nanofibres is not easy, a methodology was proposed that made it possible to identify the presence of NPs in NF-impregnated paper.

From the analysis conducted in this chapter, it was possible to conclude that the NPs dispersed in the MO tend to bound the cellulose molecules. Even when the paper is treated chemically to remove the base oil a remarkable number of NPs remain bounded to the cellulose.

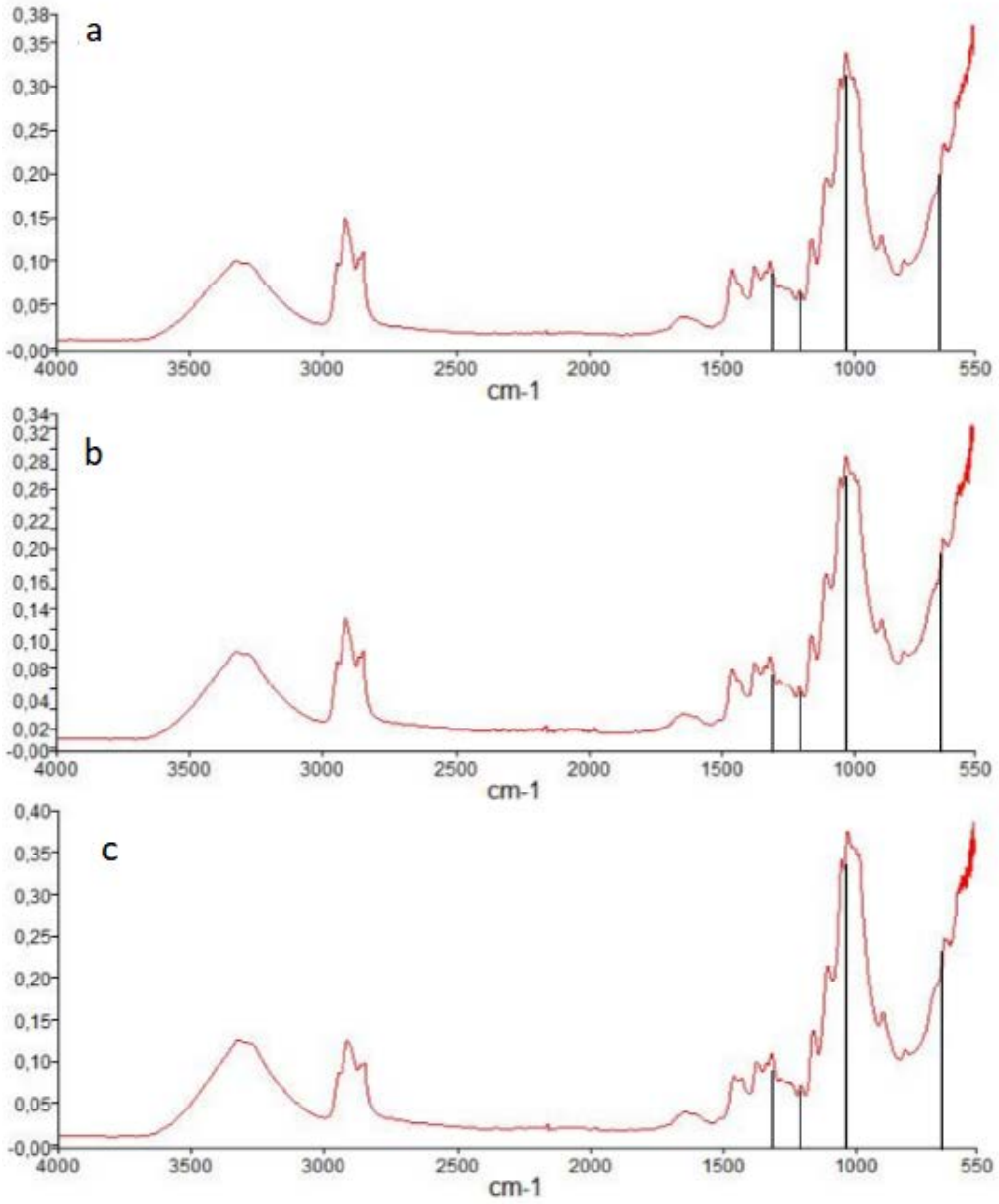

Figure 4.10. (a) FTIR spectra of MOS, (b) FTIR spectra of 0.4 g/L NFScl (c) FTIR spectra of 0.4 g/L NFS

Despite the fact that it was impossible to identify single NPs on the Kraft paper surface, NP agglomerates have been identified on it when the oil is removed by chemical methods. Also, the size of some NPs attached to an impurity were measured obtaining values that match typical NP sizes corresponding to the ones measured in the prepared NF.

An analysis based on the determination and comparison of the FTIR spectra of different samples was carried out, which suggested that chemical bonds are formed

between the cellulose and the Fe_3O_4 NPs.

Chapter 5

Dielectric response

The main goal of this chapter is to characterize the dielectric response of the NFs and also the response of pieces of cellulose insulation impregnated with those NF. The responses of the NF and NF-impregnated paper are compared with the responses responses of the MO and the MO-impregnated parer. The measurements are carried out at a reference temperature of 30^o C, and then they are repeated at different temperatures to obtain the activation energy of the different materials under analysis. The influence of the NP concentration on the dielectric response was also tested.

5.1 Dielectric response of oil-paper insulation

5.1.1 Polarization processes on dielectric materials

When a dielectric material is subjected to an electric field, a polarization process starts consisting of the alignment of the electric dipoles in the direction of the field.

Unlike what happens in conductive materials, electric charges in dielectrics materials are trapped and cannot move freely. polarization processes in insulating materials are characterised by a limited movement of the charges trapped in the material and an orientation of the dipoles that constitute the dielectric.

There are different mechanisms that contribute to the polarization of dielectrics which are governed by different time constants, such as the atomic polarization, ionic polarization, orientational polarization, interfacial polarization and hopping.

If a voltage V(t) is applied across the plates of a capacitor separated by a dielectric material, the resulting electric displacement D(t) shows a time dependency that is related with the retarded response of the different polarization processes in the dielectric:

$$D(t) = \varepsilon_0 \cdot E(t) + P(t) \tag{5.1}$$

were ε_0 is the permittivity of the vacuum, E(t) is the electric field and P(t) the polarization.

The instantaneous polarization of a material P(t) depends on the so called dielectric response function, f(t), which is a monotonous decreasing function that represents the response of a material to an impulse electric field.

For an impulse of magnitude $E\Delta t$, the resulting polarization would be:

$$P(t) = \varepsilon_0 \cdot E \cdot \Delta t \cdot f(t) \tag{5.2}$$

For a field with a different time dependency, E(t), the polarization can be obtained as:

$$P(t) = \varepsilon_0 \int_0^\infty f(\tau) E(t-\tau) d\tau \tag{5.3}$$

The dielectric response function, f(t), depends on the properties of the materials and also on its condition. Factors as the moisture content of a material or its aging condition have been demonstrated to have an impact on its dielectric response. Dielectric response measurements have been mainly used as a diagnostic method for transformer oil-paper insulation, as aging processes release water and other polar compounds that impact the dielectric response of the insulation system.

5.1.2 Determination of the dielectric response

Three methods are currently used to determine the dielectric response of oil-paper insulation: The measure of the Polarization and Depolarization Currents (PDC), the Recovery Voltage Method (RVM) and the Frequency Dielectric Spectroscopy (FDS) method. PDC and RVM determine the response of the material in the time domain, while FDS does it in the frequency domain [72]. Measuring equipment, specifically designed to monitor the condition of transformer insulation, are commercially available to perform RVM, PDC and FDS measures.

FDS is the method applied in this work to obtain the dielectric response of the NFs and the NF-impregnated cellulose insulation. With this aim cylindrical capacitors with each dielectric were prepared. A sinusoidal voltage of variable frequency is applied to the capacitor in a typical range of 1000 Hz - 0.1 mHz. The equipment returns the complex impedance of the capacitor for every applied frequency.

The dielectric material is modeled as a capacitor in parallel with a resistor (Fig. 5.1). The value of both parameters (C and R) are frequency dependent. The resistor represents the losses of active power, which are the sum of the resistive losses (dependent on the material's conductivity) and the dielectric losses (i.e. the dissipation of energy caused by the orientation of the dipoles).

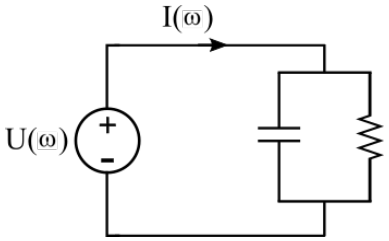

Figure 5.1. Model to represent the insulation under study

The relation between the phasor voltage and current is given by Ohm's law. Considering the association in parallel of the impedances Z_R and Z_C:

$$Z_R(\omega) = R(\omega) \qquad Z_C(\omega) = j \cdot X_C(\omega)$$

where

$$X_C(\omega) = -\frac{1}{\omega \cdot C(\omega)} \tag{5.4}$$

For a certain applied voltage, the current is:

$$\mathbf{I}(\omega) = (j \cdot \omega \cdot C(\omega) + \frac{1}{R(\omega)}) \cdot \mathbf{U}(\omega) \tag{5.5}$$

The relation between the current and the voltage is commonly expressed as:

$$I(\omega) = j \cdot \omega C_0 \cdot (\varepsilon'(\omega) - j \cdot \varepsilon''(\omega)) \cdot U(\omega) \tag{5.6}$$

were $\varepsilon(\omega)'$ and $\varepsilon(\omega)''$ are the real and imaginary parts of the so called 'complex permittivity' ($\hat{\varepsilon}(\omega)$), which depends on the capacitance and the dielectric losses of the material:

$$\varepsilon' = \frac{C(\omega)}{C_0} \qquad \varepsilon'' = \frac{1}{R(\omega) \cdot \omega \cdot C_0}$$

C_0 is the geometric capacitance, which is defined as the capacitance of the test cell with any dielectric between the electrodes.

Some other relevant magnitudes, such as the dielectric dissipation factor, also called tan delta, can be derived from these measures:

$$\tan \delta(\omega) = \frac{\varepsilon''(\omega)}{\varepsilon'(\omega)} \tag{5.7}$$

Most FDS measuring devices provide the so called complex capacitance as output parameter:

$$\hat{C}(\omega) = C'(\omega) + j \cdot C''(\omega) = C_0 \cdot \hat{\varepsilon}(\omega) \tag{5.8}$$

where

$$C' = C(\omega) \qquad C'' = \frac{1}{R(\omega) \cdot \omega}$$

As can be seen, C' is the capacitance of the test object and C" is proportional to the power loss of the material.

One of the limitations of FDS method, compared to other methods, such as PDC, is that it does not allow the direct estimation of the conductivity of the material. However, at very low frequencies the resistive part of the losses is predominant. Cigré states that, when ε'' has slope ω^{-1} and ε' is constant it is possible to identify the DC conductivity of the material with the slope of the C" curve [72].

Dielectric measures are very sensitive to temperature variations. The temperature dependence of dielectric measurements has been widely studied, observing that changes of temperature cause a frequency shift of the dielectric response frequency spectra. In most dielectric materials, such as oil-paper insulation temperature does not affect significantly the shape of the dielectric response.

The shift of the dielectric response curves with temperature can be expressed by means of an Arrhenius factor, and may be calculated using the equation proposed by Ekanayake in [73]:

$$shift = log(\omega_1) - log(\omega_2) = -\frac{E_a}{k \cdot 2.3258} \cdot (\frac{1}{T_2} - \frac{1}{T_1}) \tag{5.9}$$

where k is Boltzman's constant and Ea is the activation energy of the material.

5.2 Experimental procedure

5.2.1 Preparation of the test specimens

The responses of the MO and the NFs with different concentrations of NP were measured using a test cell for liquids with cylindrical electrodes (Fig. 5.2). The cell was filled with 2 cL of the fluid that is being characterized in each test.

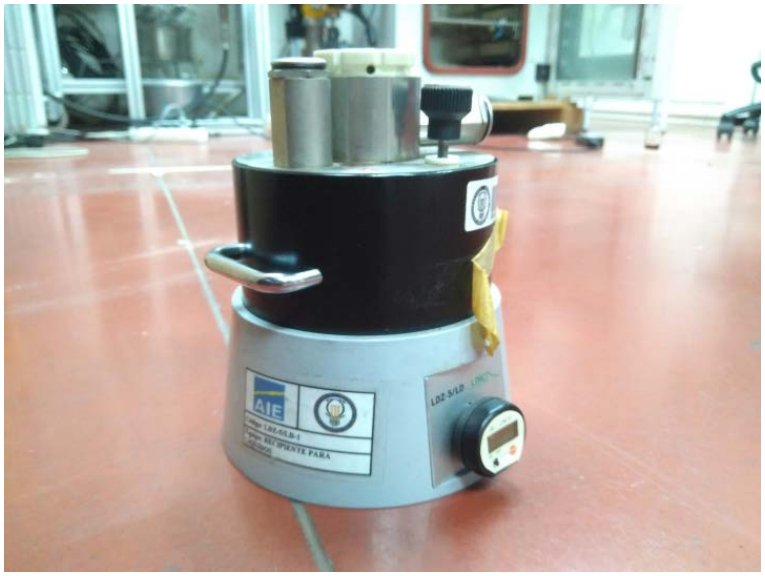

Figure 5.2. Liquids' test cell

The dielectric response of the solid insulation was tested using a cylindrical test object. The objects were prepared by winding layers of Kraft paper around an aluminium core using a winder machine to this end (Fig. 5.3). Identical test objects were

obtained with thickness of cellulose 1 mm; to reach that thickness 14 layers of Kraft paper were necessary. The resulting test object is shown in Fig. 5.4.

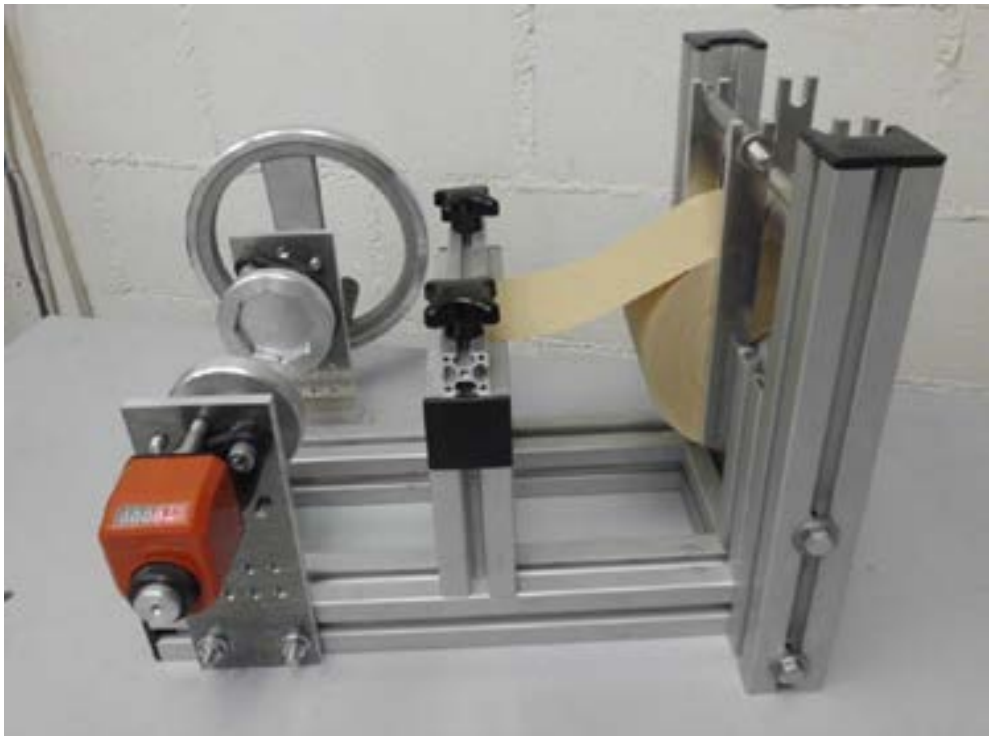

Figure 5.3. Winder machine deployed to prepare the solid insulation test-specimens

Figure 5.4. Cellulose test specimen and test cell

The drying and impregnation processes of the cellulose insulation was performed according to the method described in section 3.2 of Chapter 3.

Four pairs of test specimens were prepared by the impregnation process. Each pair was impregnated with MO, NF 0.2 g/L, NF 0.3 g/L or NF 0.4 g/L. One of the test specimens of each group was used to study the dielectric properties, and the other one was used as a control sample for moisture measurements.

The dielectric response of paper and oil insulation is strongly dependent on the moisture content of the materials [72]. Thus, in order to separate the effect of the moisture from that of the NPs, the initial moisture content of the samples included in the study was characterized using Karl Fischer titration [74]. As it can be seen in Table 5.1, all the samples had similar low moisture contents after the preparation process.

Table 5.1. Moisture content of oil and paper samples after the preparation process

Fluid	Impregnated paper	Oil
MO	1.1%	10.58 ppm
NF02	0.90%	11.62 ppm
NF03	0.89%	11.94 ppm
NF04	0.96%	12.7 ppm

To characterize the dielectric response of the cellulose test specimens they were fitted into a Teflon tank filled with oil or with NF (depending on the cellulose-impregnating fluid), so that the whole test object was immersed in oil as happens with the solid insulation in operating transformers 5.4. The aluminium core of the specimen was used as ground electrode during the measurements, and a second aluminium electrode was fastened to the external layer of the Kraft paper to be used as measuring electrode. The election of this electrode is motivated because of its fair conductivity and its capacitance to fit on the test specimens.

The measurements were done at temperatures 30, 45 and 60^o C. The test specimens were kept at constant temperature in an oven for at least 24 h prior to performing any dielectric response measurements.

5.2.2 Dielectric measurements setup

The dielectric response of the cellulose test specimens and the fluids under study was measured in the frequency domain using the dielectric response analyser Dirana (Omicron, Austria). The testing procedure is described below.

In all cases, the measurements were done under a controlled temperature, thus the test cells were placed inside of an oven as is explained below.

5.2.2.1 Solid insulation samples

The measurement protocol used to analyze the frequency response of solid-insulation samples applies a measuring voltage of 20 V and measures in a frequency range from 0.1 mHZ to 1 kHz. Although the test equipment is able to measure both in the time domain or in the frequency domain, all the measures were performed in frequency domain.

The Teflon cell containing the cellulose test specimen was placed in the oven, which was set at the test temperature for 24 hours for sample conditioning. Then, the set up of the Dirana tester was connected to the cell as shown in Fig. 5.5. The measuring configuration was Ungrounded Specimen Test (UST). The cell was kept in the oven during the FDS tests to ensure a constant temperature.

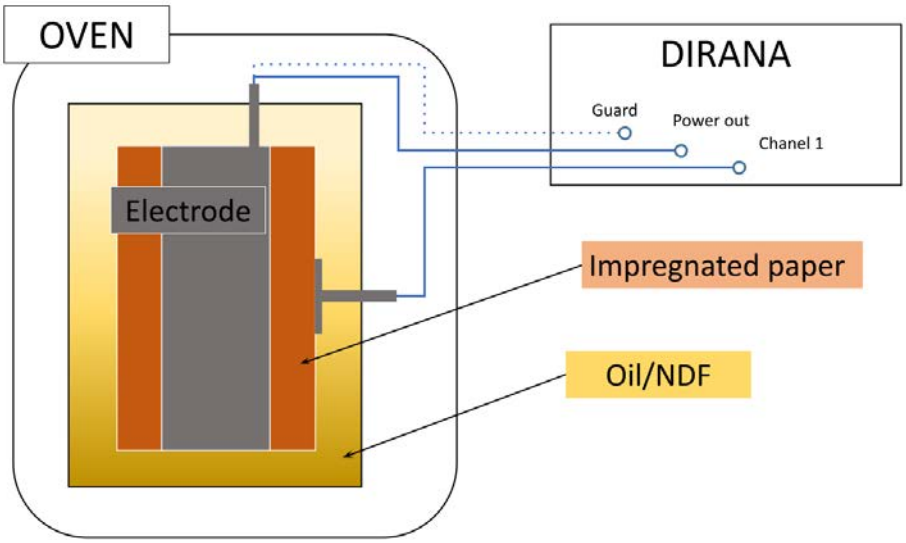

Figure 5.5. Measurement setup for the cellulose test specimens

5.2.2.2 Liquid insulation

The liquid insulation samples were placed in a vacuum oven Binder VD 53 at temperature 30^o C and vacuum of 1 mbar for 24 hours prior to the dielectric measurements. After the conditioning process the samples of the liquid were placed in the liquids' cell shown in Fig. 5.2, and were kept in the oven at the testing temperature for 24 h before performing the measurement.

As with the solid insulation, the measurements of the dielectric response of the fluids were performed using the Dirana FDS-PDC dielectric insulation analyzer. The measurement protocol used to analyze the liquid insulation samples uses a measuring voltage of 2 V and a frequency range from 1 mHz to 1 kHz. All measures were performed in the frequency domain.

5.3 Results and discussion

In this section the results of the FDS measurements that were carried out in all the tested materials are presented. First, the dielectric responses of the three prepared NFs are compared with that of the MO used as base liquid. A discussion is provided aiming at describing the physical processes that take place in those materials to justify the experimental observations. Then, the results obtained on NF-impregnated paper specimens are analyzed and compared with the recordings on MO-impregnated paper samples. Finally, the variation of the complex permittivity with temperature in analyzed.

5.3.1 Dielectric response of NFs at a reference temperature. Effect of NP concentration.

As explained before, the dielectric response of the MO and the NFs prepared with NP concentrations 0.2 g/L, 0.3 g/L and 0.4 g/L was measured in the frequency domain under constant temperature 30^o C. The results of the real and imaginary parts of the complex capacitance in those materials are shown in Figs. 5.6 and 5.7. These results are in agreement with the observations of Dai on SiO_2 based NFs [13].

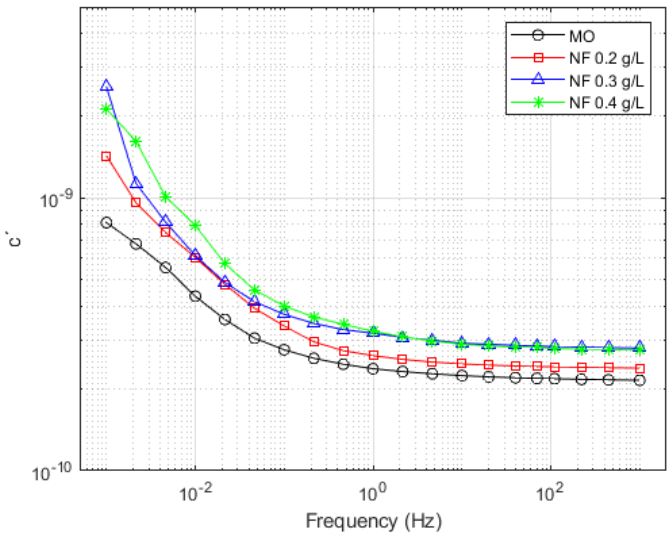

Figure 5.6. Real part of the complex capacitance of MO and NFs vs frequency.

Fig. 5.6 shows the real part of the complex capacitance for the base MO and the NFs with NP concentrations 0.2, 0.3 g/L and 0.4 g/L. It can be noted that the presence of NPs causes an increase on the values of the real part of the complex capacitance in the whole frequency range; the change is higher at lower frequencies.

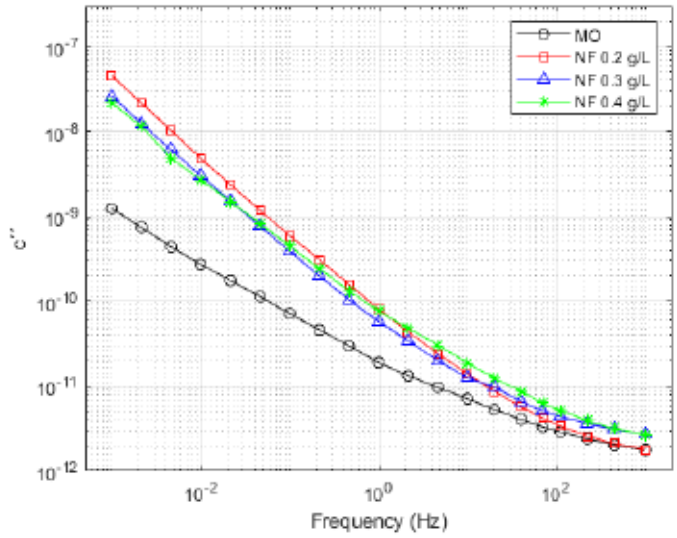

Figure 5.7. Imaginary part of the complex capacitance of MO and NFs vs vs frequency.

The measured dielectric constant (ε_r) of the three fluids is shown in Table 5.2. As it can be seen, there is an increase of more than 45% in the permittivity value; the increase is higher as the concentration of NP rises. The same pattern was reported by Du et al. in [30] for several temperatures and with different types of NPs and various NP concentrations.

Table 5.2. Dielectric constant (ε_r) of the MO and the NFs at 50 Hz

Pure MO	NF 0.2g/L	NF 0.3g/L	NF 0.4g/L
2.2	3.2	3.5	3.5

To understand the behaviour of C' (Fig. 5.6), it is important to remark that Fe_3O_4 NPs are polar compounds. Then, when a NFs is subjected to an electric field, a charge displacement takes place within the NPs that contributes to the overall polarization of the fluid. Because of this additional charge displacement, the capacitance values recorded for the NFs are higher that the ones measured in the MO. The polarization of conductive NPs is a fast event; the time constants associated to the phenomena are much shorter than the ones associated to atomic or molecular polarization in the oil. This explains the fact that the effect of NP on C' is equally noticeable in the whole frequency range.

Regarding imaginary part of the capacitance i.e. the dielectric losses of the fluids, which are displayed in Fig. 5.7, clear differences are observed between the measurements on the NF samples and those on the MO. The overall value of the dielectric losses is increased when adding NPs to the base MO, but the increase is specially noticeable at lower frequencies.

Apart from the polarization phenomenon that takes place in the NPs, the observed increase of the dielectric losses can be related with three different factors:

1. When conductive NPs are added to a base fluid, its conductivity increases significantly.

   In a previous work, the resistivity of several Fe_3O_4 based NFs was measured finding the behaviour shown in Fig. 5.8. As it can be seen, the resistivity of the MO was divided by 2.5 when 0.2 g/L of NP were added and by 8 when the concentration increased up to 0.35 g/L. As the resistivity of the NFs drops, the formation of ionic paths is more likely, what leads to an increase of the resistive losses. This effect is dominant at very low frequencies [72].

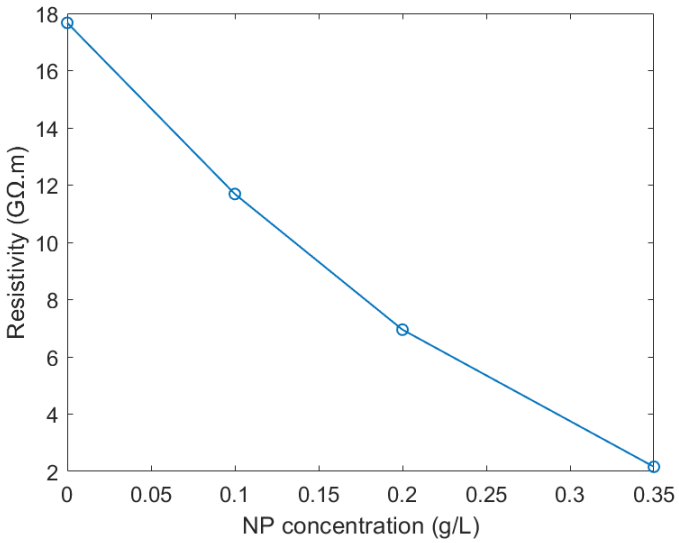

Figure 5.8. Resistivity of the MO and the NFs.

2. The addition of NPs increases the polarization losses caused by the interfacial polarization in the interfaces between the NPs and the base fluid.

   Since the electrical properties of the oil and the NPs differ greatly, an accumulation of change takes place in the interfaces between the two media when the material is subjected to an electric field. The formation of this structure of counter-ions, which is commonly referred to as the "electrical double layer" contributes to increase the dielectric losses of the material.
3. Swartz [75] described an additional mechanism that increases the dielectric losses of colloidal materials at low frequencies. As the polarization of the dielectric material progresses (i.e as the oil is polarized) there is a certain displacement of the counter-ion layer which is typically formed around the NPs when the NF is subjected to an electric field. The electrical double layer suffers a polarization in which the ions are not removed from the surface of the NPs, as this would require

larger amounts of energy to overcome the potential well, but they move within the surface of the NPs, deforming the double layer. Those movements lead to a further increase of the dielectric losses.

5.3.2 Dielectric response of NF-impregnated paper at a reference temperature. Effect of NP concentration.

Figs. 5.9 and 5.10 show the real and imaginary parts of the complex capacitance of cellulose specimens that were impregnated with MO and NFs prepared with NP concentrations 0.2, 0.3 and 0.4 g/L according to the process explained in Chapter 3.

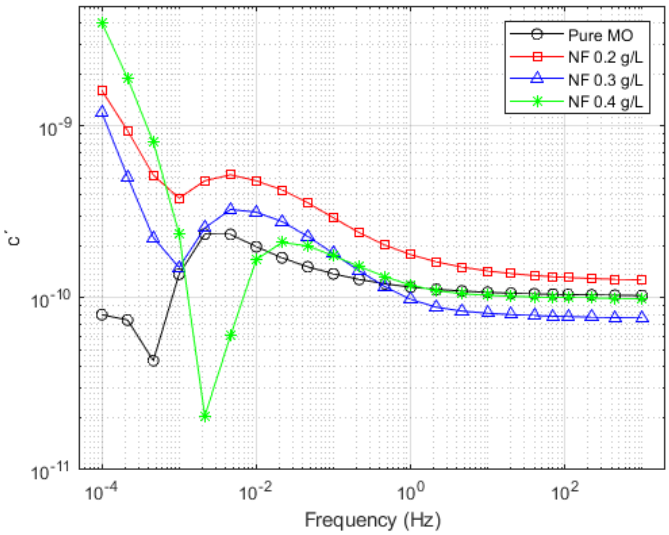

Figure 5.9. Real part of complex capacitance vs frequency for MO and NF impregnated paper.

As it can be seen, the impregnation of the cellulose with NFs has a significant impact on the dielectric response of the solid insulation. A shift towards higher frequencies can be observed for both components of the complex capacitance which increases with the concentration of NPs dispersed in the impregnating fluid. These type of relaxation peaks have also been observed on pressboard and paper samples impregnated with MO that contained high concentrations of moisture [72]. The shared polar character of water and NPs might justify the similarities between the pattern of the dielectric response of both types of specimens.

The FTIR and XPS tests presented in Chapter 4 evidenced the existence of bonds between the oxygen molecules of the cellulose and the Fe atoms of the NPs. The fact that bonds exist between the cellulose fibres and the NPs, and the limitation on the NPs mobility caused by those bonds has probably an impact on the dielectric response

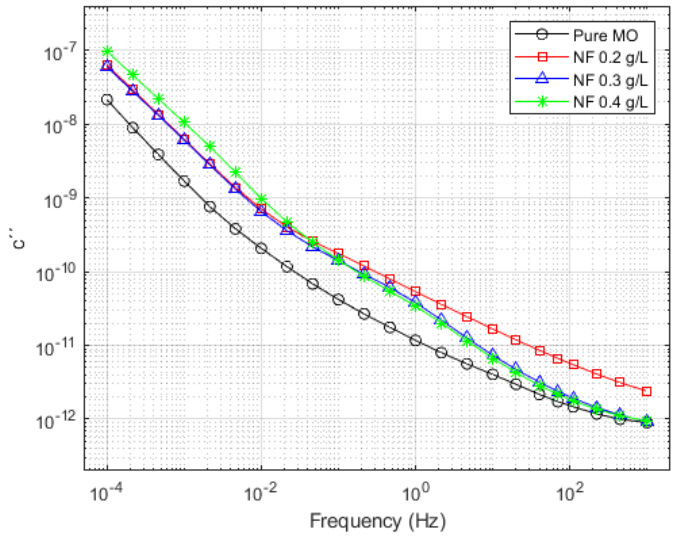

Figure 5.10. Imaginary part of complex capacitance vs frequency for MO and NF impregnated paper.

of NF-impregnated cellulose and may explain the different impact of the NPs in the response of the solid and liquid insulation.

Additionally, a change of slope appears in the dielectric losses of the three NF-impregnated specimens which indicates that an additional relaxation process appears in those specimens. The change of slope is more noticeable for the specimens impregnated with NP of concentrations 0.3 and 0.4 g/L.

The dielectric constants of the cellulose specimens are shown in Table 5.3. The value of this parameter shows a great variability as the impregnation liquid changes and do not follow a consistent tendency. A significant increase is observed for the cellulose specimens impregnated with NFs with low concentration of NPs (0.2 g/L); however the measured relative permittivity drops for the samples impregnated with liquids with higher concentrations of NPs reaching values closer to those of the oils in the case of the NF 0.3 g/L and similar to those of the MO-impregnated cellulose for the NF 0.4 g/L.

Table 5.3. Dielectric constant (ε_r) of the cellulose impregnated with MO or NFs at 50 Hz

Impregnation liquid			
MO	NF 0.2g/L	NF 0.3g/L	NF 0.4g/L
3.9	4.9	2.9	3.9

More research would be needed to explain the recorded behaviour, but the observations are probably related with the relative influence of two phenomena that occur simultaneously in the NP-cellulose composites. As was explained in Section 5.3.1, the NPs are polar compounds and they polarize in presence of an electric field; this would

contribute to increasing the capacitance and the relative permittivity of the material. However, the polarized NPs cause a distortion of the electrical field that can give rise to a decrease of other polarization processes in the cellulose, what would diminish the measured capacitance. It is likely that the first effect predominates when the NPs' content is low, but as the concentration increases the second gains more importance.

5.3.3 Influence of temperature on the dielectric response of NF-impregnated cellulose

The FDS tests on MO-impregnated and NF-impregnated paper were repeated at several temperatures to analyse the effect of temperature on the dielectric response of these type of materials.

The measurements were carried out under controlled temperature at 30, 45, and 60^o C. To this aim the test cells were placed inside of an oven and connected to the measuring system as is shown in Fig. 5.5.

Figs. 5.11 and 5.12 present the results of the imaginary part (i.e. dielectric losses) and the real part (i.e. capacitance) of the complex capacitance obtained for the MO-Kraft paper system at three temperatures. It is well known that, as temperature increases, the values of the complex capacitance are shifted towards higher frequency values [72]. The displacement of the imaginary and the real part of the complex capacitance is clear for the MO-impregnated cellulose insulation.

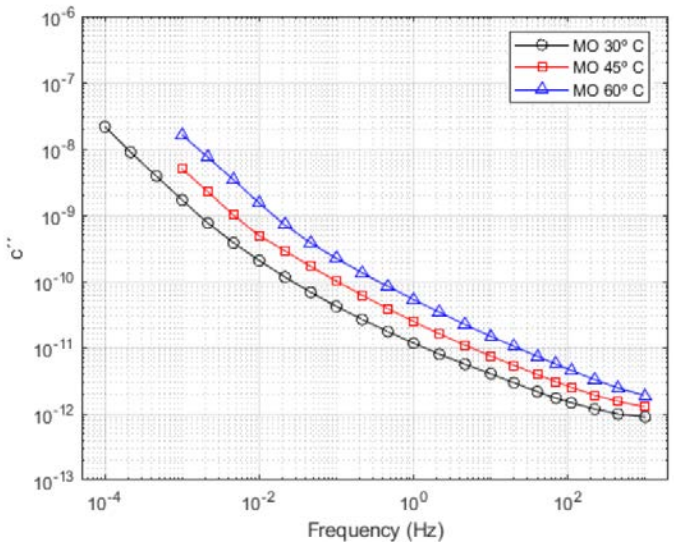

Figure 5.11. Imaginary part of the complex capacitance of MO impregnated paper vs frequency for several temperatures

Figs. 5.13 and 5.14 show the results of the FDS measurements performed on the paper specimens impregnated with NF for a NP's concentration of 0.2 g/L at the three

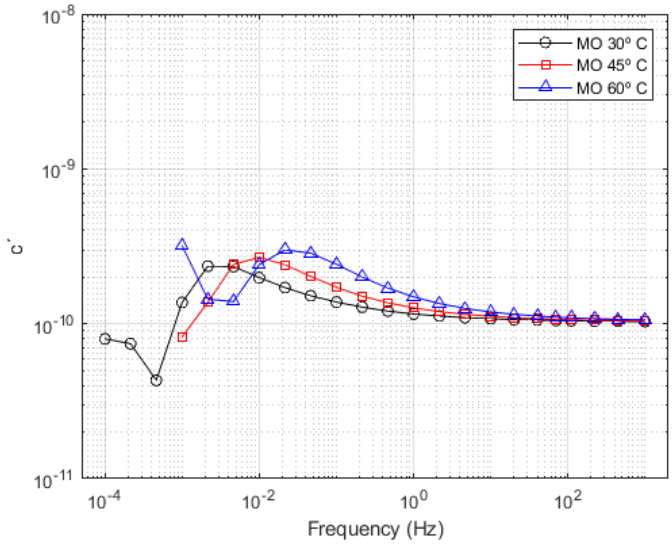

Figure 5.12. Real part of the complex capacitance of MO impregnated paper vs frequency for several temperatures

analysed temperatures. The results in the NF-paper systems are similar to those presented for the MO-impregnated paper. The NF-impregnated specimens seem to evolve similarly to MO-impregnated ones as temperature rises. However, the magnitude of the displacement in frequency changes. At first sight it is easy to note a greater displacement in the curves for the NF-impregnated specimens for both dielectric losses and capacitance. These differences could be relevant for the use of the NFs for transformer insulation.

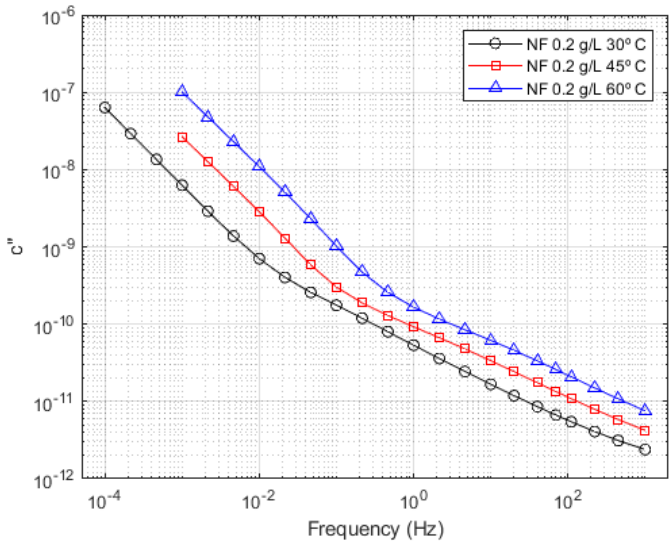

Figure 5.13. Imaginary part of the complex capacitance of NF -impregnated paper (NP concentration 0.2 g/L) vs frequency for several temperatures

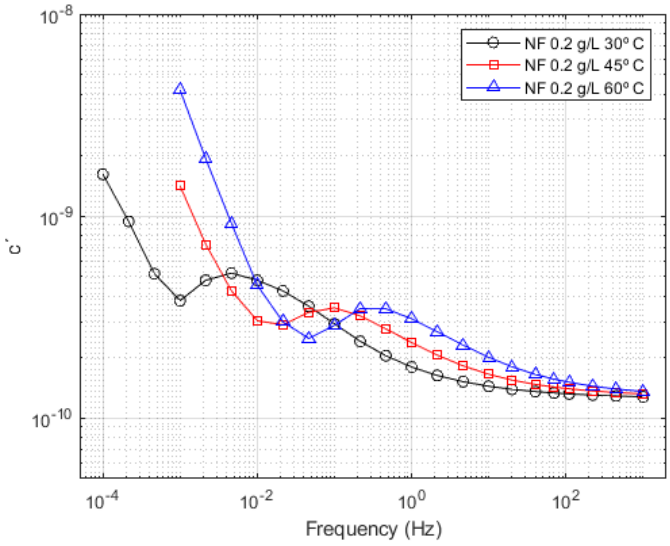

Figure 5.14. Real part of the complex capacitance of NF-impregnated paper (NP concentration 0.2 g/L) vs frequency for several temperatures

Figs. 5.15 and 5.16 show the results of the FDS measurements performed on cellulose samples impregnated with a NF with NP concentration of 0.3 g/L for the three analysed temperatures. As in the previous case, the shape of the dielectric response remains unchanged when temperature rises, but the curves are shifted towards higher frequencies. The behaviour of the paper specimens impregnated with NF with NP concentration 0.3 g/L is not very different to the one with NF of 0.2 g/L. The dielectric loses curves present almost the same shape as the previously observed for the NF 0.2 g/L impregnated test specimens.

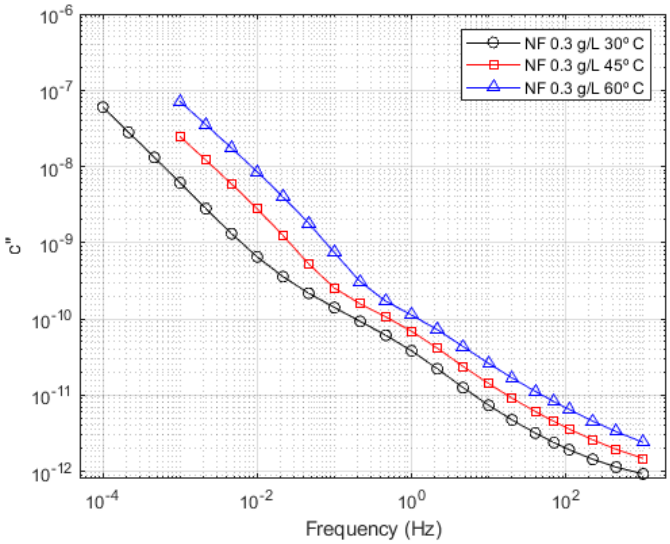

Figure 5.15. Imaginary part of the complex capacitance of NF-impregnated paper (NP concentration 0.3 g/L) vs frequency for several temperatures.

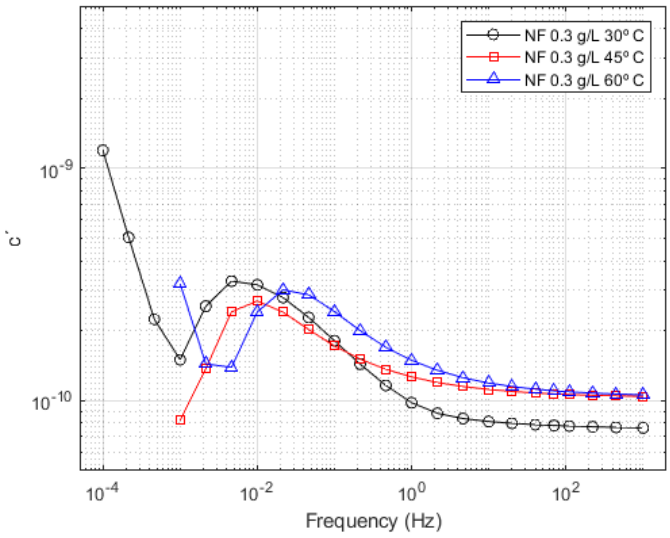

Figure 5.16. Real part of the complex capacitance of NF -impregnated (NP concentration 0.3 g/L) paper vs frequency for several temperatures

The NF-impregnated systems present a different evolution with the temperature rising due to the presence of NPs. As explained before, the polar character of the Fe_3O_4 NPs enhances the impact of the electric field. This fact is also affected by the increase of temperature that makes easier for the colloidal NPs to move inside the insulation system. As result of that effect, the charged NPs are able to move more in the NF-based specimens, making the NF impregnated specimens evolve differently with temperature.

This fact can be confirmed by studying the magnitude of the frequency shift that is observed in the three types of oil-paper insulation systems when the temperature changes. The shift of the dielectric response curves versus temperature can be expressed as an Arrhenius factor [73] according to equation 5.10. The frequency shift that can be derived from experimental curves can be used to calculate the activation energy (Ea) of the MO and NF-impregnated cellulose.

$$shift = log(\omega_1) - log(\omega_2) = -\frac{E_a}{k \cdot 2.3258} \cdot (\frac{1}{T_2} - \frac{1}{T_1}) \tag{5.10}$$

The frequency shift of the three types of specimens was determined for the three temperatures of analysis. The calculation was based on displacing horizontally the curves obtained for the imaginary part of the capacitance at temperatures 45 and 60^o C until they overlap with the 30^o C curve [72]. The shifts obtained for the three types of cellulose insulation are plotted versus the inverse of temperature in Fig. 5.17. The values of the activation energies can be obtained as the slope of the regression curves, according to eq. (5.10).

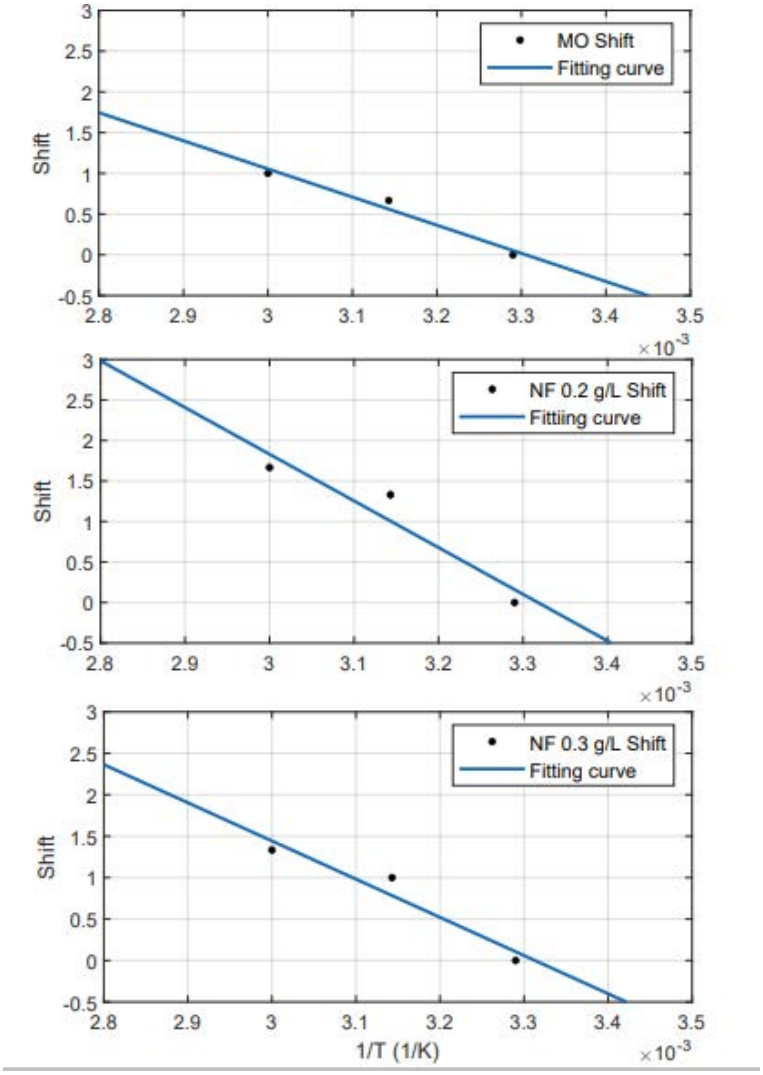

Figure 5.17. Temperature shift for the different types of samples

A value for the slope of eq. (5.10) is obtained with a linear regression and used to calculate the activation energy of the dielectric loss for the three different insulation systems. The results are presented in Table 5.4. Cigré [72] reported values of activation energy for MO-pressboard of 1.07 eV, which is in agreement with the calculation.

Table 5.4. Calculated activation energies

Fluid	Activation energy (eV)
MO	1.154
NF02	0.923
NF03	0.691

Observing the results of the calculated activation energies, it is possible to get insight into how the NPs affect the dielectric behaviour of the materials when temperature changes. The NPs interact with the dielectric liquid and the solid insulation [76].

This interaction is reflected in a change in the mobility of the NP and that changes the activation energy of the system. NF-impregnated paper have a lower activation energy than MO-impregnated paper. As result of an increase of temperature the mobility of the NPs in the oil increases. Combining this effect with the higher polarization that occurs in the NF results in a decrease on the values of activation energy in samples containing NPs.

5.4 Conclusions

The dielectric response of NFs and NF-impregnated solid insulation is investigated in this chapter observing that the presence of NP has an important impact on the permittivity and the dielectric losses of liquid and solid insulation.

The relative permittivity varies when NPs are added to both materials; for the oil, the permittivity increases consistently as the concentration of NPs rises. In the case of paper, the permittivity increases for low concentrations of NPs, but drops a little as the NP concentration is larger. This is due to the fact that two physical phenomena coexists in the dielectric: the polarization of the NPs attached to the cellulose chains, and the distortion of the electrical field in the solid caused by the presence of polarized NPs. It will be important to analyse the dielectric response of cellulose materials when those are impregnated with NFs based in semiconductive or insulating NPs in the future.

A variation of the relative permittivity also occurs when the temperature changes. The observed changes can be quantified by the change in activation energy of the solid insulation. As the concentration of NPs grows the activation energy tend to descend making easier the relaxation processes in the insulation system.

Chapter 6

Dielectric strength

In the present chapter, the dielectric strength of cellulose insulation is investigated, comparing its behaviour when it is impregnated with transformer MO and when it is impregnated with a dielectric NF. As it was explained in Chapter 2, most authors focused their studies on the oil-cellulose interfaces. In this chapter the study of the direct breakdown voltage of NF-impregnated paper is carried out. The breakdown voltage of Kraft paper samples impregnated with a Fe_3O_4-based NF was tested under AC voltages at power frequency and under lighting impulse. The tests were repeated with samples impregnated with MO to study the impact of the NP on the BDV values.

6.1 Sample preparation

Kraft-paper sheets were cut into squares of dimension 8 x 8 cm. The samples were subjected to drying under vacuum at 60^o C for 24 hours. After that, some of the samples were impregnated with MO and some others with NF.

The NFs was prepared by mixing the base MO (Nynas Nytro) with the Fe_3O_4 dispersion to a concentration of NPs 0.2 g/L. This concentration value was chosen because in previous studies the NFs with that concentration of NPs showed the highest AC BDV values, while for higher concentrations the AC BDV of the liquid decreased. Fig. 6.1 shows some of the tested samples.

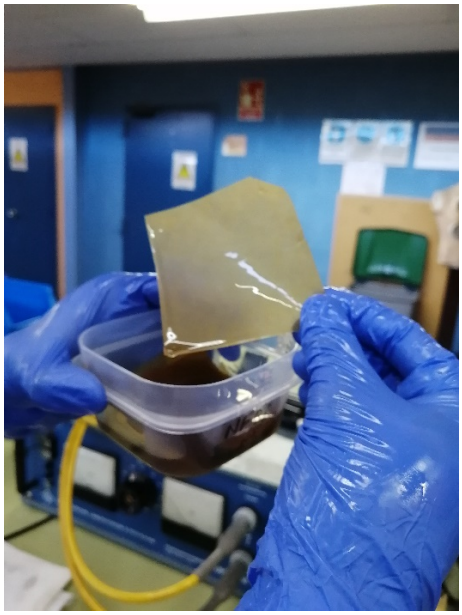

Figure 6.1. Samples tested in the AC and impulse BDV tests

6.2 AC breakdown voltage tests

6.2.1 AC Breakdown voltage test setup

The MO-impregnated and NF-impregnated samples were tested under AC voltages (50 Hz). The tests were carried out in an accredited laboratory according to Standard IEC 60243-1 [77]. The cell shown in Fig. 6.2 was used during the tests. The cell is made of a plastic material and has the shape of a cube with dimensions 20x20x20 cm. The electrode system was parallel-plate with unequal electrodes; stainless steel cylindrical electrodes of diameter 25 and 75 mm were used.

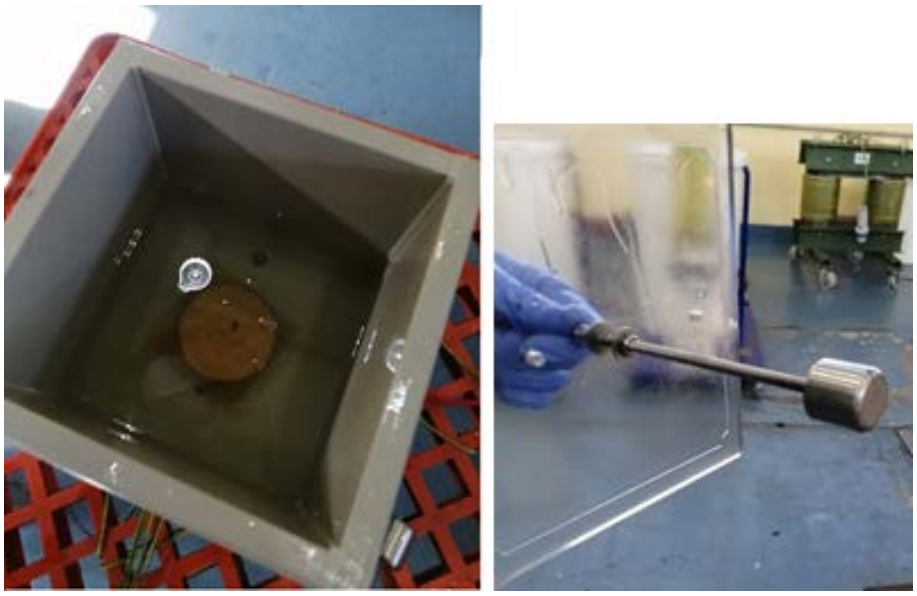

Figure 6.2. Test cell used in the study

The measuring process is described next: A sample is retired from its storage and it is placed between the electrodes of the test cell. The test-cell is filled with the dielectric fluid until the electrodes are fully covered. The bottom electrode is grounded and AC voltage is applied to the top electrode (Fig. 6.3). The testing voltage is supplied by a step up transformer (Fig. 6.4). Voltage is increased according to the specification of a rapid-rise test, i.e. applied voltage rises from zero at a rate of 1500 V/s until breakdown occurs. After breakdown, the paper sample is removed from the cell and 4 thickness measurements are made. The AC BDV (kV/mm) of each specimen is obtained as the ratio between the voltage at breakdown and the average thickness of the sample. Then, a new sample is placed in the cell and the procedure is repeated. To determine the AC BDV of each material, nine NF-impregnated samples and nine MO-impregnated samples were tested.

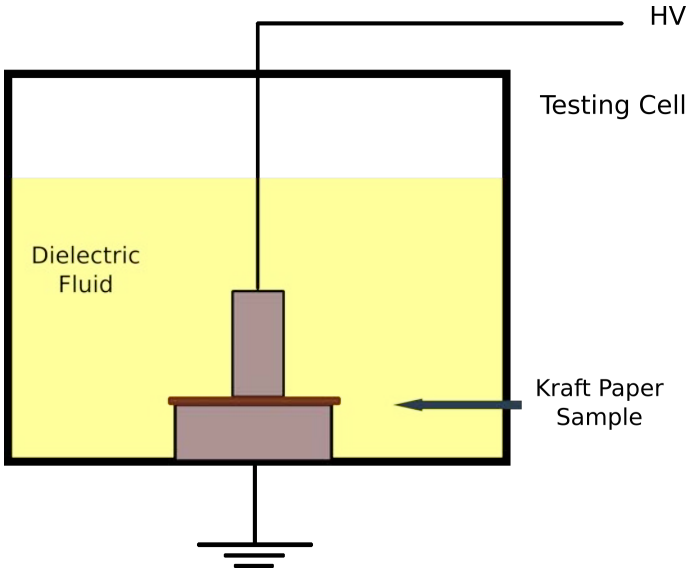

Figure 6.3. Test cell with Kraft-paper specimens surrounded by oil

Figure 6.4. Step up transformer and test cell for the AC BDV tests

6.2.2 Results of AC BDV tests

Fig. 6.5 shows the results of the AC BDV tests performed on NF-impregnated and MO-impregnated specimens displayed as a growing sequence. As it can be seen, the tests on NF-impregnated samples present higher BDV values and less dispersion. The mean values obtained for the two types of samples are 75.3 ± 0.7 kV/mm for the NF-

impregnated samples and 59.8 ± 0.4 kV/mm for those impregnated with MO, which supposes an improvement of the AC BDV of 26 %. The standard deviation of the measurements decreases from 11.24, for the MO-impregnated samples, to 5.47 for the NF-impregnated ones.

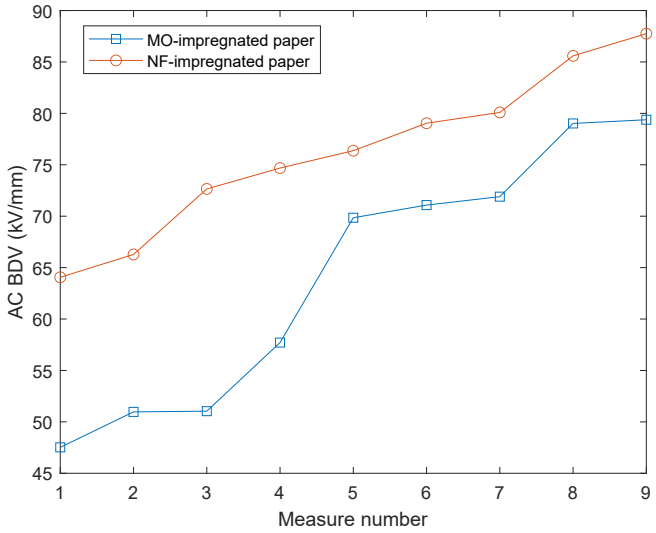

Figure 6.5. AC BDV measurements on MO-impregnated paper and NF-impregnated paper

The experimental data were fitted to a Weibull distribution eq. (6.1), which provides the failure probability associated to a certain voltage level.

$$P(V) = 1 - e^{(\frac{V}{a})^b} \tag{6.1}$$

where P(V) is the failure probability of an specimen when subjected to voltage V, a is the scale parameter (which shows the BDV at failure probability 63%) and b is the shape parameter (inversely related with the scattering of the data).

The parameters obtained for each material are shown in Table 6.1. As can be observed the values of the parameters confirm the statistical results. The shape parameter (a) reveals an increase in the dielectric strength of the NF-impregnated samples compared to those impregnated with MO. Also the shape parameter (b) confirms that the measures are less scattered when NF is used as impregnation fluid.

Table 6.1. Weibull parameters for the AC BDV tests.

Weibull parameters	MO-impregnated paper	NF-impregnated paper
a (kV/mm)	69.2	79.7
b	6.5	11.7

The plotting of the Weibull distribution obtained for the NF and MO-impregnated test specimens is shown in Fig. 6.6.

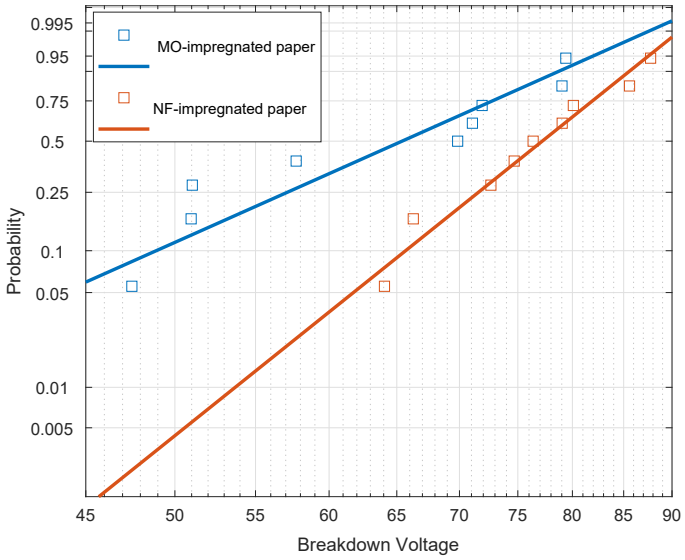

Figure 6.6. Weibull distribution of the AC BDV measures on NF-impregnated paper and MO-impregnated paper

As it can be seen, the failure probability of both materials at a certain voltage is quite different. For the MO-impregnated specimens. The lower quartile of the samples has a BDV between 45 and 55 kV/mm, while in the NF test specimens only 1% has a breakdown voltage in that range. For any value of the applied voltage, the probability of failure in the MO-impregnated paper is greater than the probability of failure in the NF-impregnated paper, although as the applied voltage increases the difference between the AC BDV of the samples impregnated with each of the fluids tend to decrease. The main values obtained from the Weibull distribution are shown in Table 6.2.

Table 6.2. Statistic analysis of the AC BDV tests for both types of specimens

AC BDV	MO-impregnated paper	NF-impregnated paper
Mean (kV/mm)	59,8	75.3
Std dv	11.24	5.47
Fail prob 5% (kV/mm)	43.8	61.7
Fail prob 25% (kV/mm)	57.1	71.6
Fail prob 50% (kV/mm)	65.4	77.2
Fail prob 90% (kV/mm)	78.7	85.6

6.2.3 Discussion on the AC BDV tests

It has been shown that the AC BDV of cellulose specimens increases by 26% when Fe_3O_4 NPs are added to the impregnation liquid.

The observed improvement might be partially due to the enhancement of the dielectric properties of the MO when the NPs are added. In a previous work [78] the dielectric properties of the NF used for the impregnation of part of the samples of the present study were obtained. The measures revealed that the AC BDV of the Fe_3O_4 based NF with NP concentration 0.2 g/L was 10% higher than the AC BDV of the MO (i.e. 95.21 kV vs. 87.02 kV).

Additionally, a significant change in the permittivities of the insulating fluid and the impregnated cellulose was observed in Chapter 5 depending on whether the impregnation fluid was MO or NF. In the case of the liquids, the permittivity changed from 2.2, for MO, to 3.2, for NF. While for the MO-impregnated and NF-impregnated paper the permittivity changed from 3.9 to 4.9 as showed in Table 5.2. The change on permittivities will lead to a variation of the electric field distribution within the test cell, what can be a factor of influence in the enhancement of the AC BDV of NF-impregnated paper.

In order to better understand the impact of the permittivity change in the AC BDV tests, a finite element study was performed using COMSOL Multiphysics. An axisymmetric 2D model was built considering the geometry of the test cell and the electrodes and the permittivity of the materials. The simulation was repeated considering the relative permittivities obtained experimentally for each combination of materials (i.e. MO and MO-impregnated paper vs. NF and NF-impregnated paper). The permittivities considered for the simulations are shown in Table 6.3.

The testing voltage considered for both simulations was 5.5 kV, which is the average testing voltage at which the breakdown of MO-impregnated paper samples takes place. The same voltage was considered for the NF-impregnated samples, aiming at comparing the effect in the same testing conditions of the two combinations of materials.

Figs. 6.7 and 6.8 compare the results of the finite element simulations for the MO and the MO-impregnated paper specimen (Fig. 6.7) and for the NF and NF-impregnated paper specimens (Fig. 6.8). Both figures show the electric potential lines in the cell and the electric field in the region of maximum stress.

In the MO-impregnated samples, the lines of potential converge in the limit between the top electrode and the paper (Fig. 6.7). This is also the region that withstands the maximum electric field, as can be observed in the detail provided at the bottom of the figure. In particular, the most stressed area of the whole cell is the volume of oil in that region. It is also interesting to see that there is a big gradient of electric field between the oil and the paper.

The NF-impregnated samples present a similar distribution of electric potential lines than the MO-impregnated samples (Fig. 6.8), and the difference between the two cases is not noticeable at first sight. However, the representation of the electric field

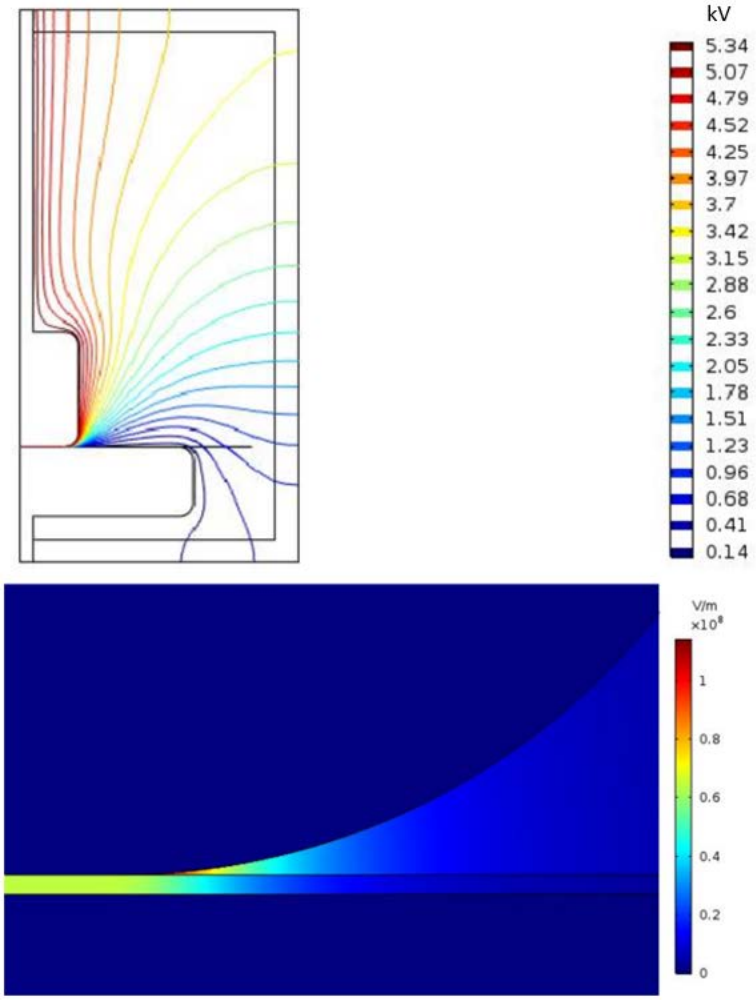

Figure 6.7. Finite element simulation of the test cell for the MO-impregnated paper immersed in MO

at the bottom image reveals differences in the distribution of the electric field when compared with Fig. 6.7. For the case of NF-impregnated samples the electric field is lower in the point of contact of the upper electrode and the paper sample. Additionally, the electric field is less concentrated in that point and the field gradient between oil and paper is significantly smaller than in the previous case.

The value of the maximum electric field (E) in the oil and in the paper obtained for each simulation are shown in Table 6.3. As can be seen, the value of the maximum electric field in the paper samples for both combinations of materials is almost the same in the two cases, but the maximum electric field in the liquid is a 15% lower in the case of the NF and NF-impregnated paper specimens. Additionally, the maximum electric field in the NF-impregnated paper immersed in NF was recalculated for an applied voltage of 6.4 kV, which is the average voltage at which breakdown takes place in this combination of materials. The simulation calculated that the maximum electric

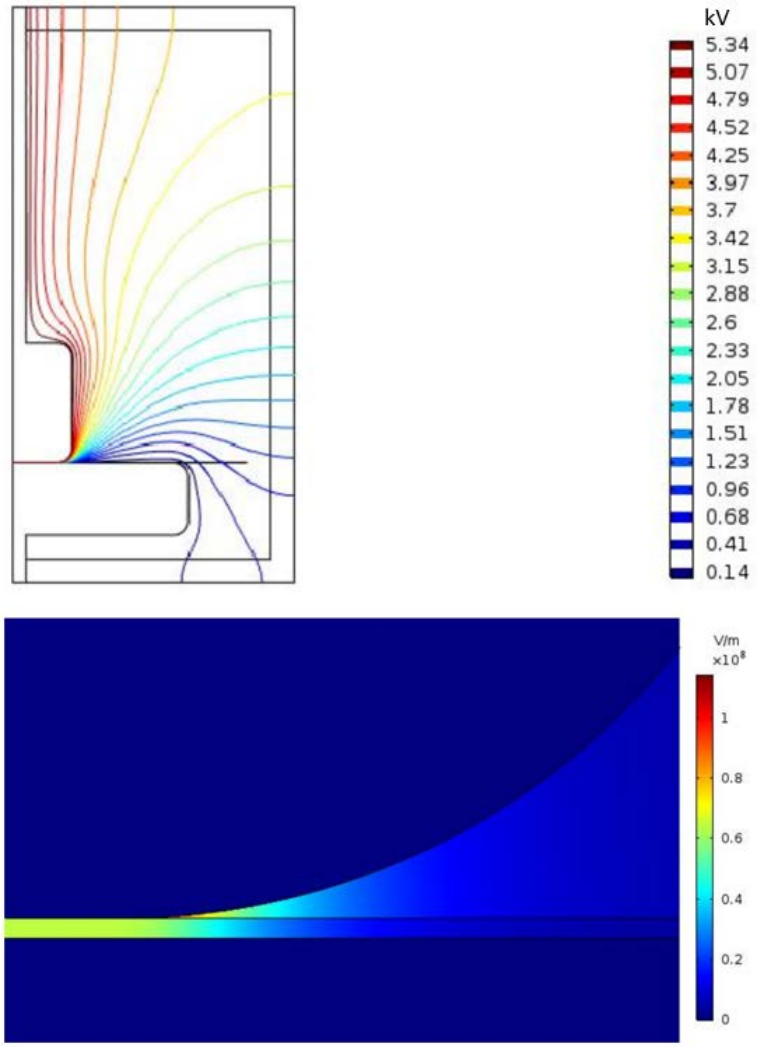

Figure 6.8. Finite element simulation of the test cell for the NF-impregnated paper immersed in NF

field for the oil was 116.35 kV/mm while the maximum field for the paper was 75.99 kV/mm.

Table 6.3. Maximum electric field in paper and oil for a testing voltage of 5.5 kV

	Kraft paper-MO		Kraft paper-NF	
	Oil	Paper	Oil	Paper
Relative permittivity	2.2	3.9	3.2	4.9
Maximum E (kV/mm)	114.42	64.95	99.30	64.86

The simulation results suggest that the breakdown process starts in the fluid. The ionization of the fluid would start in the region of maximum stress and the streamer progresses through the fluid until it reaches the paper and causes its perforation.

This mechanism is in agreement with the visual inspection of the samples. Fig. 6.9 shows an image of two of the paper samples after the breakdown test. The breakdown

point and the mark of the upper electrode on the paper surface can be appreciated in the upper image; the breakdown point and the shape of the upper electrode have been highlighted at the bottom figure for better identification. As it can be seen, the breakdown point is located at the limit of the upper electrode which, according to the simulations, is the region where the maximum electric field is obtained. The same situation was observed in most of the tested samples, since they showed perforation at the edge of the top electrode.

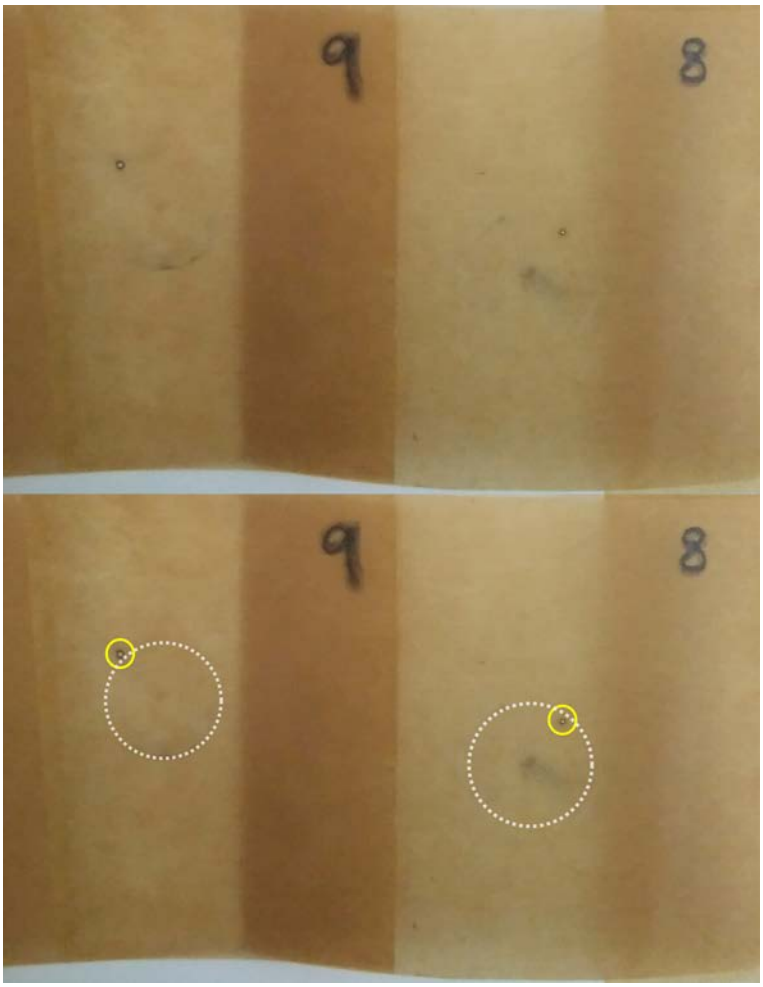

Figure 6.9. Image of two samples after the breakdown

The conclusion of the previous analysis is that the improvement of the AC BDV observed in the NF-impregnated samples is mainly due to two phenomena:

1. The decrease in the maximum electric field in the fluid, caused by the change in the permittivity of the materials, reduces the probability of streamer inception. Note that the maximum electric field in the NF was a 15% smaller than the maximum field in the most stressed area of the MO.
2. The presence of NPs in the NF hinders the streamer progression in it. This phenomenon was studied by several authors attributing it to the accumulation of

charges around the NPs [79] and to the reduction of the streamer speed by the trapping and de-trapping of charges in shallow traps that increases sharply when MO is doped with NPs [80]. The improvement of the AC BDV of the NF used in this work is a 10 % according to previous works of the authors. [78].

6.3 Lightning impulse tests

6.3.1 Testing procedure

In order to complete the analysis of the dielectric performance of the NF-impregnated paper, MO and NF-impregnated paper samples were tested under positive lightning impulse (1.2/50 μs). Positive impulse tests were chosen since they pose a higher risk for the insulation, and also because greater improvements were reported for the positive impulse BDV of oils when NPs were added to it [81].

Impulse tests were carried out using the same test cell and electrodes described in the previous section and shown in Fig. 6.2.

The tests were performed in accordance with IEC 60243-3 [82] using an impulse generator Haefely Type P35 and an oscilloscope Tektronix TDS 744A. The testing procedure is described next: a paper sample is located between the electrodes of the test cell, which is filled with the insulating fluid. A first impulse is applied with peak voltage value 70% of the expected breakdown value. In this case, the initial impulses were of value 7 kV. If no breakdown takes place, two more impulses of the same voltage are applied. After applying three impulses without breakdown, the voltage is raised in steps of 1 kV and three new impulses are applied until the breakdown happens. After a breakdown occurs, the sample is extracted from the cell and three thickness measurements are carried out. The impulse strength of the sample is obtained as the ratio between the voltage at which the breakdown occurred and the average thickness of the sample. Finally, a fresh sample is placed in the testing cell and the same measuring sequence is repeated. For the lightning impulse study eight MO-impregnated paper samples and six NF-impregnated samples were tested.

6.3.2 Impulse BDV results

Tables 6.4 and 6.5 present the total number of impulses applied on each type of sample and the number of breakdowns recorded for each voltage level. As can be seen, all the samples withstood the impulses with a voltage lower than 8 kV. For testing voltages above 9 kV, a variable number of breakdowns occurred in both types of samples. The average values of the impulse strength of MO-impregnated paper immersed in MO was

121.8 ± 0.8 kV/mm, and the impulse BDV of NF-impregnated paper immersed in NF was 124.1 ± 0.8 kV/mm.

Table 6.4. Impulse test applied with and without breakdown for MO-impregnated samples

Voltage (kV)	Impulses applied	Number of breakdowns
7	3	0
8	15	0
9	18	2
10	11	3
11	8	1
12	1	1

Table 6.5. Impulse test applied with and without breakdown for NF-impregnated samples

Voltage (kV)	Impulses applied	Number of breakdowns
7	3	0
8	18	0
9	12	1
10	6	3
11	3	1
12	1	1

Fig 6.10 shows the probability of breakdown for each voltage level for the MO-impregnated and the NF-impregnated samples. It can be seen that for both impregnation fluids the probability of breakdown is zero for voltages 7 and 8 kV. For higher voltage levels, the probability of both fluids is quite similar and for voltage 12 kV the probability of breakdown is 100% for the two types of samples.

As in the previous study, the experimental data were fitted to a Weibull distribution. The parameters of the Weibull fitting for the impulse test data are shown in Table 6.6; it can be noted that the scale parameter is about 2 kV/mm higher for NF-impregnated samples, and the shape parameter is almost equal for both cases. The representation of the Weibull distribution for both materials, shown in Fig. 6.11, also reveals a very similar behaviour for both kinds of samples.

Table 6.6. Weibull parameters for the impulse BDV of MO-impregnated and NF-impregnated paper

Weibull parameters	MO-impregnated paper	NF-impregnated paper
a (kV/mm)	127.9	129.8
b	10.3	10.2

The main values obtained from the Weibull distribution for the impulse test are summarized in Table 6.7. The analysis reveals a small improvement of the dielectric

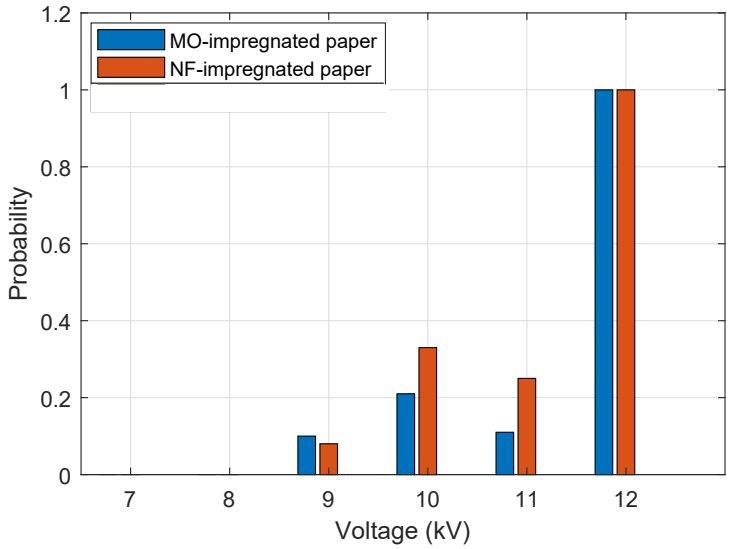

Figure 6.10. Probability of breakdown in impulse tests

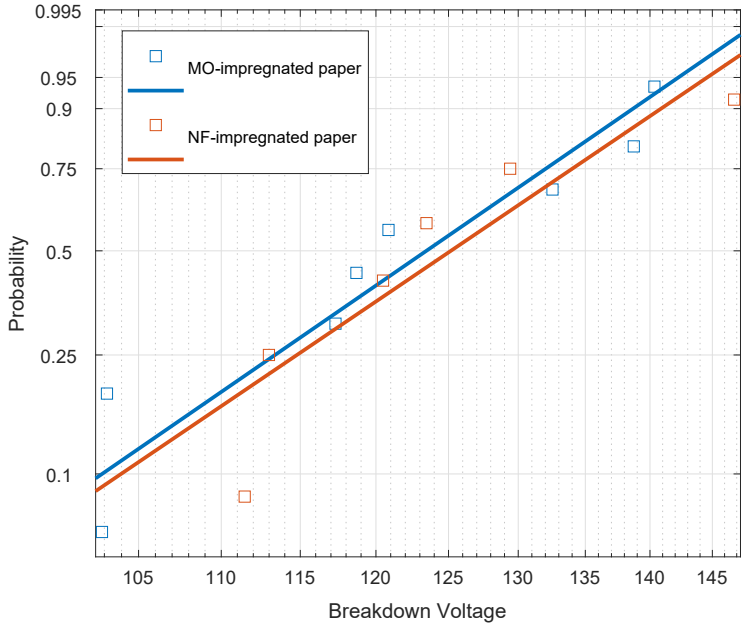

Figure 6.11. Weibull distribution of the impulse measures on NF-impregnated paper and MO-impregnated paper

strength of the NF impregnated samples under positive lighting impulse. The mean value of the impulse strength for the NF-impregnated samples is only a 2% higher than that of the MO-impregnated samples. The values for the different failure probabilities of both liquids are also very similar.

Table 6.7. Main values obtained from the Weibull fit of the results of the impulse BDV tests for both types of specimens

Impulse strength	MO-impregnated paper	NF-impregnated paper
Mean (kV/mm)	121.8	124.1
Std dv (kV/mm)	7.45	8
Fail prob 5% (kV/mm)	95.9	96.8
Fail prob 25% (kV/mm)	113.4	114.8
Fail prob 50% (kV/mm)	123.4	125.2
Fail prob 90% (kV/mm)	138.7	140.9

6.3.3 Discussion on the lighting impulse tests

Although the NF-impregnated papers present a slightly higher impulse BDV than the MO-impregnated samples, the difference is much lower than for the AC BDV tests.

In a previous work [81] the same NF used for this test was subjected to impulse tests, considering different NP-concentrations. The results obtained for positive impulses are shown in Table 6.8. It can be seen that, although for higher NP concentrations the impulse BDV improves significantly, the effect of the presence of NP in the oil with a NP concentration of 0.2 g/L on the impulse BDV is almost negligible. The same tendency was observed by other authors [83].

Table 6.8. BDV obtained for positive lightning impulse for MO and two NFs with different Fe_3O_4 concentrations

	MO	NF 0.2 g/L	NF 0.6 g/L
Impulse BDV (kV)	34.37	35.7	51.46

The effect of the change in the permittivity of the materials on the electric field distribution is not easy to evaluate by simulation in this case. However, an additional round of impulse measurements was carried out in which the test cell was filled with MO and the test specimens were paper samples impregnated with NF. The average impulse BDV in this case was 123.9 $\pm$ 1 kV/mm, which is between the results of the two types of samples analysed.

6.4 Conclusions

In the present chapter an experimental study of AC and impulse BDV of NF-impregnated Kraft paper has been carried out.

The tests carried out showed an improvement of 26% on the AC BDV values of the NF-impregnated samples. The improvement may be due to the effect of the NPs on the dielectric performance of the fluid and also to the modification of the electric field

distribution within the oil and paper insulation that is caused by the variation of the permittivities of the liquid and solid insulation when NPs are present.

The improvement is less noticeable for the impulse tests and the values of the average impulse BDV of NF-impregnated samples are only 2% higher than that of MO-impregnated specimens. More research is needed to determine if higher concentrations of NPs could lead to higher values of the impulse BDV of NF-impregnated cellulose insulation.

Chapter 7

Thermal ageing.

One of the aspects that might be clarified before NFs might be considered for transformer insulation is to understand the impact of the NPs in the ageing processes of cellulose insulation.

Transformer's life expectancy is linked to the life of its solid insulation. Several degradation reactions take place in the solid insulation during transformer operation which rate mainly depends on the operation temperature but also on the moisture content of the insulation system and on the presence of oxygen. Paper degradation derives into a worsening of its mechanical properties becoming more brittle and being more likely to be broken.

This chapter studies the aging process of cellulose impregnated with a NE-based NF and compares it with the process that takes place when the impregnation liquid is a NE.

7.1 Experimental procedure

The main objective of the experimental study was to evaluate the effect of the NPs on the aging process of paper-impregnated insulation. Two kinds of samples were subjected to accelerated aging tests and further investigation: samples composed of Kraft paper impregnated and immersed in an NE, and samples of Kraft paper impregnated and immersed in an NF with the same NE as base fluid. The reasons for using these materials was explained in Section 3.1.3 and was related with guaranteeing the long-term stability of the NFs at high temperatures.

7.1.1 Preparation of the samples

The commercial NE Bioelectra was used as the base fluid to prepare the NF characterized in this chapter. The same liquid was used to prepare the control samples that were used to compare results with those of NF-based samples. The preparation method of the NF was described in Section 3.1.3.

The aging vessels were crystal vials of volume 100 mL with silicone septa.

In order to allow a statistical analysis of the results obtained and to guarantee a sufficient quantity of samples to perform the tests, five strips of Kraft paper with a total mass of 0.03 g were introduced in each vial, as can be seen in Fig. 7.1.

The vials with the paper samples were dried in two stages: firstly they remained under vacuum at 60^o C for 48 h, then, the temperature was raised to 80^o C for 2 h.

The NE and the NF were also preconditioned before filling the testing vials. The process of fluid drying was also performed in a vacuum oven, keeping the fluids at 60^o C for 48 h.

Figure 7.1. NF and NE aging test vials.

Once the paper and the two fluids were conditioned, the aging vials were filled with NE or NF and sealed with silicone septa. Then, the vials were kept at room temperature for 2 days to allow the samples to stabilize. After the stabilization process, the vials were treated by bubbling nitrogen in the NE or NF for 5 min (Fig. 7.2). This nitrogen treatment was used to avoid undesirable oxidation processes of the samples.

Figure 7.2. Bubbling treatment with nitrogen.

7.1.2 Accelerated aging tests

For the aging tests, the vials were kept in a temperature-controlled oven at a temperature of 110^o C for 60 days. The selected test temperature was 110^o C because the NE-based NF used in this work showed good stability at this temperature for at least 60 days [35], whereas for higher temperatures, stability problems were observed.

Throughout the tests, two vials, one of them filled with NE and the other one filled with NF, were removed from the oven after 3, 6, 11, 16, 23, 30, 39, 50, and 60 days of testing. Additionally, samples of both specimens not subjected to aging were fully characterized, with these results considered as "fingerprints". The evolution of the two insulating fluids throughout the aging process can be seen in Fig. 7.3. The coloration of the new NF samples was darker than that observed in the NE samples; this effect is due to the black color of the NPs used in the experiment. The evolution of the colors as aging advanced was clear in both experiments. As can be seen, both types of fluids became darker due to the aging of the NE.

Figure 7.3. NF and NE aged fluid at several points of the accelerated aging test.

7.1.3 Characterization of the Samples during the aging process

The control variables that were considered during the aging tests were the tensile strength (TS) of the paper and the moisture content of paper and oil. Additionally, FTIR and XPS analysis were carried out on the samples to gain insight into the chemical structure of the materials.

7.1.3.1 Tensile strength measurements

Although the measurement of the polymerization degree (DP) is commonly acknowledged as a more reliable parameter to assess the aging condition of paper, that technique was not used in this work because NPs cannot be digested by the solvent that is

used to perform DP measurements and their presence might lead to erroneous results. For this reason, the aging condition of the paper samples at different stages of the aging tests was characterized by TS measurements.

The TS of the new and aged paper samples was evaluated using an MTC-100 Vertical Universal Tensile Tester (IDM) showen in Fig. 7.4. Five paper samples were prepared for each vial of the study by cutting paper strips 15 cm long. Each of these strips was tested with the tensile strength tester. The parameters used for the test were adjusted to the ASTM D828-97 Standard [84]. Finally, the obtained TS data were statistically treated by discarding the outlier measures and calculating the average value of the remaining values, as will be discussed in the results section.

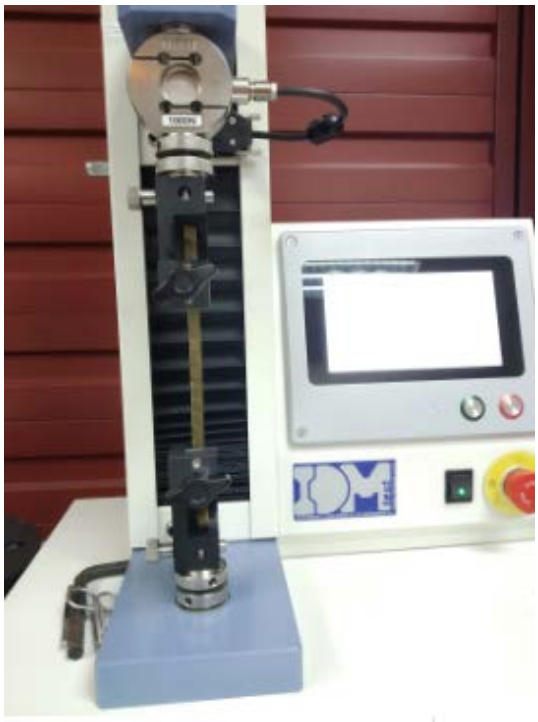

Figure 7.4. MTC-100 Vertical Universal Tensile Tester (IDM)

7.1.3.2 Moisture content of oil and paper

The water content of the liquids and that of the cellulose samples was measured with the Karl Fischer (KF) method, using a KF Coulometer Methrom 831 combined with a KF Thermoprep oven.

7.1.3.3 X-ray Photoelectron Spectroscopy

X-ray photoelectron spectroscopy was performed on some of the samples included in the study to understand how the presence of NPs alters the chemical reactions involved

in the degradation process, and to investigate the changes in the chemical bonds that are present in the oil-paper insulation as the aging process advanced.

The XPS measurements of the study, including the full width at half maximum (FWHM), were performed using an energy analyzer PHOIBOS 150 9MCD (SPECS GmbH) at the Institute of Catalysis and Petrochemistry of the Spanish Council for Scientific Research (CSIC), Spain.

7.1.3.4 FTIR

FTIR spectra were performed on cellulose samples to compare how NF and NE affect the degradation process of the cellulose immersed in each fluid during the accelerated aging.

The reason for using both XPS and FTIR to gain insight into the aging process is that each method is better suited to detect certain functional groups inside the molecules.

7.2 Results and discussion

In this section, the results of the aforementioned tests throughout their aging process are presented. Additionally, the evolution of the moisture content of the paper and fluids are analyzed in both cases: NF and NE.

7.2.1 Tensile strength

Fig. 7.5 shows the evolution of the TS of the Kraft paper samples vs. aging time in days. It can be seen that the results are quite scattered. The Kraft paper strips are thin and quite brittle, and tend to break inconsistently. It can be observed that the TS values measured for the samples of paper immersed in NF are slightly lower than those of the paper immersed in NE for the same aging times. As the aging advances, the results tend to approximate.

The relationship between TS and DP of Kraft paper was analyzed by Frimpong et al. [85], who reported that, in the first stage of the aging process (i.e. DP above 600), there is a drop in the paper DP that is not accompanied by a decrease of its TS [72]. This may be due to the fact that as long as the glucose chains are long enough, there is no clear impact on the mechanical properties of the material.

The aging process of the same type of Kraft paper used in this experiment immersed in an NE was thoroughly analyzed in a previous work for longer aging times and at several temperatures [86]. The evolution of the DP measured in this experiment is shown in Fig. 7.6.

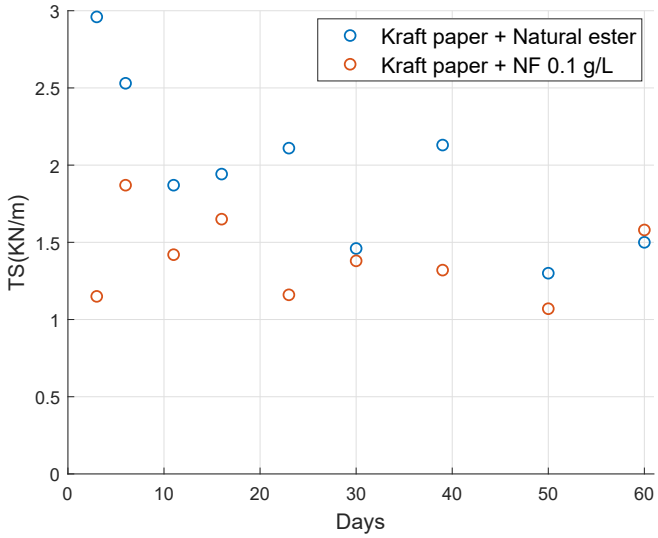

Figure 7.5. Tensile strength of paper vs. aging time.

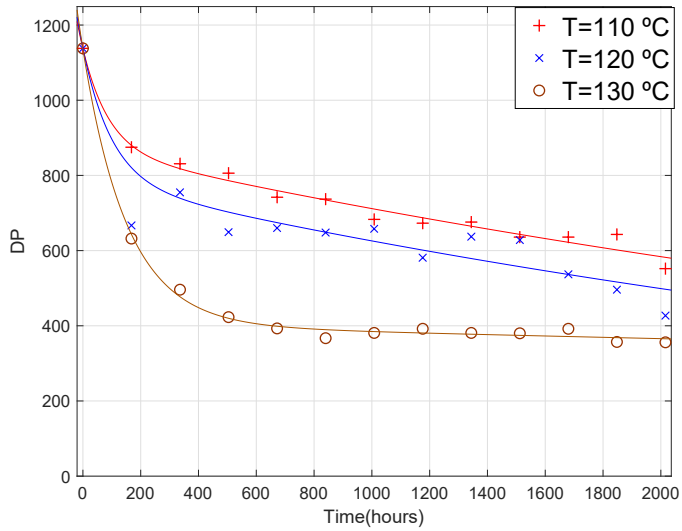

Figure 7.6. DP evolution vs. aging time of paper impregnated with NE. Taken from [86].

As can be seen, for the testing times of the last sample of the present study (60 days, 1440 h), Fig. 7.6 shows a DP of about 670. As the TS remains almost stable until the aging starts to degrade the cellulose fibers, the most important drop of this variable starts when the DP of the samples is below 600. Thus, for a DP of 670, only a slight decrease of the TS was observed.

The main conclusion that can be extracted from the analysis of the TS of the NF-based and the NE-based samples is that the TS of both types of insulation behave similarly. Thus, a major effect of the NPs on the rate of loss of the mechanical properties of the cellulose can be discarded.

7.2.2 Water content analysis

Fig. 7.7 shows the evolution of the moisture content of the NE and the NF during the aging process. Those measurements were taken on samples of fluid extracted from the aging vials.

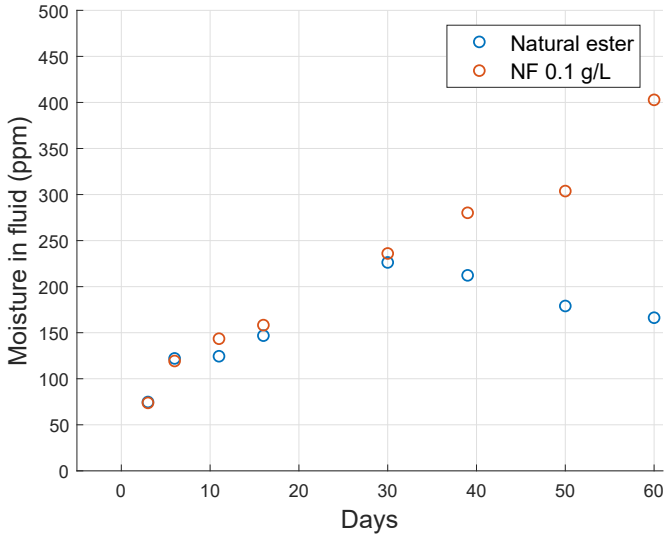

Figure 7.7. Moisture content in the fluid vs. aging time.

It is possible to observe two well-differentiated stages in the aging process: before day 30 and after day 30. In the first stage, the moisture content present in the NE and the NF was almost the same. In the second stage, the trend of the moisture content in both fluids diverged: while the moisture in the NF kept rising until the end of the experiment, in the case of the NE it stabilized or even decreased.

The reduction of the moisture in the NE was reported before [86]. It is produced by a chain of chemical reactions that take place when the NE begins to degrade as a result of the aging process. The process of degradation of the fatty acids takes place through a hydrolysis reaction (Fig. 7.8), which consumes water molecules. Thus, as the experiment advanced, the tendency was for a reduction of the moisture content of the dielectric fluid.

The presence of the free fatty acids produced in the hydrolysis reaction protects cellulose from degradation, since fatty acids are able to bind the hydroxyl groups of alcohols of cellulose chains, preventing the cellulose polymer from breaking down into shorter chains. This reaction is called transesterification and is illustrated in Figure 7.9. The transesterification reactions that occurred in the system NE-cellulose are shown in Fig. 7.9.

In the case of the NF-immersed cellulose, the NPs seemed to interfere with the previously described chemical reactions, meaning that the amount of water consumed

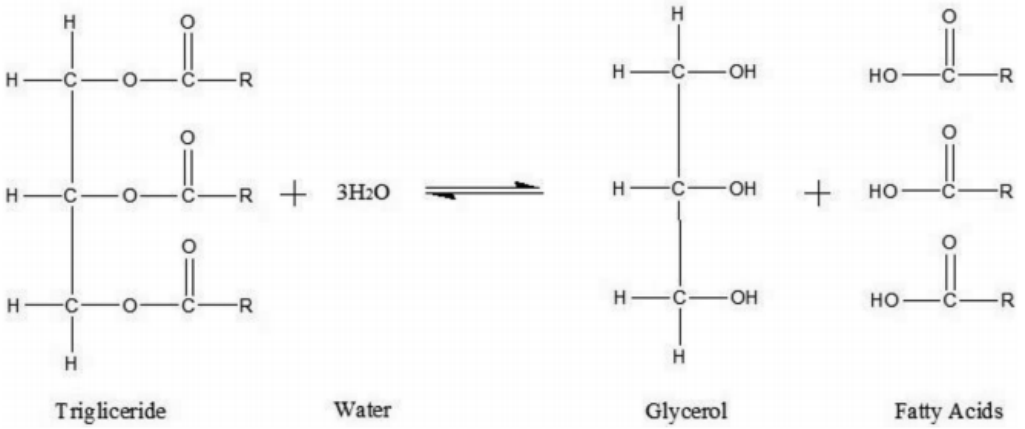

Figure 7.8. Hydrolysis of a NE.

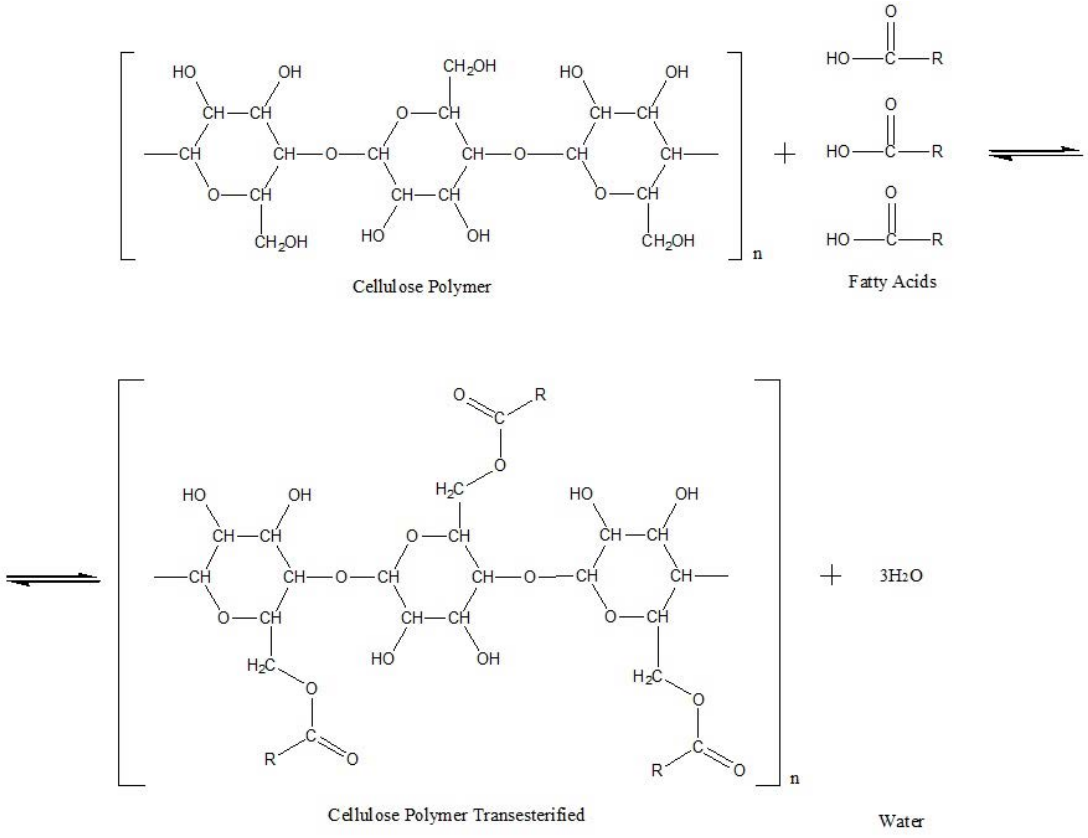

Figure 7.9. Transesterification reaction of cellulose.

was less than in the case of the NE-immersed samples. This effect could be produced by the high capacity of the NPs to trap water; if the water molecules are bound to the NPs, they will not be available for other reactions such as the hydrolysis of ester. In addition, chemical bonds might have been created between the NPs and the hydroxyl groups of alcohols of the cellulose molecules [87]. This would also inhibit the transesterification reaction that is typically involved in the aging process of cellulose in the presence of

ester [86, 88].

Fig. 7.10 shows the results of the moisture tests on the aged paper samples as the experiment progressed. It is possible to see how moisture in the paper samples tended to stabilize at a value around 1% in weight. This final value is quite similar to the value at the beginning of the experiment. This effect, associated with the NE or NF moisture test, could reveal that dielectric fluid tends to accumulate most of the water molecules present in the system. This behavior has been observed previously by several authors [86, 89].

7.2.3 X-Ray Photoelectron spectroscopy analysis of the samples

For a deeper analysis of the chemical reactions that take place in the different types of oil-paper insulation, an XPS analysis was carried out. Fig. 7.11 shows the results of a high-resolution XPS spectroscopy performed on two Kraft paper samples; the first sample was aged in presence of NE, and the second was aged in presence of NF. As can be observed,

O1s and C1s peaks are shifted around 2-3 eV from the results found by other authors [90]. The reason for this is that the samples are made of non-conductive materials. Since this study compares the width of the peaks of both samples, the conclusions are not affected by the shift.

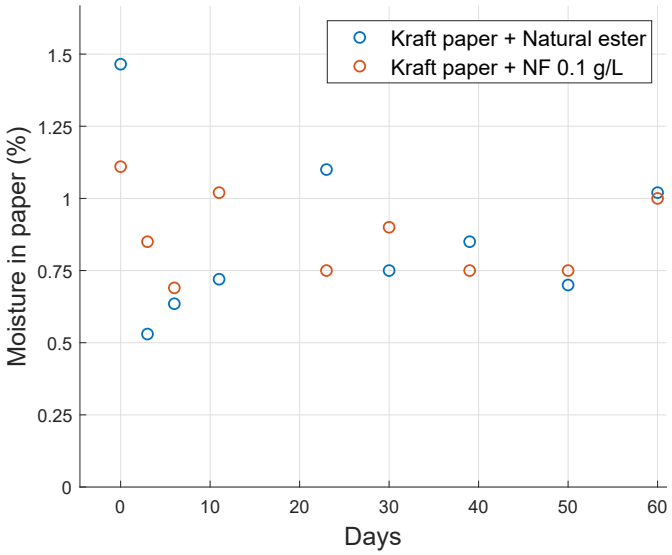

Figure 7.10. Moisture content in cellulose vs. aging time for NF- and NE-based insulation.

The XPS spectrum is sensitive to chemical changes related to the way carbon and oxygen bond with various elements. These changes are observed in the binding energy of the carbon and oxygen atoms: the shape of the spectrum is displaced to higher or

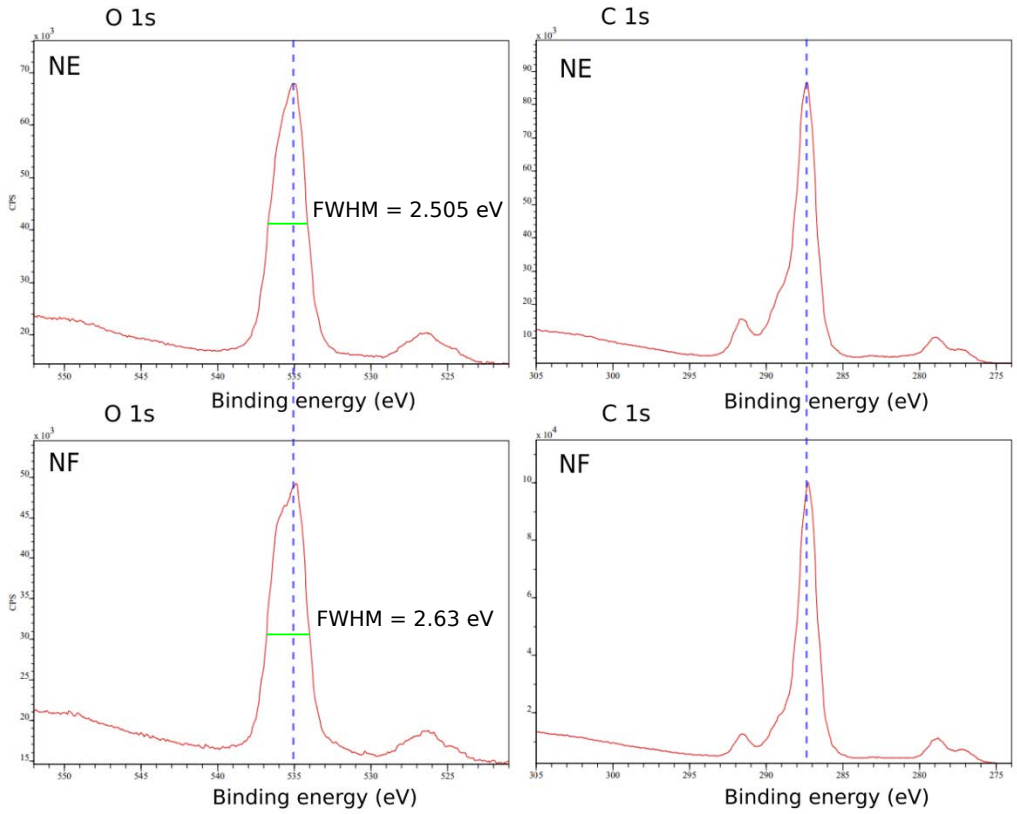

Figure 7.11. High-resolution XPS spectra of the O 1s (left) and C 1s (right), performed on paper samples.

lower energies depending on the new bonds formed [90, 91]. In Fig. 7.11, it can be seen how the chemical environment changes around the carbon and oxygen atoms when the paper samples are aged in NF.

The shape of the XPS spectrum of the oxygen 1s band is the contribution of the O^{1-} bond energy and the O^{2-} bond energy, which are very close to each other. Therefore, a widening of this area towards higher energies is an indication of the formation of chemical compounds with a higher content of O^{2-} bonds. In our case, the signal of the oxygen 1 s band (shown in the figures at the left) was displaced to higher binding energies in NF-immersed samples, as can be observed by the values of the full width at half maximum (FWHM) of the O 1s band that grows from 2.505 eV for the NE to 2.63 eV for the NF. The contribution of the oxygen atoms as O^{2-} increases, making the O 1 s maximum wider. This O^{2-} contribution is related to bonds that present a high polarization. The observed effect reflects the fact that NPs have bonded to cellulose molecules by substituting H atoms, which form less polarized bonds with oxygen than the hydroxyl groups of alcohols (OH).

The shape of the XPS spectrum of C at the 1s orbital is the contribution of the different saturation grades of carbon bonds in the molecule (C1, C2, C3...) [92]. In the

case of the samples of the Thesis, the change was less noticeable in the carbon binding energies (figures on the right); thus, the carbon bonds were not modified in the aging process.

These changes in the chemical structure of the cellulose are compatible with the hypothesis that NPs bind to the cellulose molecules, preventing the degradation of NE and hindering the advance of the transesterification. In Fig. 7.12, a schematic representation of the chemical interactions that are proposed to explain the interaction between NPs and cellulose molecules within the Kraft paper is shown. According to this explanation, the Fe_3O_4 NPs may replace the hydrogen of the alcohol groups. These bonding mechanisms were obtained based on the results of the performed XPS tests.

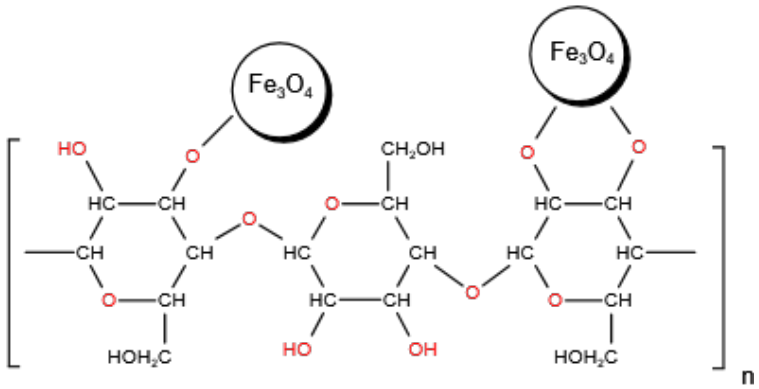

Figure 7.12. Fe_3O_4 NPs binding with cellulose molecules.

7.2.4 FTIR analysis

The FTIR spectra of some of the NE and NF-impregnated papers were analyzed to identify the chemical products generated during the accelerated aging process and to confirm the conclusions drawn from XPS tests. In order to compare the aging processes of both types of samples and the influence of the NPs on the aging process, the FTIR spectra of three samples of paper impregnated with NF aged for 6, 30, and 60 days, and equivalent samples impregnated with NE are shown in Fig. 7.13.

The first important band that changes from one sample type to another is the one centered around 3450 cm^{-1}. This band corresponds to O-H bonds, mostly due to the presence of water molecules and the hydroxyl groups of alcohols of the cellulose, and is always present in cellulose FTIR spectra [93]. In order to improve the observation of the main differences among the spectra of the six samples, a detail of the spectra centered at 3350 cm^{-1} is plotted in Fig. 7.14. It is possible to observe how the NF-impregnated samples aged for 30 and 60 days present a lower transmittance in this band; this fact is related to the H_2O molecules generated during the accelerated aging

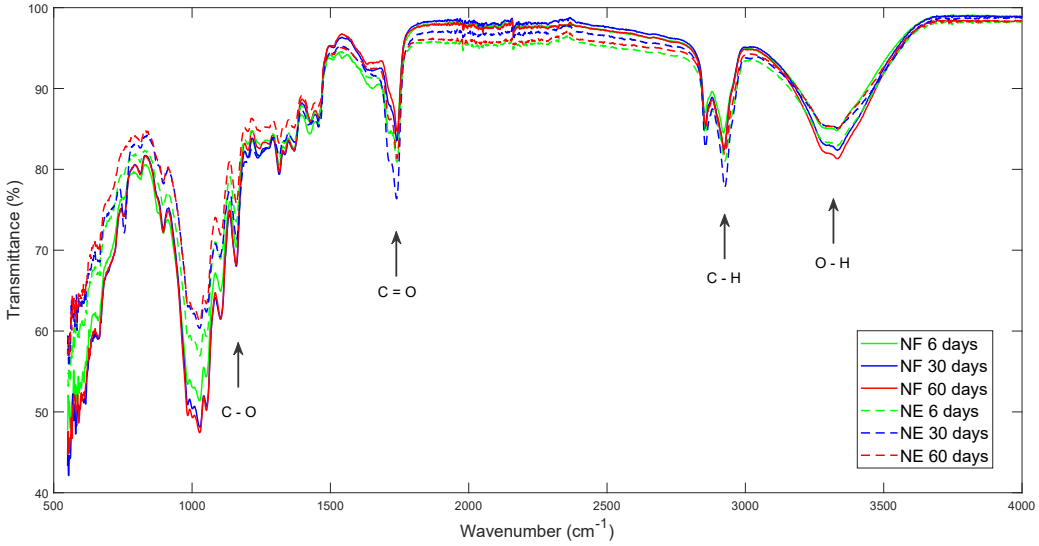

Figure 7.13. FTIR spectrum of cellulose impregnated with NF and NE, subjected to different aging times.

process, and agrees with the observations on the moisture tests presented in Section 7.2.2. On the other hand, the NE-impregnated samples present a higher transmittance and, in consequence, a lower content of OH groups, which is in agreement with the hypothesis that water is consumed during the aging process in the presence of NE.

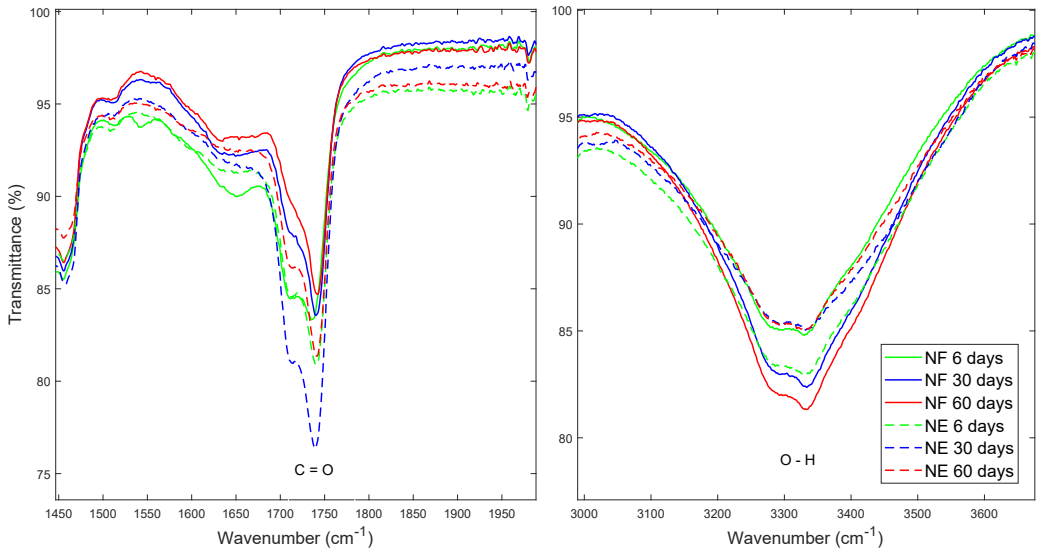

Figure 7.14. Details of FTIR spectrum of cellulose impregnated with NF and NE, subjected to different aging times

The band centered around 2800 cm^{-1} represents the C-H functional groups. As can be seen, the transmittance of the NF-impregnated samples in this band decreased as the aging progressed; this fact is due to the products generated by the hydrolysis of the fatty acids [94]. For the NE-impregnated samples, the evolution was different; the

transmittance grows after 30 days of aging and then, for samples of 60 days of aging, decreased to a value almost equal to that of the 6-day aging sample. This behaviour is consistent with the results of the moisture tests and with the mechanisms proposed in Figs. 7.8 and 7.9. As the transesterification progresses, it is more likely that water molecules and free fatty acids are consumed in the NE-impregnated samples.

It is easier to differentiate variations in C-O and C=O functional groups by means of FTIR tests than with XPS tests. The band around wavelength 1700 cm^{-1} corresponds to the transmittance of the C=O functional groups. In Fig. 7.14, a zoom of the spectra centered at 1750 cm^{-1} is plotted. It is possible to observe how the intensity of the band that represents the C=O functional groups changes as the aging progresses; this observation is related with the degradation of fatty acids reported by Frimpong et al. [85]. It can be observed how the NF-impregnated paper presented a lower increase of C=O groups in this band as the aging progressed compared with the NE-impregnated samples. This effect could represent better conservation of the insulating system when the cellulose samples are impregnated with NF. The changes of shape in this band also represent how free fatty acids bond to cellulose molecules; this fact is in agreement with previous observations of XPS tests (Fig. 7.11 left).

Finally, in the band around 1000 cm^{-1}, the response of the two types of paper was opposite to that analyzed in the 1000 cm^{-1} band, with the C–O groups turning into C=O groups as the aging progressed.

7.3 Conclusions

In the present chapter, a variety of tests were performed on samples of paper impregnated with a Fe_3O_4-based NF treated subjected to an accelerated temperature aging process.

As a first conclusion of the present study, it was observed that the evolution of the TS of Kraft paper samples impregnated with NE and NF are very similar. The addition of NP does not affect the rate of loss of mechanical properties of the cellulose, regardless of whether the samples are fresh or aged.

When comparing the results of the moisture tests carried out on the different materials, remarkable differences were observed between the behavior of NF-impregnated samples and NE-impregnated samples. We conclude that the NPs interfere in the degradation mechanisms of the NE and slow down transesterification reactions in the cellulose. This hypothesis was confirmed by the XPS and FTIR results, which clearly show a change in the carbon-oxygen bonds of the NF-impregnated samples when compared with those impregnated with the base NE.

It can be concluded that NPs affect the aging process of both NE and Kraft paper. Some chemical reactions were proposed (mainly transesterification and hydrolysis), but it could not be stated which is the most predominant, since the oil-paper system allows the mobility of water molecules, meaning that water produced in the paper could be transferred to the oil and trapped by the NPs.

Chapter 8

Conclusions

In this chapter the conclusions obtained during the thesis and the original contributions are presented. Additionally some lines for future research are suggested.

8.1 General conclusions

The interaction between Kraft paper and NFs prepared with Np of Fe_3O_4 has been studied from various points of view to understand how the presence of NPs affects different aspects of the paper-oil insulation system relevant to the transformer operation.

The main conclusions of the Thesis are presented in this section.

8.1.1 Conclusions in relation to the morphology of Kraft paper impregnated with NF

- The impregnation process proposed in the Thesis emulates the one performed in transformer production plants and allows the preparation of Kraft paper samples intimately impregnated with MO or with NFs. The samples impregnated with NF showed clear evidences that the NPs were bounded to cellulose structure.
- Visual differentiation between NPs and cellulose nanofibres is not easy and to identify the presence of NPs the combination of several characterization techniques is required.
- ICP analysis showed a significant concentration of Fe even when the paper-impregnated samples were washed with chloroform, suggesting that NPs are not only present in the fluid but also bound to the paper.
- Cryo-SEM combined with EDX was successfully used to identify NPs in cellulose. The technique demonstrated to be useful for the characterization of oil-impregnated samples, in which SEM is not an option due to the corrosive character of the dielectric oils.
- EDX confirms the conclusions obtained by applying ICP: that is, the amount of Fe that remains bound to the paper after washing is high, suggesting a chemical interaction between Fe and paper in paper-NF impregnated samples.
- The combination of Cryo-SEM and EDX technique provide visual and elemental composition information that allows to identify the NPs in the cellulose structure. Each technique separately is insufficient to conclude in a proper identification of the NPs in a complex structure as the cellulose.
- The FTIR analysis performed to the samples suggested that chemical bonds are formed between the cellulose and the Fe_3O_4 NPs. This hypothesis was confirmed by the XPS analysis, which clearly show a change in the carbon-oxygen bonds in the NF-impregnated samples.

- The study proved that the NPs dispersed in the NF tend to ingress into the paper and bind with cellulose molecules. Even when the paper is treated chemically to remove the base oil, a remarkable number of NPs remain bound to the cellulose.
- The observation of NF-impregnated Kraft paper samples that had been chemically treated to remove the oil, made possible the identification of aggregated NPs in the paper when oil is eliminated. This observation reinforces the importance of using of a suitable surfactant to avoid the agglomeration of the NP, and to obtain stable NFs.

8.1.2 Conclusions in relation to the dielectric response of the NF-impregnated Kraft paper

Although the main focus of interest of this Thesis is the study of the behaviour of NF-impregnated paper, before carrying out tests to obtain the dielectric response of solid insulation, a study on the dielectric response of NFs has been carried out.

The studies related with the dielectric response of NF-impregnated paper samples consider two main factors of influence: the concentration of NPs in the NF and the influence of the temperature. The conclusions related with each of these factors are presented below.

8.1.2.1 Dielectric response of NFs

- The real part of the complex capacitance increases as the NP concentration increases.
- The 50 Hz permittivity of NF is higher than that of the base oil, but it does not present a dependence with the concentration of NP.
- The observed phenomena can be explained by the polar structure of the NPs used. The polarization of conductive NP is a fast event; this explains the fact that the effect of NP on the real part of the capacitance is equally noticeable in the whole range of frequencies.
- The dielectric losses of the liquid is modified when NPs are added, but the losses are very similar regardless of the NP concentration of the NF. The increase of dielectric losses is related with three phenomena: The aforementioned NP polarization, the increment in conductivity, the interfacial polarization in the interface NP-base oil (electrical double layer).

8.1.2.2 Dielectric response of NF-impregnated paper. Influence of the NP concentration

The dielectric response of paper impregnated with NF presents important variations with respect to that of paper impregnated with MO.

- The capacitance in the frequency domain and the relative permittivity of the NF-impregnated paper samples depend on the concentration of NPs in the NF used for the impregnation.
- The permittivity consistently increases for paper samples impregnated with NFs with NP concentrations 0.2 g/L and 0.3 g/L. When NP concentration rises to 0.4 g/L the tendency is reversed.
- The capacitance spectrum presents a relative maximum. The frequency at which the maximum is obtained shifts towards higher frequencies as the NP content increases.

  The justification for the movement of the maximum is found in the polar character of the NPs. The polar character of the NPs is due to the bonds between the oxygen molecules of the cellulose and the Fe atoms on the NP, as shown by the FTIR and XPS analysis carried out.
- The dielectric losses of the NF-impregnated Kraft paper also show changes compared to MO-impregnated samples. On one hand, the dielectric losses increase in paper samples impregnated with NF. On the other hand, a new slope appears in the spectra, what corresponds to an additional relaxation peak that is not present in MO-impregnated samples.

  The increase in dielectric losses and the appearance of a new resonance peak are consistent with the hypothesis that NPs react with cellulose molecules giving rise to new compounds.

  The phenomena involved in the variation of the dielectric response, are the polarization of the NPs attached to the cellulose chains and the distortion of the electrical field on the NF-impregnated samples caused by the polarized NPs. The double layer formed around Fe_3O_4 NP also has an influence on dielectric response,

8.1.2.3 Dielectric response of NF-impregnated paper. Temperature dependency

The conclusions related with the temperature dependency of NF-impregnated samples are as follows:

- The increase of temperature produces a frequency shift in the curve of the capacitance and the dielectric losses both for MO-impregnated and NF-impregnated paper.

- Changes in the dielectric response with temperature were quantified by means of the activation energy concluding that, as the concentration of NPs grows the activation energy tend to descend making the relaxation processes in the insulation system easier.

8.1.3 Conclusions in relation to the AC and impulse BDV of NF-impregnated Kraft paper

The dielectric performance of the NF-impregnated Kraft paper samples was tested under AC BDV and under lightning impulse tests. The conclusions obtained are presented next:

- NF-impregnated paper showed a 26% improvement in AC BDV values compared to paper impregnated with MO. In addition, the standard deviation of the AC BDV is lower in the case of paper impregnated with NF. These two factors make the voltage necessary to cause breakdown with a 5% probability (obtained through a Weibull adjust of the obtained data) to be much lower in paper impregnated with NF.
- The observed improvement could be due in part to the enhancement of the dielectric properties of the fluid surrounding the tested samples, as breakdown generally initiates in the fluid. The analysis of the electric field distribution within the test cell in MO and NF based systems, led to the conclusion that, due to the change in the permittivities of solid and liquid insulation, the maximum electric in the fluid is 15% lower in NF-based systems. This fact reduces the probability of streamer inception in NF based systems.

  Furthermore, the streamer propagation in the NF-impregnated paper and in the NF is slowed down by the presence of NPs that act as electrons traps.
- Under positive lightning impulse, NF-impregnated samples show a reduced improvement (2%) of the BDV value compared to that of MO-impregnated samples.

8.1.4 Conclusions regarding the aging of the NF-impregnated Kraft paper

The conclusions extracted from the ageing tests carried out on NE-based NF-impregnated paper are as follows:

- Kraft paper samples impregnated with a NE-based NF seem to age at similar rate as NE-impregnated ones. The presence of NPs does not seem to affect the evolution of the tensile strength trough the aging process. The values of the TS

observed for the fresh NE-impregnated samples and the NF-impregnated ones was also quite similar.

- The evolution of the moisture content along the ageing test was one of the main differences that could be observed when comparing the aging of both types of systems. In case of NE-impregnated samples, water in the fluid surrounding the samples rises as the ageing test progress to certain aging degree and then water in the fluid decreases. On the contrary, in case of NF-impregnated samples, water in the fluid rises along the whole process.

  The reduction in moisture content in case of NE-impregnated samples is due to the degradation reactions of the fatty acids of the NE. In case of NF-impregnated samples the reactions of degradation of the fatty acids seems to slow down. This effect could be produced by the great capacity of NPs to trap water. In addition to the above, the aging process of cellulose in presence of NE is quite different from that in presence of NF, as the chemical bonds between cellulose molecules and NP inhibit transesterification reactions.
- XPS and FTIR analysis provides information into the mechanisms that may cause the observed differences in moisture contents. NPs interfere with degradation reactions and slow down transesterification reactions in NE-impregnated cellulose. The presence of NPs also affect the hydrolysis of the NE. Both the XPS results and the FTIR results show that the NF-impregnated paper samples have a higher content of O^{2-} bonds that are more susceptible to being polarized. The presence of O^{2-} bonds also accounts for the dielectric properties. As the aging test progresses, FTIR shows a decrease in the hydroxyl groups on NF-impregnated cellulose chains related to water generation during the ageing.
- The pattern in the evolution of CH groups along the aging of the NF-impregnated paper is different from that of the NE-impregnated paper, as in the first case fatty acids are produced constantly in the whole ageing period while in the second case there is a point in which ceases the production of fatty acids. This is consistent with the water generation studied in Chapter 7.

  The FTIR band corresponding to C=O groups allows to infer a lower degradation of NF-impregnated paper compared NE impregnated paper.

  On the contrary the band corresponding to C-O groups has a dramatic change during aging, showing than in NF-impregnated paper there is a higher conversion of C-O groups into C=O groups, much more than in NE-impregnated paper.

8.2 Original contributions of the Thesis

The field of study of the Thesis is very new and not many authors in the literature have conducted similar studies to the ones presented in it. Thus, most of the work included in the study has a high level of novelty.

One of the main problems of the research field of the Thesis, is that a great number of NPs are currently available in the market and thus, the materials investigated by different authors are diverse and the results are not totally comparable or can be interpreted in a general context. This work has addressed this problem by conducting all the tests with materials based in Fe_3O_4 NPs and using repetitive preparation procedures and experimental methods.

The NFs that were applied in the Thesis had been analysed in depth in a previous work, so the main focus of interest in this Thesis is the interaction and properties of paper and NF.

The Thesis provides a comprehensive study in which the same material (Kraft paper impregnated with a Fe_3O_4 based NF) was analysed from several perspectives which included morphology, dielectric properties and the ageing processes. The behaviour of the material was compared with that of paper impregnated with MO and NE.

The Thesis is a breakthrough in the research field, as it can serve as a starting point to study how a transformer insulated with NF would behave globally.

In summary, the main characteristics of the Thesis are:

- The morphology of the NF-impregnated paper system was studied in depth using many complementary techniques (ICP, EDX, Cryo-SEM, FTIR, XPS). Fe_3O_4 NPs were identified on the surface and in the inner part of NF impregnated Kraft paper.
- In view of the difficulty of analyzing CryoSEM results separately, a method based on the combination of the Cryo-SEM and EDX techniques were proposed to analyze NF-impregnated cellulose samples in presence of oil. The proposed methodology may be used to characterize other combinations of materials in the future.
- A mechanism of chemical interaction between Fe_3O_4 NP and cellulose was proposed compatible with the results of the analytical techniques used, as FTIR. This interaction is a key factor to understand the variation of properties that are observed in the NF impregnated cellulose.
- The influence of Fe_3O_4 NP in the dielectric response of the NF-impregnated paper was studied. Values of relative permittivities and dielectric losses were derived from the tests that can be used for the analysis of the electric field distribution in the NF-based transformer. The temperature dependency of the dielectric response was been investigated, obtaining values for the activation energies of

NF-impregnated paper with different NP concentrations.

- The AC BDV of NF-impregnated paper was investigated demonstrating that the presence of NPs may increase the average AC BDV values by more than 25 %, what is a very important enhancement. This suggests that the use of NF-based materials as transformer insulation may lead to transformers with larger safety margins or might make possible the design of more compact insulation systems.
- The lighting impulse breakdown voltage of NF-impregnated paper was also tested but the increase in that case was only a the 2% than that of conventional insulation.
- The ageing process of NF-impregnated paper was studied proving that the ageing rate of paper does not seem to be affected by the presence of NPs, although XPS and FTIR tests suggest that NPs interfere in the chemical reactions that takes place between the cellulose and the dielectric oil during the ageing process. Theoretical processes were proposed to explain the experimental observations on ageing.

8.3 Lines of future research

As was stated throughout the Thesis, the study of NF-impregnated cellulose is still in the first stages of its development. Extensive research is needed yet to expand the studies that have been carried out in the Thesis and those conducted by other authors to apply NFs to real transformers with enough safely. In this context some future lines are proposed:

- Morphology studies might be completed with other analytical techniques which can show changes in the elementary state of the materials, such as X-ray photoelectron spectroscopy.
- Further morphological characterization might be carried out on materials based in other NPs that have demonstrated good performance as NF. The interaction between these NPs and the cellulose may be different than for the case of the Fe_3O_4-based NFs studied in the Thesis.
- Analyse how the changes on the permittivities observed in the Thesis may impact on the electric field distribution of the transformer by means of finite elements models. In the future, studies will be needed to determine the values of these parameters and probably some modifications in the design of the oil-paper insulation may proposed for NF based transformers.
- Study how the interaction between the NP and the cellulose may affect other physic-chemical properties of the materials to better understand and predict the

possible challenges to overcome.

- Characterize the impact of NPs on other dielectric parameters, as the partial discharge inception voltage, the switching impulse BDV or the DC BDV.
- Determine if higher concentrations of NPs could lead to higher values of the impulse BDV of NF-impregnated cellulose insulation.
- Study how other types of NPs (specially semiconductive and insulating) affect the dielectric properties of NF-impregnated cellulose materials.
- Complete the aging study to consider other factors that can impact the aging process, such as the testing temperature, NP concentration, or the base fluid and NPs used to produce the NF.
- Advance in the development of new surfactants that allow to improve the long-term stability of NF, and avoid the aggregation of NP.
- Study the properties and behaviour of nanoparticle-modified cellulose material impregnated with NFs. A combination of the this two novel materials can lead to important improvement on the properties of the solid and liquid insulation.

References

[1] D. Martin, C. Beckett, J. Brown, and S. Nielsen, "Analysis and Mitigation of Australian and New Zealand Power Transformer Failures Resulting in Fires and Explosions," *IEEE Electr Insul M*, vol. 35, no. 6, pp. 7–14, 2019.

[2] J. Marks, D. Martin, T. Saha, *et al.*, "An Analysis of Australian Power Transformer Failure Modes, and Comparison with International Surveys," *Austr Univ Pow Eng*, pp. 1–6, 2016.

[3] D. Martin, J. Marks, and T. Saha, "Survey of Australian Power Transformer Failures and Retirements," *IEEE Electr Insul M*, vol. 33, no. 5, pp. 16–22, 2017.

[4] M. J. Heathcote, "Basic materials," in *J & P Transformer Book*, Elsevier, 2007.

[5] Z. Ma, J. Liu, Y. Liu, X. Zheng, and K. Tang, "Green synthesis of silver nanoparticles using soluble soybean polysaccharide and their application in antibacterial coatings," *International Journal of Biological Macromolecules*, vol. 166, pp. 567–577, 2021.

[6] H. Setälä, H. L. Alakomi, A. Paananen, *et al.*, "Lignin nanoparticles modified with tall oil fatty acid for cellulose functionalization," *Cellulose*, vol. 27, no. 1, pp. 273–284, 2020.

[7] E. J. Kadim, Z. A. Noorden, Z. Adzis, and N. Azis, "Nanoparticles Application in High Voltage Insulation Systems," *IEEE Transactions on Dielectrics and Electrical Insulation*, vol. 28, no. 4, pp. 1380–1399, 2021.

[8] V. Segal and K. Raj, "An Investigation of Power Transformer Cooling with Magnetic Fluids," *Indian J Eng Mater S*, vol. 5, no. 6, pp. 416–422, 1998.

[9] X. Wang and X. Xu, "Thermal Conductivity of Nanoparticle–fluid Mixture," *J Thermophys Heat Tr*, vol. 13, no. 4, 1999.

[10] S. Özerinç, S. Kakaç, and A. G. Yazıcıoğlu, "Enhanced Thermal Conductivity of Nanofluids: A State-of-the-art Review," *Microfluid Nanofluid*, vol. 8, no. 2, pp. 145–170, 2010.

[11] N. Weijun Yin, *Patent No; US 2013/0285781*, 2013.

[12] Y. Du, Y. Lv, C. Li, *et al.*, "Effect of Nanoparticles on Charge Transport in Nanofluid-impregnated Pressboard," *J Appl. Phys*, vol. 111, no. 12, 2012.

[13] J. Dai, M. Dong, Y. Li, and J. Zhou, "Influence of Nanoparticle Concentration on the Frequency Domain Spectroscopy Properties of Transformer Oil-based Nanofluids," *IEEE Conf on Electrical Insulation and Dielectric Phenomena*, pp. 587–590, 2016.

[14] G. Shukla and H. Aiyer, "Thermal Conductivity Enhancement of Transformer Oil Using Functionalized Nanodiamonds," *IEEE T Dielect El In*, vol. 22, no. 4, pp. 2185–2190, 2015.

[15] G. D. Peppas, A. Bakandritsos, V. P. Charalampakos, *et al.*, "Ultrastable Natural Ester-Based Nanofluids for High Voltage Insulation Applications," *Acs Appl Mater Inter*, vol. 8, no. 38, pp. 25 202–25 209, Sep. 2016.

[16] F. M. O'Sullivan, "A Model for the Initiation and Propagation of Electrical Streamers in Transformer Oil and Transformer Oil Based Nanofluids," *Thesis (Ph. D.)–Massachusetts Institute of Technology, Dept. of Electrical Engineering and Computer Science, 2007.*, 2007.

[17] J. Kudelcik, P. Bury, P. Kopcansky, and M. Timko, "Dielectric Breakdown in Mineral Oil ITO 100 Based Magnetic Fluid," 2, vol. 9, 2010, pp. 78–81.

[18] Y. Du, Y. Lv, C. Li, *et al.*, "Effect of water adsorption at nanoparticle – oil interface on charge transport in high humidity transformer oil-based nanofluid," *Colloids and Surfaces A: Physicochemical and Engineering Aspects*, vol. 415, pp. 153–158, 2012.

[19] A. M. Abd-Elhady, M. E. Ibrahim, T. A. Taha, and M. A. Izzularab, "Effect of temperature on AC breakdown voltage of nanofilled transformer oil," *IET Science, Measurement and Technology*, vol. 12, no. 1, pp. 138–144, 2018.

[20] B. Shan, Q. Sun, C. Li, *et al.*, "Breakdown strength of transformer oil modified by TiO2 nanoparticles under AC-DC combined voltage," *2017 IEEE 19th International Conference on Dielectric Liquids, ICDL 2017*, vol. 2017-January, no. Icdl, pp. 1–4, 2017.

[21] M. H. Abdo, "Electrical Discharge Analysis on Application," no. December, pp. 19–21, 2017.

[22] M. Rafiq, C. Li, Y. Lv, K. Yi, and S. Hussnain, "Preparation and study of breakdown features of transformer oil based magnetic nanofluids," in *2017 International Conference on Electrical Engineering (ICEE)*, 2017, pp. 1–4.

[23] D. Liu, Y. Zhou, Y. Yang, and L. Zhang, "Characterization of High Performance AlN Nanoparticle-Based Transformer Oil Nanofluids," *IEEE Transactions on Dielectrics and Electrical Insulation*, vol. 23, no. 5, pp. 2757–2767, 2016.

[24] D. Pérez, V. Primo, B. García, and J. C. Burgos, "Analysis of Water Solubility in natural-ester based nanodielectric fluids .," in *IEEE International Conference on Dielectrics*, 2019.

[25] H. Jin, "Dielectric Strength and Thermal Conductivity of Mineral Oil based Nanofluids," Ph.D. dissertation, Delft University of Technology, the Netherlands, 2015.

[26] W. Yu, D. France, S. Choi, and J. Routbort, "Review and Assessment of Nanofluid Technology for Transportation and Other Applications," *Energy Systems Division, Argonne National Laboratory work*, 2007.

[27] V. A. Primo, B. García, D. Pérez, and J. C. Burgos, "Analysing the impact of moisture on the ac breakdown voltage on natural ester based nanodielectric fluids," in *2019 IEEE 20th International Conference on Dielectric Liquids (ICDL)*, 2019, pp. 1–4.

[28] H. Jin, T. Andritsch, I. A. Tsekmes, R. Kochetov, P. H. F. Morshuis, and J. J. Smit, "Properties of mineral oil based silica nanofluids," *IEEE Transactions on Dielectrics and Electrical Insulation*, vol. 21, no. 3, pp. 1100–1108, 2014.

[29] D.-e. A. Mansour and A. M. Elsaeed, "Heat Transfer Properties of Transformer Oil-Based Nanofluids Filled with Al2O3 Nanoparticles Diaa-Eldin," *2014 IEEE International Conference on Power and Energy (PECon)*, pp. 123–127, 2014.

[30] B. X. Du, X. L. Li, and J. Li, "Thermal Conductivity and Dielectric Characteristics of Transformer Oil Filled with BN and Fe 3 O 4 Nanoparticles," pp. 2530–2536, 2015.

[31] E. G. Atiya, D. E. A. Mansour, R. M. Khattab, and A. M. Azmy, "Dispersion behavior and breakdown strength of transformer oil filled with TiO2nanoparticles," *IEEE Transactions on Dielectrics and Electrical Insulation*, vol. 22, no. 5, pp. 2463–2472, 2015.

[32] J. B. Dumitru, S. Member, A. M. Morega, S. Member, M. Morega, and S. Member, "Nanofluid Cored Miniature Electrical Transformer with Planar Spiral Windings," pp. 11–16, 2014.

[33] H. Jiang, H. Li, C. Zan, F. Wang, Q. Yang, and L. Shi, "Temperature dependence of the stability and thermal conductivity of an oil-based nanofluid," *Thermochimica Acta*, vol. 579, pp. 27–30, 2014.

[34] K. N. Koutras, I. A. Naxakis, A. E. Antonelou, V. P. Charalampakos, E. C. Pyrgioti, and S. N. Yannopoulos, "Dielectric strength and stability of natural ester oil based TiO2 nanofluids," *Journal of Molecular Liquids*, vol. 316, 2020.

[35] V. A. Primo, D. Pérez-Rosa, B. García, and J. C. Cabanelas, "Evaluation of the Stability of Dielectric Nanofluids for Use in Transformers under Real Operating Conditions," *Nanomaterial-Basel*, vol. 9, no. 2, 2019.

[36] R. Karthik, F. Negri, and A. Cavallini, "Influence of Ageing on Dielectric characteristics of silicone di oxide , tin oxide and ferro nanofluids based mineral oil," *2016 2nd International Conference on Advances in Electrical, Electronics, Information, Communication and Bio-Informatics (AEEICB)*, pp. 40–43,

[37] H. U. Zhi-feng, M. a. Kai-bo, W. Wei, *et al.*, "Thermal Aging Properties of Transformer Oil-Based TiO 2 Nanofluids," *Proceedings - IEEE International Conference on Dielectric Liquids*, pp. 1–4, 2014.

[38] D. Zmarz and D. Dobry, "Analysis of Properties of Aged Mineral Oil Doped with C 60 Fullerenes," *IEEE Transactions on Dielectrics and Electrical Insulation*, vol. 21, no. 3, pp. 1119–1126, 2014.

[39] V. Antonio and P. Cano, "Application of nanodielectric fluids for the improvement of the insulation system of power transformers," 2019.

[40] R. Hollertz, D. Ariza, C. Pitois, and L. Wågberg, "Dielectric response of kraft paper from fibres modified by silica nanoparticles," *Annual Report - Conference on Electrical Insulation and Dielectric Phenomena, CEIDP*, vol. 2015-December, pp. 459–462, 2015.

[41] M. M. Katun, A. Smith, R. Kadzutu-Sithole, C. Gomes, C. Nynamupangedengu, and N. Moloto, "Impact of Fibres and Reinforced Nanoparticles on Tensile Strength of Transformer Oil-impregnated Paper," *Proceedings - 30th Southern African Universities Power Engineering Conference, SAUPEC 2022*, pp. 2–7, 2022.

[42] J. Zheng, K. Nagashima, D. Parmiter, J. de la Cruz, and A. K. Patri, "Sem x-ray microanalysis of nanoparticles present in tissue or cultured cell thin sections," in *Characterization of Nanoparticles Intended for Drug Delivery*, S. E. McNeil, Ed. Totowa, NJ: Humana Press, 2011, pp. 93–99.

[43] R. Sadeghy, M. Haghshenasfard, S. G. Etemad, and E. Keshavarzi, "Investigation of alumina nanofluid stability using experimental and modified population balance methods," *Advanced Powder Technology*, vol. 27, no. 5, pp. 2186–2195, 2016.

[44] A. Jain, J. G. Sheridan, R. Xing, F. Levitov, S. Yasharzade, and H. Nguyen, "Sem imaging and automated defect analysis at advanced technology nodes (di: Defect inspection and reduction)," in *2017 28th Annual SEMI Advanced Semiconductor Manufacturing Conference (ASMC)*, 2017, pp. 240–248.

[45] S. Licht, V. Naschitz, L. Halperin, *et al.*, "Analysis of ferrate(VI) compounds and super-iron Fe(VI) battery cathodes: FTIR, ICP, titrimetric, XRD, UV/VIS, and electrochemical characterization," *Journal of Power Sources*, vol. 101, no. 2, pp. 167–176, 2001.

[46] G. V. Andrievsky, V. K. Klochkov, A. B. Bordyuh, and G. I. Dovbeshko, "Comparative analysis of two aqueous-colloidal solutions of C60 fullerene with help of FTIR reflectance and UV-Vis spectroscopy," *Chemical Physics Letters*, vol. 364, no. 1-2, pp. 8–17, 2002.

[47] J. C. Dupin, D. Gonbeau, H. Benqlilou-Moudden, P. Vinatier, and A. Levasseur, "XPS analysis of new lithium cobalt oxide thin-films before and after lithium deintercalation," *Thin Solid Films*, vol. 384, no. 1, pp. 23–32, 2001.

[48] M. Descostes, F. Mercier, N. Thromat, C. Beaucaire, and M. Gautier-Soyer, "Use of XPS in the determination of chemical environment and oxidation state of iron and sulfur samples: Constitution of a data basis in binding energies for Fe and S reference compounds and applications to the evidence of surface species of an oxidized pyrite in a carbonate medium," *Applied Surface Science*, vol. 165, no. 4, pp. 288–302, 2000.

[49] Y. Zhou, Y. X. Zhong, M. T. Chen, *et al.*, "Effect of Nanoparticles on Electrical Characteristics of Transformer Oil-based Nanofluids Impregnated Pressboard," *IEEE Int Sym Elec In*, pp. 650–653, 2012.

[50] M. Kai-Bo, L. Yu-Zhen, W. Wei, Z. You, Z. Sheng-Nan, and L. Cheng-Rong, "Influence of semiconductive nanoparticle on sulfur corrosion behaviors in oil-paper insulation," *Annual Report - Conference on Electrical Insulation and Dielectric Phenomena, CEIDP*, pp. 715–718, 2013.

[51] Y. Mo, Y. Yuan, and R. Liao, "Study on improving the space charge behavior in insulating paper by depositing nanostructured alumina on its surface via magnetron sputtering," *Thin Solid Films*, vol. 709, no. December 2019, p. 138 219, 2020.

[52] D. U. Yue-fan, L. V. Yu-zhen, Z. Jian-quan, *et al.*, "Effect of Ageing on Insulating Property of Mineral Oil-based TiO_2 Nanofluids," pp. 0–3, 2011.

[53] J. Miao, M. Dong, and L. P. Shen, "A modified electrical conductivity model for insulating oil-based nanofluids," in *Proceedings of 2012 IEEE International Conference on Condition Monitoring and Diagnosis, CMD 2012*, 2012, pp. 1126–1129.

[54] M. Rafiq, Y. Lv, C. Li, and Q. Sun, "Effect of Al2O3 nanorods on the performance of oil-impregnated pressboard insulation," *Electrical Engineering*, vol. 102, no. 2, pp. 715–724, 2020.

[55] B. Shan, M. Huang, Y. Ying, *et al.*, "Research on creeping flashover characteristics of nanofluid-impregnated pressboard modified based on Fe 3 O 4 nanoparticles under lightning impulse voltages," *Nanomaterials*, vol. 9, no. 4, 2019.

[56] M. Huang, L. Wang, Y. Ge, Y. Z. Lv, B. Qi, and C. R. Li, "Creeping flashover characteristics improvement of nanofluid/pressboard system with TiO2 nanoparticles," *AIP Advances*, vol. 8, no. 3, 2018.

[57] B. Shan, Y. Wu, H. Song, *et al.*, "Research on DC Breakdown Performance of Nanofluid-impregnated Pressboard Based on TiO2 Nanoparticles," *Proceedings of the 2020 IEEE 3rd International Conference on Dielectrics, ICD 2020*, pp. 169–172, 2020.

[58] R. Liao, C. Lv, L. Yang, Y. Zhang, W. Wu, and C. Tang, "The insulation properties of oil-impregnated insulation paper reinforced with nano-TiO2," *Journal of Nanomaterials*, vol. 2013, 2013.

[59] M. Maharana, N. Baruah, S. K. Nayak, and N. Sahoo, "Comparative study of mechanical and electrical strength of kraft paper in nanofluid based transformer oil and mineral oil," vol. 2, pp. 646–649, 2017.

[60] P. Trnka, M. Svoboda, and J. Hornak, "Insulation System," pp. 148–151, 2015.

[61] S. Yan, R. Liao, Y. Lü, X. Zhao, and L. He, "Influence of Nano-Al2O3 on Electrical Properties of Insulation Paper under Thermal Aging," *Diangong Jishu Xuebao/Transactions of China Electrotechnical Society*, vol. 32, no. 11, pp. 225–232, 2017.

[62] K. Swati, R. Sarathi, and K. S. Sharma, "Understanding the surface discharge activity with thermally aged nanofluid impregnated paper insulating material," *International Journal on Electrical Engineering and Informatics*, vol. 9, no. 4, pp. 762–775, 2017.

[63] A. Ibrahim, L. Nasrat, A. Elnoby, and S. Eldebeiky, "Thermal ageing study of zno nanofluid–cellulose insulation," *IET Nanodielectrics*, vol. 3, no. 4, pp. 124–130, 2020.

[64] R. Cimbala, S. Bucko, L. Kruželák, and M. Kosterec, "Thermal Degradation of Transformer Pressboard Impregnated with Magnetic Nanofluid Based on Transformer Oil," *Int Sci C Pow Eng*, no. 26220120055, pp. 1–5, 2017.

[65] M. Franchek and A. Levin, "Insulations ® DPE," *Transformers Magazine*, vol. 3, 2016.

[66] V. A. Primo, B. García, J. C. Burgos, and D. Pérez, "Ac breakdown voltage of fe3o4 based nanodielectric fluids. part 1: Analysis of dry fluids," *IEEE Transactions on Dielectrics and Electrical Insulation*, vol. 27, no. 2, pp. 352–359, 2020.

[67] E. Smiechowicz, B. Niekraszewicz, P. Kulpinski, and K. Dzitko, "Antibacterial Composite Cellulose Fibers Modified with Silver Nanoparticles and Nanosilica," *Cellulose*, vol. 25, no. 6, pp. 3499–3517, 2018.

[68] M. S. Alsalhi, A. S. Aldwayyan, A. H. Jasas, M. Atif, and W. Aslam Farooq, "Study of the Structural Analysis of Dye-Silica Core-Shell Nanoparticles (DSC-SNPs)," *9th Int Conf High Capacity Optical Networks and Enabling Technologies*, pp. 175–178, 2012.

[69] A. Lay-Ekuakille, M. Di Paola, F. Conversano, *et al.*, "Determining Shapes and Sizes Using TEM Images: Functionalized Nanoparticles," *Nanotechnology for Instrumentation and Measurement*, pp. 5–16, 2018.

[70] Ł. Klapiszewski, J. Zdarta, K. Antecka, *et al.*, "Magnetite Nanoparticles Conjugated with Lignin: A Physicochemical and Magnetic Study," *Appl. Surf. Sci.*, vol. 422, pp. 94–103, 2017.

[71] G. J. Hildeman and M. J. Koczak, "Powder-metallurgy Aluminum Alloys," in, ser. Treatise on Materials Science & Technology, vol. 31, Elsevier, 1989, pp. 323–364.

[72] TF D1.01.09, "Cigré Brochure 254. Dielectric response methods for diagnostics of power transformers.," vol. 33, no. 0, 2004.

[73] C. Ekanayake, S. M. Gubanski, A. Graczkowski, and K. Walczak, "Frequency response of oil impregnated pressboard and paper samples for estimating moisture in transformer insulation," *IEEE Transactions on Power Delivery*, vol. 21, no. 3, pp. 1309–1317, 2006.

[74] Commission International Electrotechnical, "CEI/IEC 60814:1997; Insulating liquids – Oil-impregnated paper and pressboard – Determination of water by automatic coulometric Karl Fischer titration Numéro," Tech. Rep., 1997.

[75] G. Schwarz, "A theory of the low-frequency dielectric dispersion of colloidal particles in electrolyte solution," *Journal of Physical Chemistry*, vol. 66, no. 12, pp. 2636–2642, 1962.

[76] D. Pérez-Rosa, B. García, J. C. Burgos, and A. Febrero, "Morphological analysis of transformer Kraft paper impregnated with dielectric nanofluids," *Cellulose*, vol. 27, no. 15, pp. 8963–8975, 2020.

[77] IEC Standard 60243-1, "Electric strength of insulating materials Test methods-Part 1: Tests at power frequencies," 2013.

[78] V. A. Primo, B. García, J. C. Burgos, and D. Pérez, "Ac breakdown voltage of fe3o4 based nanodielectric fluids. part 2: Analysis of fluids with high moisture content," *IEEE Transactions on Dielectrics and Electrical Insulation*, vol. 27, no. 2, pp. 360–367, 2020.

[79] J.-W. G. Hwang, "Elucidating the Mechanisms Behind Pre-Breakdown Phenomena in Transformer Oil Systems," Ph.D. dissertation, Massachusetts Institute of Technology, 2010.

[80] Y. Du, Y. Lv, C. Li, *et al.*, "Effect of electron shallow trap on breakdown performance of transformer oil-based nanofluids," *Journal of Applied Physics*, vol. 110, no. 10, p. 104 104, 2011.

[81] V. A. Primo, B. García, J. C. Burgos, and D. Pérez-Rosa, "Investigation of the lightning impulse breakdown voltage of mineral oil based fe3o4 nanofluids," *Coatings*, vol. 9, no. 12, 2019.

[82] IEC Standard 60243-3, "Electric strength of insulating materials Test methods-Part 3: Additional requirements for 1,2/50 s impulse tests," 2013.

[83] F. Negri, "FUNDAMENTAL STUDY AND MODELING OF NANOFLUIDS," Ph.D. dissertation, 2017.

[84] ASTM, "Standard Test Method for Tensile Properties of Paper and Paperboard Using Constant-Rate-of-Elongation Apparatus," Tech. Rep., 1997, pp. 1–7.

[85] G. K. Frimpong, T. V. Oommen, and R. Asano, "A survey of aging characteristics of cellulose insulation in natural ester and mineral oil," *IEEE Electrical Insulation Magazine*, vol. 27, no. 5, pp. 36–48, 2011.

[86] B. García, T. García, V. Primo, J. C. Burgos, and D. Urquiza, "Studying the loss of life of natural-ester-filled transformer insulation: Impact of moisture on the aging rate of paper," *IEEE Electrical Insulation Magazine*, vol. 33, no. 1, pp. 15–23, 2017.

[87] C. Tang, S. Zhang, J. Xie, and C. Lv, "Molecular simulation and experimental analysis of al2o3-nanoparticle-modified insulation paper cellulose," *IEEE Transactions on Dielectrics and Electrical Insulation*, vol. 24, no. 2, pp. 1018–1026, 2017.

[88] T. V. Oommen, R. N.C., C. C. Claiborne, and S. Pa, “"Electrical transformers containing electrical insulating fluids comprising high oleic acid oil compositions, Patent No: 5949017,” pp. 4–7, 1999.

[89] D. Liu, Z. Guo, J. DIng, and X. Xu, “Thermal Aging Effect on Properties of Pure and Doped Nano-TiO2Cellulose Pressboard,” *IEEE Transactions on Dielectrics and Electrical Insulation*, vol. 28, no. 1, pp. 133–141, 2021.

[90] L. Yang, R. Liao, S. Caixin, and M. Zhu, “Influence of vegetable oil on the thermal aging of transformer paper and its mechanism,” *IEEE Transactions on Dielectrics and Electrical Insulation*, vol. 18, no. 3, pp. 692–700, 2011.

[91] S. Beldar, R. Dolasiya, G. Morde, and C. Narasimhan, “Ftir and x-ray photoelectron spectral (xps) evidence for interaction between natural ester and cellulose paper,” in *2019 IEEE 20th International Conference on Dielectric Liquids (ICDL)*, 2019, pp. 1–4.

[92] A. Junior de Menezes, G. Siqueira, A. A. Curvelo, and A. Dufresne, “Extrusion and characterization of functionalized cellulose whiskers reinforced polyethylene nanocomposites,” *Polymer*, vol. 50, no. 19, pp. 4552–4563, 2009.

[93] S. Y. Oh, D. I. Yoo, Y. Shin, and G. Seo, “FTIR analysis of cellulose treated with sodium hydroxide and carbon dioxide,” *Carbohydrate Research*, vol. 340, no. 3, pp. 417–428, 2005.

[94] A. Munajad, C. Subroto, and Suwarno, “Study on the effects of thermal aging on insulating paper for high voltage transformer composite with natural ester from palm oil using fourier transform infrared spectroscopy (ftir) and energy dispersive x-ray spectroscopy (EDS),” *Energies*, vol. 10, no. 11, 2017.

Appendix A

Microscopy images

The following pages include the SEM and Cryo-SEM images that form the extensive morphological study performed to the NF impregnated Kraft paper samples.

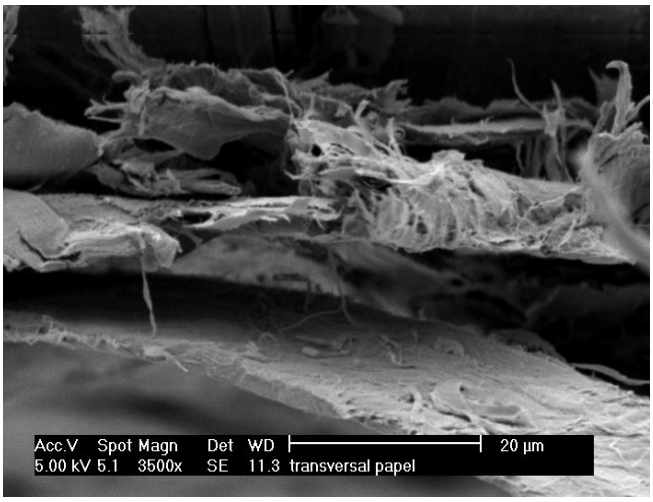

SEM image of the 0.2 g/L nanofluid impregnated Kraft paper sample cross section. It is possible to observe the nanofibers of cellulose broken when cutted to be observed. Performed in UC3M.

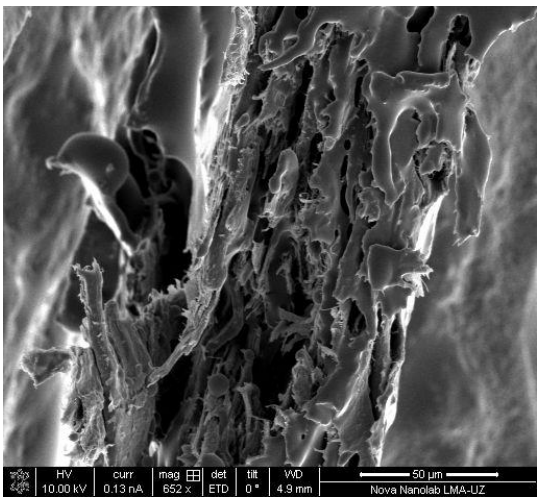

Cryo-SEM image of the 0.2 g/L nanofluid impregnated Kraft paper sample cross section. It is possible to observe the nanofibers of cellulose that are more compact due to the platinum coating needed to observe the samples. Performed in LMA-Unizar.

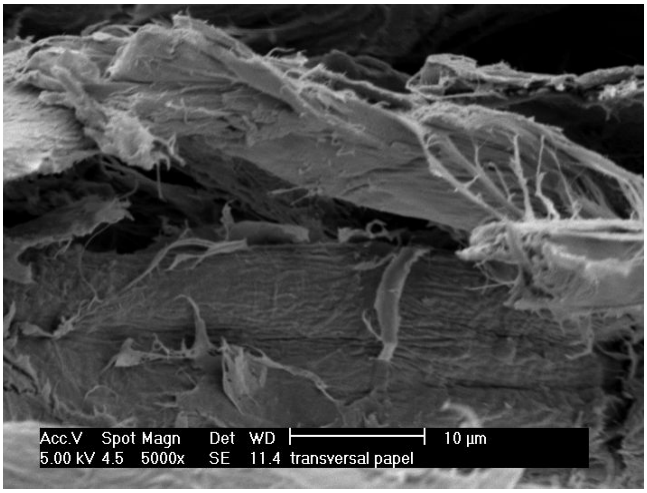

SEM image of the 0.2 g/L nanofluid impregnated Kraft paper sample cross section. It is possible to observe the nanofibers of cellulose broken when cutted to be observed. Performed in UC3M.

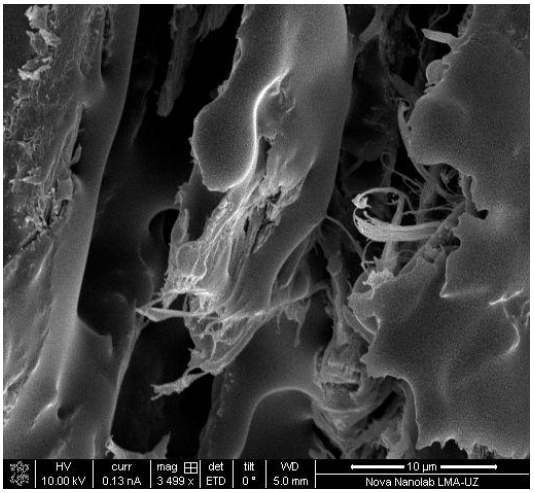

Cryo-SEM image of the 0.2 g/L nanofluid impregnated Kraft paper sample cross section. In the image is difficult to distinguish the cellulose fibers due to the platinum coating. Performed in LMA-Unizar.

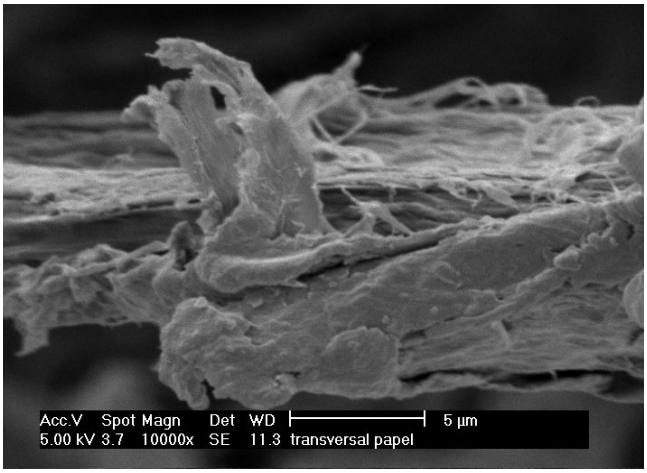

SEM image of the 0.2 g/L nanofluid impregnated Kraft paper sample cross section. It is possible to observe the nanofibers of cellulose, in this case the cellulose appears more compact compared with the previous images. Performed in UC3M.

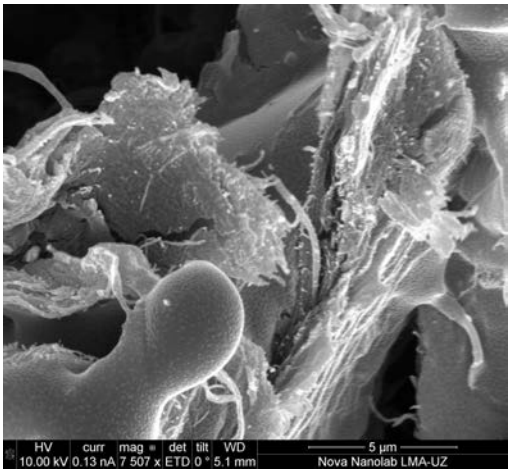

Cryo-SEM image of the 0.2 g/L nanofluid impregnated Kraft paper sample cross section. In the image is possible to observe in the right part the nanfibres despite the platinum coating. Performed in LMA-Unizar.

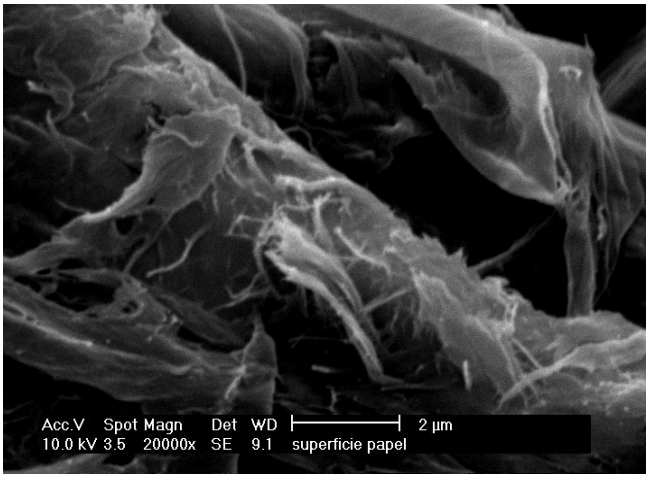

SEM image of the 0.2 g/L nanofluid impregnated Kraft paper sample surface. In this case is not possible to observe the nanofibres due to the perspective of the surface. Performed in UC3M.

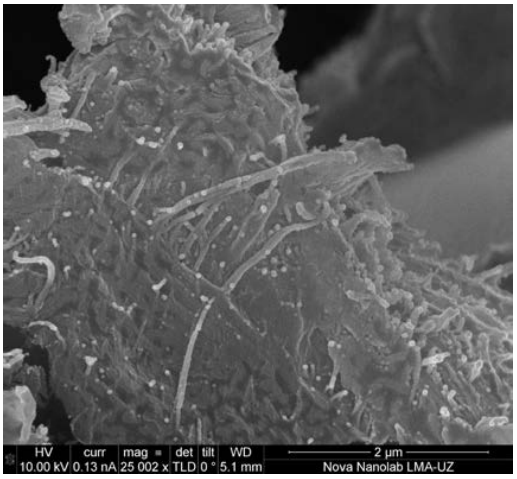

Cryo-SEM image of the 0.2 g/L nanofluid impregnated Kraft paper sample. In this image the nanofibres of cellulose are clearly observed, also some spherical forms are observed. Performed in LMA-Unizar.

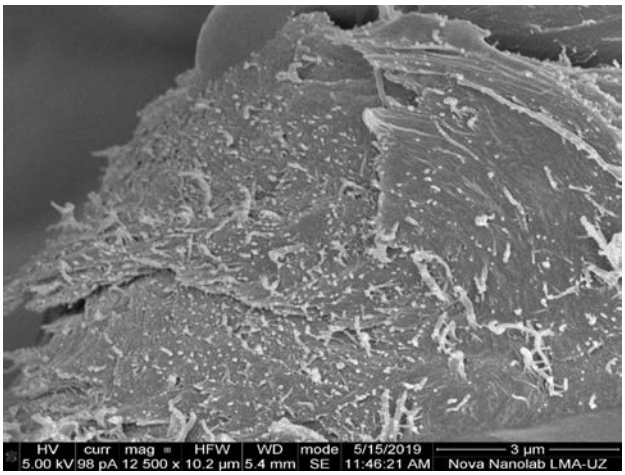

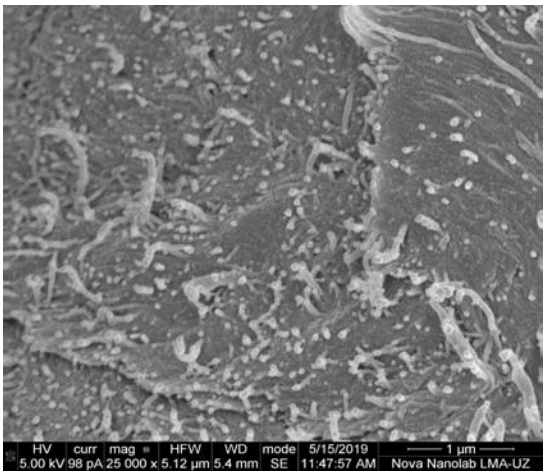

Cryo-SEM image of Mineral oil impregnated Kraft paper sample. The images belong to the surface of the same sample. Is possible to observe the cellulose fibres and its directionality, the cutted fibres are brighter due to the accumulation of negative charge in it when are irradiated with the electron beam. Performed in LMA-Unizar.

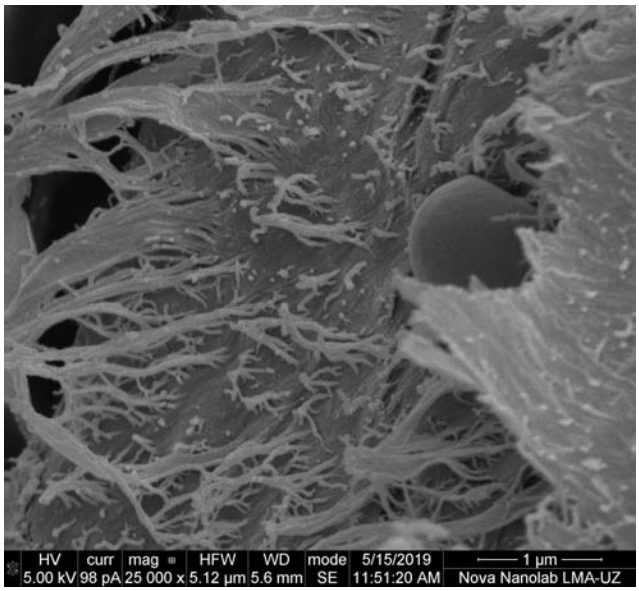

Cryo-SEM image of Mineral oil impregnated Kraft paper sample. The image belong to the surface of the same sample. The image reflects the cellulose fibres and also a drop of mineral oil (on the right part). Performed in LMA-Unizar.

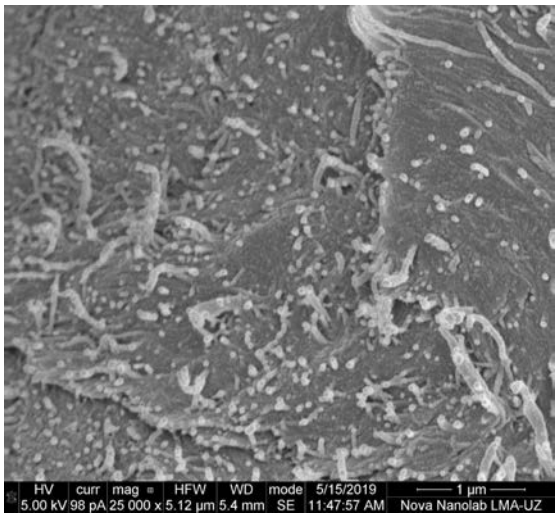

Cryo-SEM image of the mineral oil impregnated Kraft paper sample. In this image the nanofibres of cellulose are clearly visible Performed in LMA-Unizar.

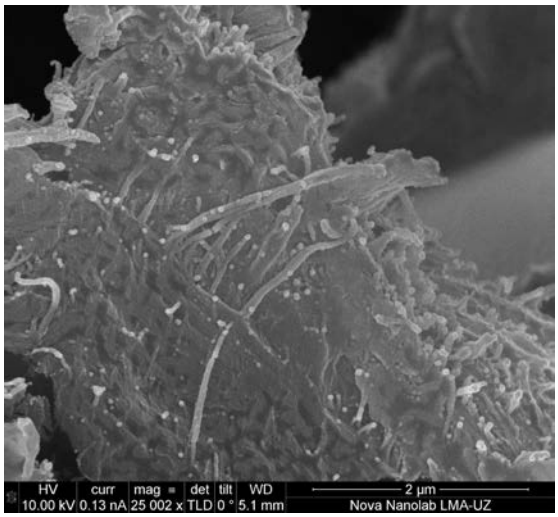

Cryo-SEM image of the 0.2 g/L nanofluid impregnated Kraft paper sample. In this image the nanofibres of cellulose are clearly observed, also some spherical forms are observed. Performed in LMA-Unizar.

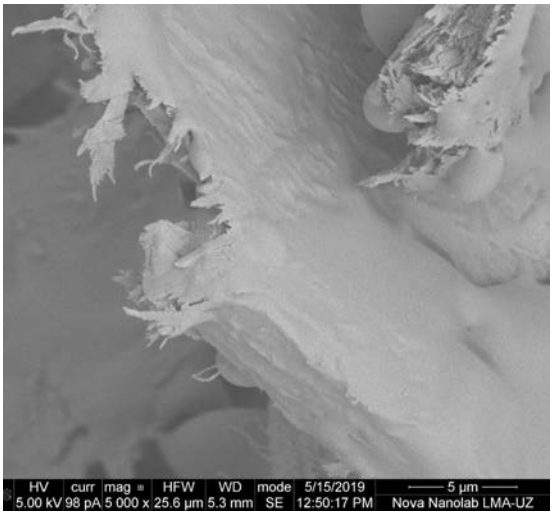

Cryo-SEM image of the mineral oil impregnated Kraft paper sample. The images belong to the interior of the Kraft paper sample. Performed in LMA-Unizar.

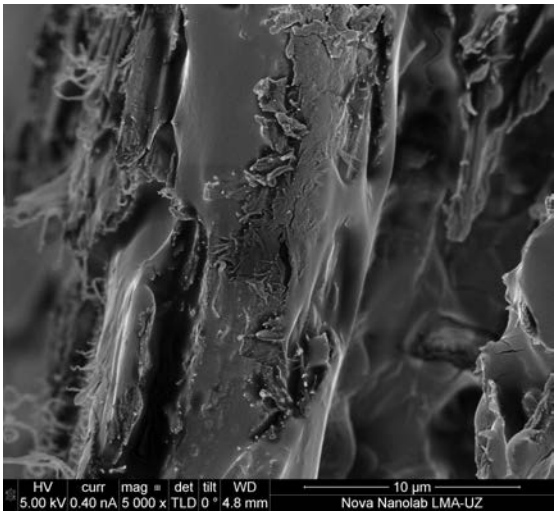

Cryo-SEM image of the 0.2 g/L nanofluid impregnated Kraft paper sample. The images belong to the interior of the Kraft paper. Performed in LMA-Unizar.

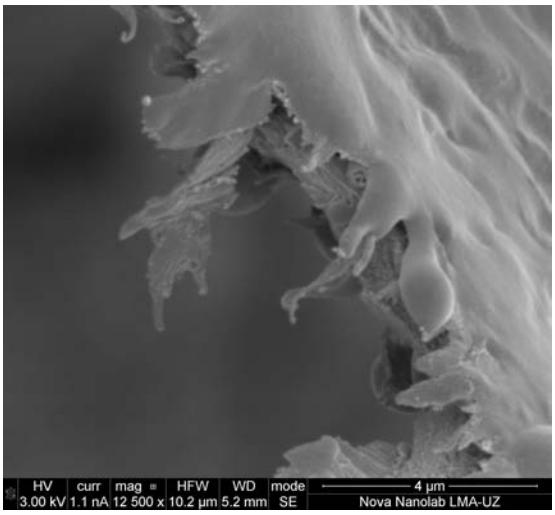

Cryo-SEM image of the mineral oil impregnated Kraft paper sample. The images belong to the interior of the Kraft paper Performed in LMA-Unizar.

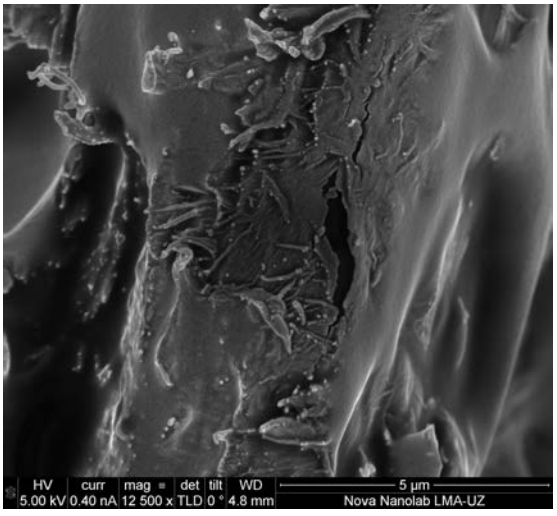

Cryo-SEM image of the 0.2 g/L nanofluid impregnated Kraft paper sample. The images belong to the interior of the Kraft paper. Performed in LMA-Unizar.

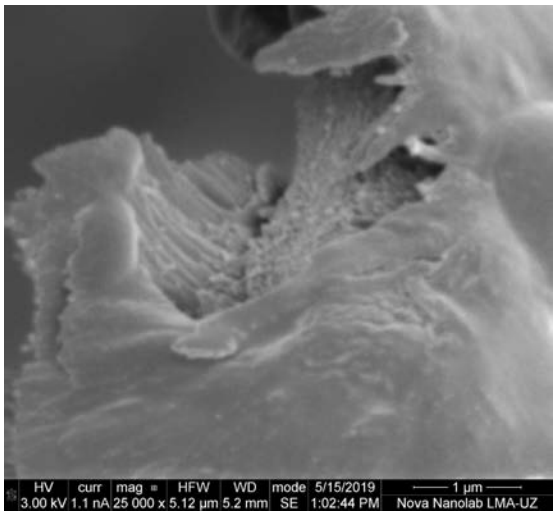

Cryo-SEM image of the mineral oil impregnated Kraft paper sample. The images belong to the interior of the Kraft paper. The cutted cellulose fibre is visible on the center of the image. Performed in LMA-Unizar.

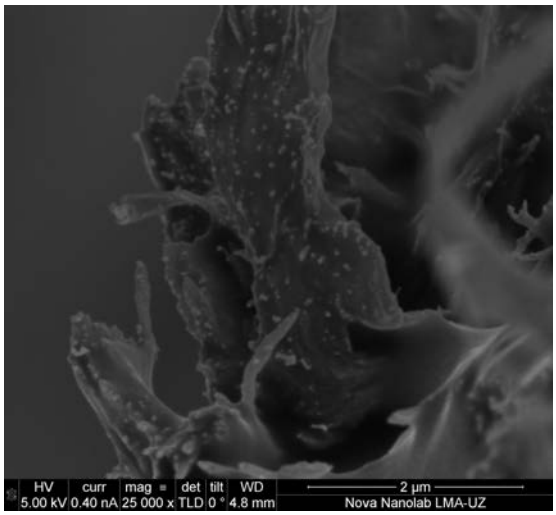

Cryo-SEM image of the 0.2 g/L nanofluid impregnated Kraft paper sample. The images belong to the interior of the Kraft paper. A macrofibre of the cellulose cutted is visible on the center of the image Performed in LMA-Unizar.

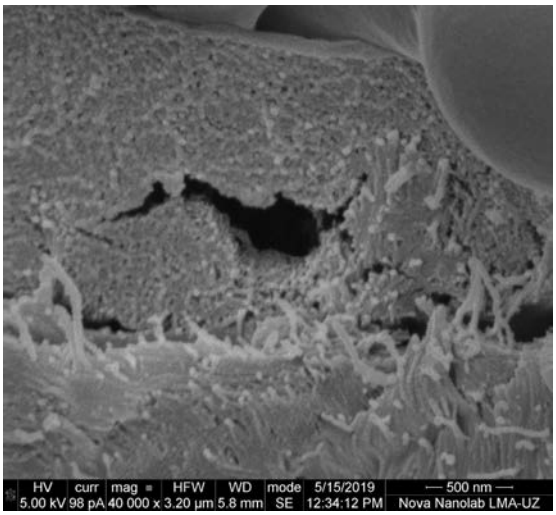

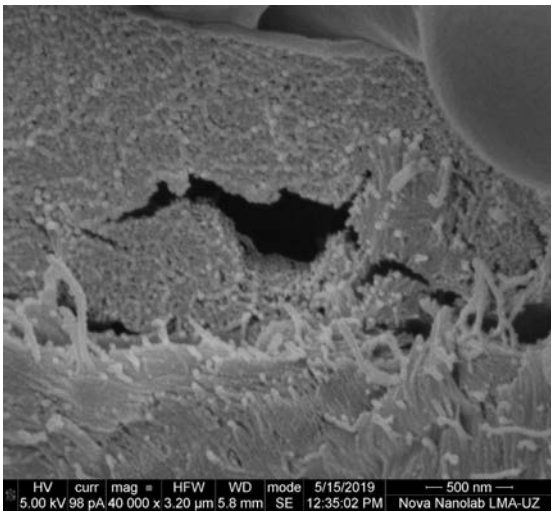

Cryo-SEM image of nanofluid 0.2 g/L impregnated Kraft paper sample. The images belong to the section of a sample . The image reflects the cellulose nanofibres during the study, section on the picture is the same with less than a minute of difference. The degradation of the samples is evident due to the energy of the electron beam . Performed in LMA-Unizar.

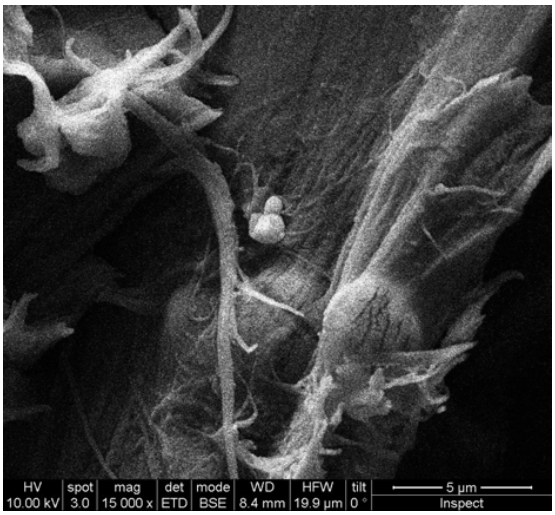

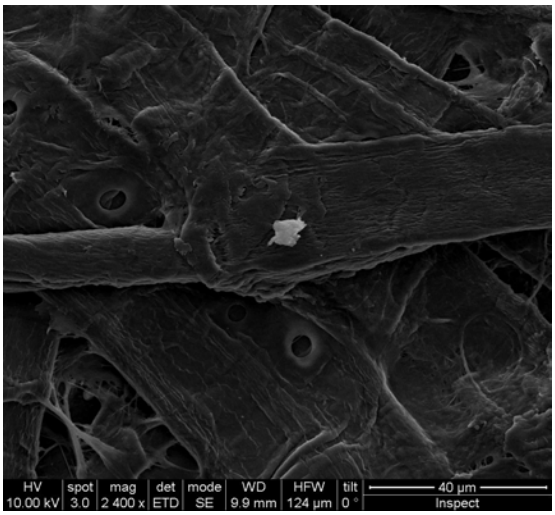

Cryo-SEM image of Mineral oil impregnated Kraft paper sample. The images reflect some impurities that appear after a treatment with chloroform. This impurities could be formed or content NPs from the NF. The impurities were then analyzed. Performed in LMA-Unizar.

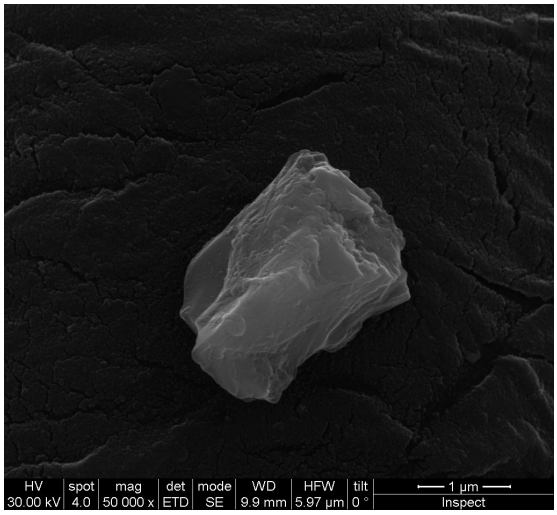

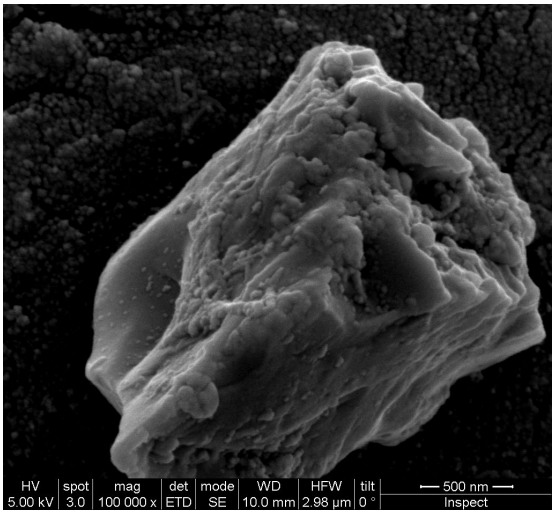

Cryo-SEM image of Mineral oil impregnated Kraft paper sample. The images reflect a impurity that appear after a treatment with chloroform, this impurity was then analyzed. Performed in LMA-Unizar.

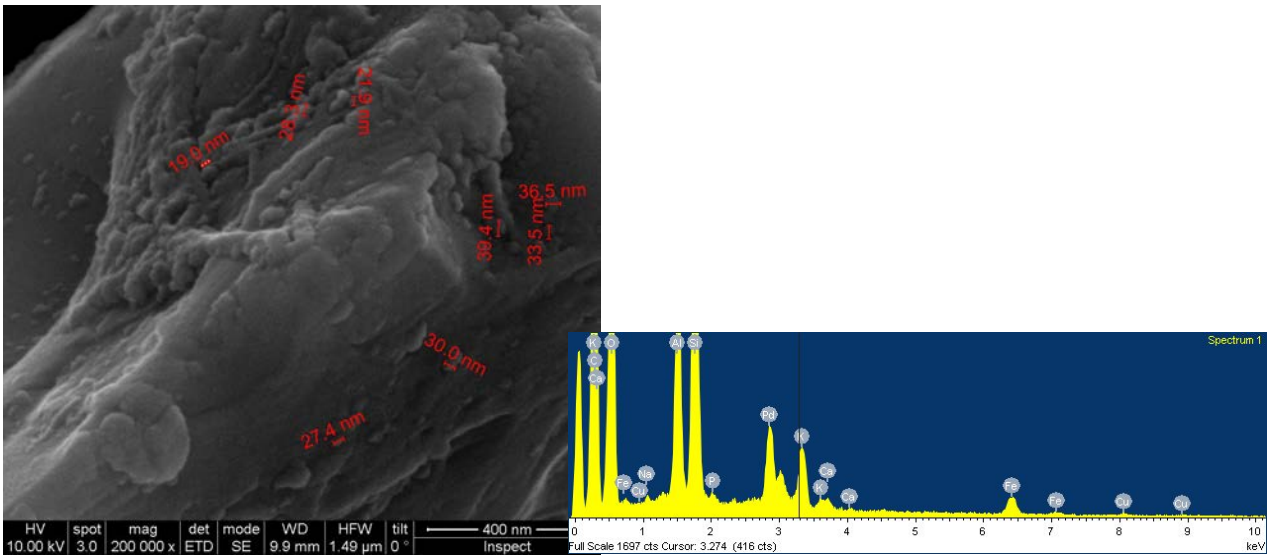

Cryo-SEM image of Mineral oil impregnated Kraft paper sample. The images reflect some impurities that appear after a treatment with chloroform. The globular forms are measured and then analyzed using EDX technique, also the analysis EDX is added were the chemical composition could be observed. Performed in LMA-Unizar.

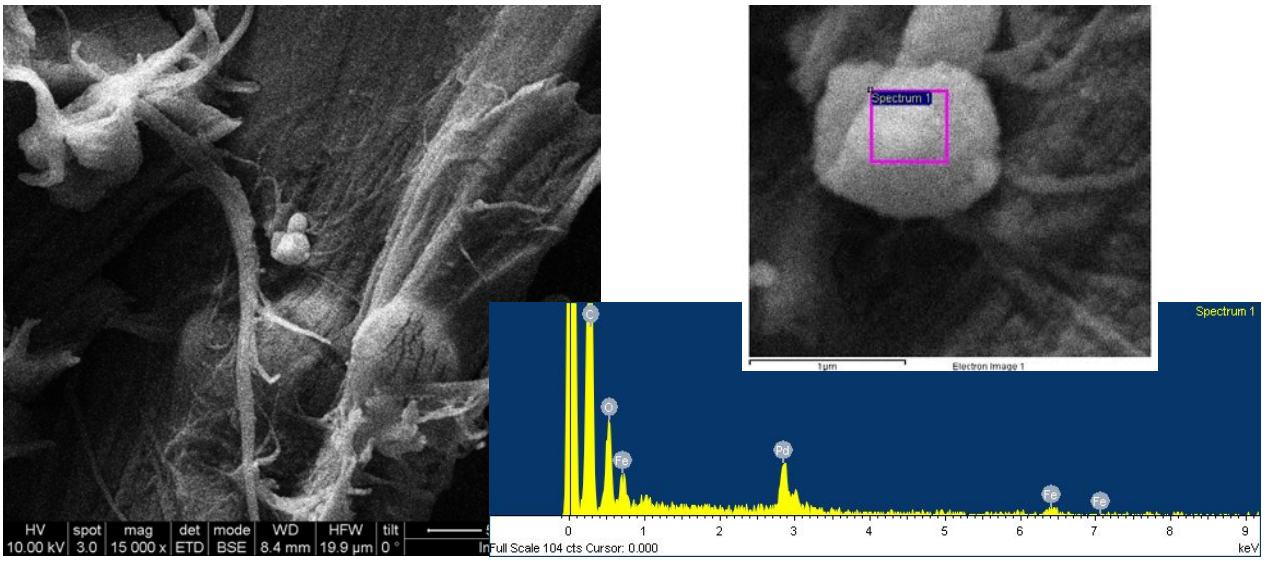

Cryo-SEM image of Mineral oil impregnated Kraft paper sample. The images reflect some impurities that appear after a treatment with chloroform. The impurity is observed in the superior zoom and the analysis EDX is added were the chemical composition could be observed. Performed in LMA-Unizar.

Appendix B

Sheet of characteristics of the base fluids

The following pages include the technical sheets of the dielectric oils used in the Thesis (Nynas Nytro 4000X and Bio Electra).

PRODUCT DATA SHEET

NYTRO® 4000X

Property	Unit	Test Method	Specification Limits		Typical Data
			Min	Max	
1 - Function					
Viscosity, 40°C	mm^2/s (cSt)	ISO 3104		12	9.2
Viscosity, -30°C	mm^2/s (cSt)	ISO 3104		1800	851
Pour point	°C	ISO 3016		-40	-54
Water content	mg/kg	IEC 60814		30	< 20
Breakdown voltage	kV	IEC 60156			
- Before treatment	kV	IEC 60156	30		40-60
- After treatment	kV	IEC 60296	70		> 70
Density, 20°C	kg/dm^3	ISO 12185		0.895	0.864
DDF at 90°C		IEC 60247		0.005	< 0.001
2 - Refining/stability					
Colour		ISO 2049		< 0.5	< 0.5
Appearance at 15°C		IEC 60296	Clear, Free from Sediment		Clear, Free from Sediment
Acidity	mg KOH/g	IEC 62021		0.01	< 0.01
Interfacial tension at 25°C	mN/m	IEC 62961	43		49
Total sulphur content	%	ISO 14596		0.05	< 0.01
Corrosive sulphur		DIN 51353	Non-Corrosive		Non-Corrosive
Potentially corrosive sulphur		IEC 62535	Non-Corrosive		Non-Corrosive
Corrosive sulphur		ASTM D1275	Non-Corrosive		Non-Corrosive
DBDS	mg/kg	IEC 62697-1	Not Detectable		Not Detectable
Antioxidants	wt %	IEC 60666	0.34	0.40	0.38
Metal passivator additives	mg/kg	IEC 60666	Not Detectable		Not Detectable
Other additives *			None		None
2-Furfural and related compounds content	mg/kg	IEC 61198		< 0.05	< 0.05
Aromatic content	%	IEC 60590			4
Stray gassing under thermo-oxidative stress		IEC 60296			
- Hydrogen	µl/l	clause A.4		< 50	< 5
- Methane	µl/l	clause A.4		< 50	< 1
- Ethane	µl/l	clause A.4		< 50	< 1
3 - Performance					
Oxidation stability at 120°C, 500 h		IEC 61125			
- Total acidity	mg KOH/g	IEC 61125		0.3	0.02
- Sludge	wt %	IEC 61125		0.05	< 0.01
- DDF at 90°C		IEC 61125		0.050	< 0.005
Inhibitor content after 500 h	wt %	IEC 60666	0.08		0.18
4 - Health, safety and environment (HSE)					
Flash Point, PM	°C	ISO 2719	135		148
PCA	wt %	IP 346		< 3.0	< 3.0
PCB	mg/kg	IEC 61619	Not Detectable		Not Detectable

*this product contains no undeclared additives

NYTRO 4000X is a Super Grade inhibited insulating oil meeting IEC 60296 Ed. 5 (2020) Type A, TVAI and it is 100% recyclable. Breakdown voltage after treatment as per definition in IEC 60296, section 6,4

Severely hydrotreated insulating oil

Issuing date: 18-05-2021

BIO ELECTRA

INDUSTRY

Lubricants

Description

Dielectric oil based on plant-derived esters, rapidly biodegradable and non-toxic for both aquatic and land ecosystems. It is an increased safety fluid thanks to its high ignition point and the lack of risk factors on its safety sheet.

To be used as a dielectric insulator in transformers, reactors, and electrical switches. Can be used in both new electrical equipment as well as to fill equipment that was previously using a different type of dielectric fluid. Especially for those cases that require a fluid with a high flash point or for use in environmentally sensitive areas.

Properties

- Vegetable oil in a percentage greater than 99%.
- No synthetic antioxidants.
- No silicones, halogens, or any other component that could pose a risk to health or the environment.
- Ignition point over 300 °C. Reduces risk of fires and their consequences.
- Classified as a type K fluid according to IEC 61100.

Quality levels

- IEC 62770

Technical specifications

Physical and chemical properties	UNIT	METHOD	GUARANTEED VALUE	TYPICAL VALUE
Fire point	°C	ASTM D92	>300	362
Flash point	°C	ASTM D92	>250	330
Density at 20 °C	g/ml	ASTM D4052	<1	0.91
Kinematic viscosity at 100 °C	cSt	ASTM D455	<15	8.5
Kinematic viscosity at 40 °C	cSt	ASTM D455	<50	39.2
Kinematic viscosity at 0 °C	cSt	ASTM D455	<500	275.9
Pour point	°C	ASTM D97	<-10	-22
Appearance	--	ASTM D1524	Clear and bright	
Thermal expansion coefficient 0-50 °C	$°C^{-1}$	ASTM D1903		0.00072
Thermal conductivity at 25 °C	W/K m	ASTM D2717		0.1691
Specific heat at 25 °C	J/kg	ASTM D2766		1.97
Acidity (neutralisation index)	mgKOH/g	ASTM D974	<0.06	0.05

A safety data sheet is available on request.

repsol.com
+34 901 111 999

Technical data sheet for Lubricants. Revision 1. July 2016.

BIO ELECTRA

INDUSTRY

Lubricants

Water content	mg/kg	IEC 60814	<200	150
Oxidation stability				
Total acidity	mgKOH/g	IEC 61125 C	0.6	0.16
Diel. dissipation factor 90 °C, 50 Hz	--	IEC 60247	0.5	0.065
Viscosity increase	%	ASTM D445	<30	10.4

Electrical properties	UNIT	METHOD	GUARANTEED VALUE	TYPICAL VALUE
Dielectric strength	kV	IEC 60156	>35	65
Diel. dissipation factor 90 °C, 50 Hz		IEC 60247	<0.050	0.03
Diel. dissipation factor 25 °C, 50 Hz		ASTM D924		0.002
Electrical conductivity at 25 °C	pS/m	ASTM D2624		3
Dielectric constant at 25 °C		IEC 60247		3.1
Gassing tendency	µl/min	IEC 60628 A		-31.2

Environmental properties	UNIT	METHOD	GUARANTEED VALUE	TYPICAL VALUE
Biodegradability - 28 days	%	OECD 301B	>60	85
Ecotoxicity in aquatic environment	mg/l	OECD 201 OECD 202 OECD 203	>100 >100 >100	>1000 >1000 >1000
Ecotoxicity in land environment	mg/kg	OECD 207 OECD 208	>100 >100	>1000 >1000

A safety data sheet is available on request.

repsol.com
+34 901 111 999

Technical data sheet for Lubricants. Revision 1. July 2016.